Supporting Information

PRIMO: A Transferable Coarse-grained Force Field for Proteins

Parimal Kar[1], Srinivasa Murthy Gopal[1], Yi-Ming Cheng[1], Alexander Predeus[1], Michael Feig[1,2*]

[1]Department of Biochemistry and Molecular Biology and [2]Department of Chemistry, Michigan State University, East Lansing, MI 48824, USA

Keywords: Coarse-grain, force field, implicit solvent, molecular dynamics, replica exchange

*Corresponding author:
Email: feig@msu.edu
Phone: +1 (517) 432-7439
Fax: +1 (517) 353-9334.

Table S1: The mapping between all-atom and PRIMO CG levels.

Residues	PRIMO		CHARMM
	NAME	TYPE	ATOM
ACE	COY	COY	CY OY
	SCT	SCT3	CAY
CT3	NTT	NTT	NT
	SNT	SCT3	CAT
ALA	SC1	SC1A	CB
ARG	SC1	SC1R	CB CG
	SC2	SC2R	CD
	SC3	SC3R	NE
	SC4	SC4R	NH1
	SC5	SC4R	NH2
ASP	SC1	SC1D	CB
	SC2	SC2D	CG OD1
	SC3	SC2D	CG OD2
ASN	SC1	SC1N	CB
	SC2	SC2N	CG OD1
	SC3	SC3N	ND2
CYS	SC1	SC1C	CB SG
GLN	SC1	SC1Q	CB CG
	SC2	SC2Q	CD OE1
	SC3	SC3Q	NE2
GLU	SC1	SC1E	CB CG
	SC2	SC2E	CD OE1
	SC3	SC2E	CD OE2
HSD	SC1	SC1H	CB CG
	SC2	SC2HD	ND1
	SC3	SC3HD	NE2
HSE	SC1	SC1H	CB CG
	SC2	SC2HE	ND1
	SC3	SC3HE	NE2
ILE	SC1	SC1I	CB CG1 CG2
	SC2	SC2I	CD
LEU	SC1	SC1L	CB
	SC2	SC2L	CG CD1
	SC3	SC2L	CG CD2
LYS	SC1	SC1K	CB CG
	SC2	SC2K	CD
	SC3	SC3K	CE
	SC4	SC4K	NZ
MET	SC1	SC1M	CB CG
	SC2	SC2M	SD
	SC3	SC3M	CE

PHE	SC1	SC1F	CB CG
	SC2	SC2F	CE1
	SC3	SC2F	CE2
PRO	SC1	SC1P	CB CG CD
SER	SC1	SC1S	CB OG
THR	SC1	SC1T	CG OG1
	SC2	SC2T	CG2
TRP	SC1	SC1W	CB CG
	SC2	SC2W	NE1
	SC3	SC3W	CE3
	SC4	SC4W	CZ2
TYR	SC1	SC1Y	CB CG
	SC2	SC2Y	CE1
	SC3	SC2Y	CE2
	SC4	SC4Y	OH
VAL	SC1	SC1V	CB CG1
	SC2	SC1V	CB CG2

Table S2: List of virtual atom constructions and the associated interaction potentials. Following the nomenclature in the main text, virtual atoms are suffixed by an asterix (*). # indicates a CG particle of the next residue. All interactions are harmonic with a spring constant (k_b) of 10.0 kcal/(mol Å^2) and k_θ of 5.0 kcal/(mol rad^2) for bonds and angles respectively. A virtual atom A is constructed using either Scheme I or Scheme II. Scheme I refers to a construction of an atom A, using the A-B bond, the A-B-C angle and the dihedral A-B-C-D as input. In scheme II, an atomic site B, is obtained from a CG site located at the midpoint AB by extrapolation from A. For a more detailed discussion of the above methods, the reader is referred to refs 1 and 2.

	Construction of Virtual atoms			Potential		
Residue	Virtual Atoms	Construction Method	CG /Virtual particles used for construction	Type	Particles Involved	Minima
ALL Except Gly/Pro	C*	I	CO, N1#, CA1	Bond	N1, C*	2.480 Å
				Angle	N1, C*, CO	113.000°
Gly	C*	I	CO, N1#, CA1	Bond	N1, C*	2.510 Å
				Angle	N1, C*, CO	115.000°
Pro	C*	I	CO, N1#, CA1	Bond	N1, C*	2.530 Å
				Angle	N1, C*, CO	116.000°
Arg	Cβ*	I	CA1, N1, C*	Bond	SC1, Cβ*	0.770 Å
				Angle	CA1, Cβ*, SC1	114.5°
	Cγ*	II	Cβ*, SC1	Bond	SC1, Cγ*	1.540
				Angle	SC1, Cγ*, SC2	113.5°
	Cζ*	I	SC3, SC5, SC4	Angle	SC3, Cζ*, SC2	124.285°
Asn	Cγ*	I	SC1, SC3, SC2	Angle	SC1, Cγ*, CA1	111.020°
Asp	Cγ*	I	SC1, SC2, SC3	Angle	SC1, Cγ*, CA1	111.010°
Cys	Cβ*	I	CA1, N1, C*	Bond	SC1, Cβ*	0.915 Å
				Angle	CA1, Cβ*, SC1	113.000°
Gln	Cβ*	I	CA1, N1, C*	Bond	SC1, Cβ*	0.775 Å
				Angle	CA1, Cβ*, SC1	114.500°

Glu	Cβ*	I	CA1, N1, C*	Bond	SC1, Cβ*	0.775 Å
				Angle	CA1, Cβ*, SC1	114.500°
	Cγ*	II	Cβ*, SC2	Bond	SC2, Cγ*	1.960 Å
				Bond	SC3, Cγ*	1.960 Å
Hsd/Hse	Cβ*	I	CA1, N1, C*	Bond	SC1, Cβ*	0.755 Å
				Angle	CA1, Cβ*, SC1	114.5°
	Cγ*	II	Cβ*, SC1	Bond	SC2, Cγ*	1.380
				Angle	SC1, Cγ*, SC2	123.780°
Ile	Cβ*	I	CA1, N1, C*	Bond	SC2, Cβ*	2.580 Å
				Angle	CA1, Cβ*, SC1	129.490°
Leu	Cγ*	I	SC1, SC2, SC3	Bond	CA1, Cγ*	2.620 Å
				Angle	SC1, Cγ*, CA1	115.530°
Lys	Cβ*	I	CA1, N1, C*	Bond	SC1, Cβ*	0.775 Å
				Angle	CA1, Cβ*, SC1	112.000°
	Cγ*	II	Cβ*, SC1	Bond	SC2, Cγ*	1.540
				Angle	SC1, Cγ*, SC2	112.700°
Met	Cβ*	I	CA1, N1, C*	Bond	SC1, Cβ*	0.775 Å
				Angle	CA1, Cβ*, SC1	115.000°
	Cγ*	II	Cβ*, SC1	Bond	SC1, Cγ*	1.820
				Angle	SC1, Cγ*, SC2	114.130°
Phe	Cβ*	I	CA1, N1, C*	Bond	SC1, Cβ*	0.775 Å
				Angle	CA1, Cβ*,SC1	112.000°
	Cγ*	II	Cβ*, SC1	Bond	SC1, Cγ*	2.440
				Angle	SC1, Cγ*, SC3	149.800°
Pro	Cβ*	I	CA1, N1, C*	Bond	SC1, Cβ*	1.240 Å
				Angle	CA1, Cβ*,SC1	84.605°
Ser	Cβ*	I	CA1, N1, C*	Bond	SC1, Cβ*	0.715 Å

				Angle	CA1, Cβ*, SC1	108.610°
Thr	Cβ*	I	CA1, N1, C*	Bond	SC1, Cβ*	0.710 Å
				Angle	CA1, Cβ*, SC1	108.630°
Trp	Cβ*	I	CA1, N1, C*	Bond	SC1, Cβ*	0.775 Å
				Angle	CA1, Cβ*, SC1	115.650°
	Cγ*	II	Cβ*, SC1	Bond	SC1, Cγ*	2.240
				Angle	SC1, Cγ*, SC2	160.450°
Tyr	Cβ*	I	CA1, N1, C*	Bond	SC1, Cβ*	0.775 Å
				Angle	CA1, Cβ*, SC1	112.000°
	Cγ*	II	Cβ*, SC1	Bond	SC1, Cγ*	2.440
				Angle	SC1, Cγ*, SC3	149.800°
Val	Cβ*	I	CA1, SC1, SC2	Bond	SC1, Cβ*	0.770 Å
					SC2, Cβ*	0.770 Å
				Angle	CA1, Cβ*, N1	111.900°

Table S3: Average solvent-accessible surface areas (SASA) obtained from PRIMO and CHARMM simulations in comparison with SASA values of PDB structures. Standard deviations are provided in the parentheses.

PDB	PRIMO ($Å^2$)	CHARMM ($Å^2$)	PDB ($Å^2$)
1VII	3127.4 (88.7)	3232.3 (111.2)	3183.3
3GB1	4289.2 (92.6)	3853.8 (81.5)	3888.5
1BDD	3748.1 (95.9)	3568.3 (91.7)	3332.6
1D3Z	5209.0 (129.1)	5074.7 (82.0)	4965.7
2PTL	4647.9 (145.4)	4335.8 (84.7)	4095.7
1BTA	5723.0 (132.1)	5466.3 (111.9)	5341.1
1FKS	6750.0 (183.0)	6718.5 (230.0)	6561.6
1A2P	7004.6 (158.1)	6241.1 (117.5)	5994.2
2AAS	7555.0 (182.0)	7440.9 (188.9)	6580.2
1CYE	7100.8 (151.8)	7010.5 (115.7)	6189.5
2RN2	9894.4 (208.3)	8839.6 (207.6)	8492.0

Table S4**:** C_α RMSD obtained from PRIMO-MD simulations with OPEP4-MD simulations. Standard deviations are provided in the parentheses.

PDB	C_α RMSD (PRIMO) (Å)	C_α RMSD (OPEP) (Å)	rigid core
1GYZ	3.7 (0.5)	3.5 (0.2)	60-86, 92-115
2DA1	4.4 (0.8)	3.2 (0.4)	16-63
1FAF	3.4 (0.5)	3.3 (0.1)	5-41, 50-69
1PRA	3.8 (0.5)	3.4 (0.4)	1-63
2VXD	3.5 (0.5)	3.4 (0.4)	1-54
1BW6	4.2 (0.5)	3.6 (0.2)	10-64
1QHK	3.5 (0.5)	3.6 (0.2)	6-13, 18-52
1E0G	3.7 (0.5)	3.6 (0.3)	2-47
1CLB	3.4 (0.5)	2.9 (0.2)	3-14, 20-39, 47-53, 60-73
1FCL	3.0 (0.3)	2.8 (0.3)	3-55
1PGB	2.8 (0.7)	3.3 (0.20	1-56
1B75	3.5 (0.7)	2.9 (0.2)	1-8, 26-31, 38-78, 88-92
2KTE	6.1 (0.9)	3.6 (0.4)	1-36, 41-52, 62-105, 118-152
1E0L	2.9 (0.5)	2.1 (0.5)	7-33
2B86	2.8 (0.4)	2.8 (0.3)	3-14, 20-51, 57-58
1AFP	2.9 (0.7)	2.9 (0.2)	1-16, 24-27, 37-51
1SHG	3.2 (0.7)	2.4 (0.3)	8-11, 29-61

Table S5: The efficiency of 1 ns simulations of 11 proteins with three different simulation methodologies. CPU times are provided in second (s). Speedups are provided in parentheses.

PDB	PRIMO (s)	CHARMM/GBMV (s)	CHARMM/TIP3P (s)
1VII	4116	41256 (10.0)	55548 (13.5)
3GB1	6510	63900 (9.8)	94536 (14.5)
1BDD	5184	53208 (10.3)	61776 (11.9)
1D3Z	9360	98712 (10.5)	188928 (20.2)
2PTL	7162	70776 (9.9)	119592 (16.7)
1BTA	10260	116856 (11.4)	94320 (9.2)
1FKS	13536	135936 (10.0)	169272 (12.5)
1A2P	12168	128232 (10.5)	135648 (11.2)
2AAS	15048	147024 (9.8)	147456 (9.8)
1CYE	16272	118440 (7.3)	169344 (10.4)
2RN2	19944	194112 (9.8)	238680 (12.0)

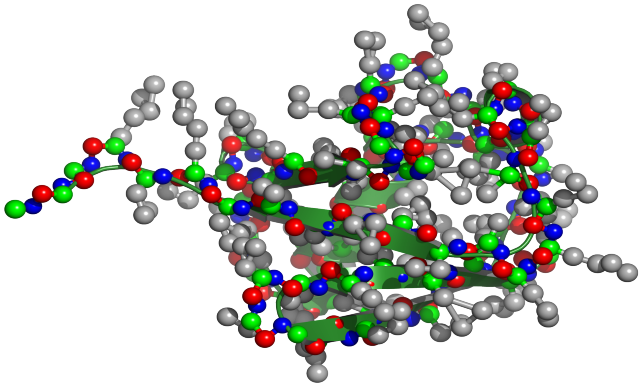

Figure S1: Ubiquitin (PDB ID: 1D3Z) in PRIMO representation together with a cartoon representation of the secondary structure. All side chain CG sites are shown as gray, the backbone is shown in color (green: CA1, blue: N1, and red: CO).

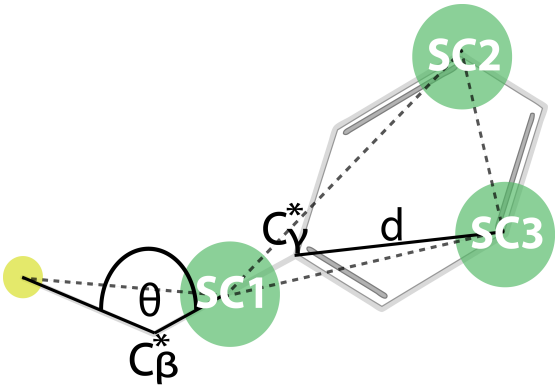

Figure S2: Reconstruction of virtual atoms c_β* and c_γ* for phenylalanine.

Hydrogen bond reconstruction and its derivatives:

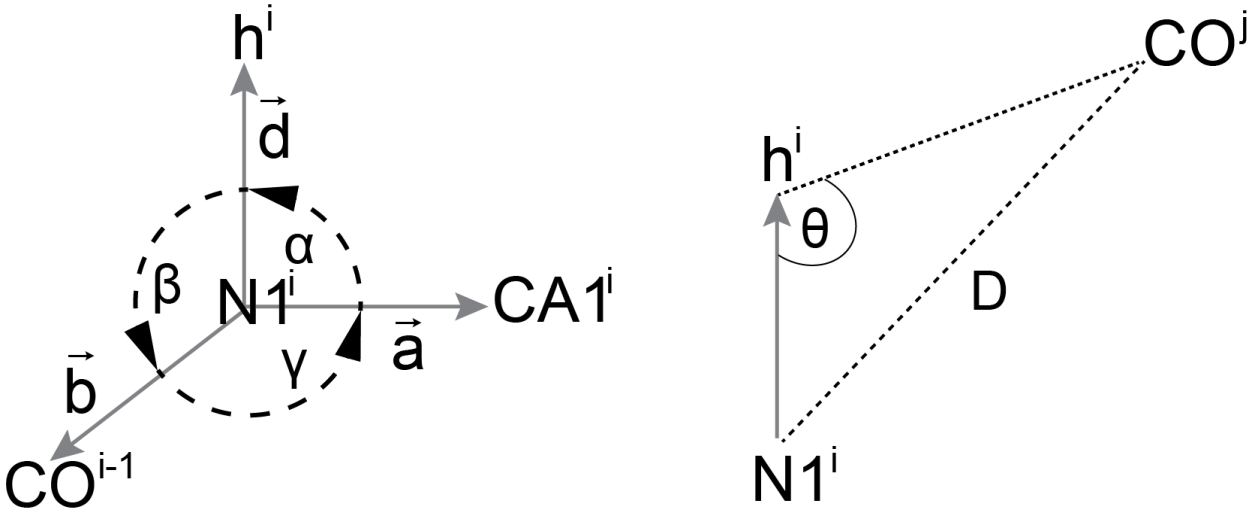

Figure S3. Construction of the amino hydrogen atom using CG particles for the i^{th} residue. Also shown is the calculation of the hydrogen bonding potential for residues i and j using the **$N1^i$-h^i-CO^j** angle (**θ**) and the distance (**D**) between **$N1^i$** and **CO^j** particles.

The hydrogen atom on the i^{th} residue is constructed (See Fig. S1) using three CG particles, N1 and CA1 of the i^{th} residue as well as CO of the $(i-1)^{th}$ residue.

First, we define $\vec{a}\,(x_a, y_a, z_a)$ and $\vec{b}\,(x_b, y_b, z_b)$ as

$$\begin{aligned} q_a &= q^i_{CA1} - q^i_{N1} \quad \text{for } q = x, y, z \\ q_b &= q^{i-1}_{CO} - q^i_{N1} \quad \text{for } q = x, y, z \end{aligned} \tag{1}$$

Since the vectors $\vec{a}$, $\vec{b}$ and the hydrogen atom bonded to the nitrogen are in the same plane, it can be shown from elementary trigonometric (or alternatively using vector cross-product definition) that the position of hydrogen atom $\vec{h}\,(x_h, y_h, z_h)$ is given by the relation

$$\vec{d} = F_A\vec{a} + F_B\vec{b}$$
$$F_A = -\frac{d}{\sin\gamma}\left(\frac{\sin\beta}{a}\right)$$
$$F_B = -\frac{d}{\sin\gamma}\left(\frac{\sin\alpha}{b}\right) \quad (2)$$
$$q_h^i = q_{N1}^i + q_d \text{ for } q = x, y, z$$

where the angles α, β and γ, as well as the magnitudes of vectors a and b are based on atomistic simulations. These parameters together define the constant parameters F_A and F_B used in the reconstruction.

The hydrogen bond potential ($s_{2d}(\cos\theta,D)$) is a 2D spline-interpolated potential, a knowledge-based potential based on statistical analysis of 2000+ high resolution crystal structures. The potential is a function of the distance between the donor (N1 particle of i^{th} residue) and the acceptor (CO of j^{th} residue), and the angle formed between them with the reconstructed hydrogen atom.

The derivatives of this potential are applied to CG particles used in the construction of hydrogen atom and the acceptor CO particle. The derivatives in Cartesian co-ordinate system are given as

$$\frac{\partial s_{2d}(\cos\theta,D)}{\partial q_k} = \frac{\partial s_{2d}(\cos\theta,D)}{\partial\cos\theta}\cdot\frac{\partial\cos\theta}{\partial q_k}$$
$$\frac{\partial s_{2d}(\cos\theta,D)}{\partial q_k} = \frac{\partial s_{2d}(\cos\theta,D)}{\partial D}\cdot\frac{\partial D}{\partial q_k} \quad (3)$$
$$\text{for } q = x, y, z \text{ and } k = CO^{i-1}, N1^i, CA1^i \text{ and } CO^j$$

where $\frac{\partial s_{2d}(\cos\theta,D)}{\partial\cos\theta}$ and $\frac{\partial s_{2d}(\cos\theta,D)}{\partial D}$ are numerically determined during the spline interpolation.

The procedure for determining the derivatives of the distance (D) and the angle (cosθ) is as follows:

First, the distance D and the angle (cosθ) are given by the relation

$$D = \sqrt{\sum_{q = x, y, z} (q^{j}_{CO} - q^{i}_{N1})^2}$$

$$\cos\theta = - \frac{\sum_{q = x, y, z} (q^{i}_{h} - q^{j}_{CO})(q^{i}_{h} - q^{i}_{N1})}{\sqrt{\sum_{q = x, y, z} (q^{i}_{h} - q^{j}_{CO})^2}\, d_{N1h}} \qquad (4)$$

where d_{N1h} is the constant bond length used in the hydrogen bond reconstruction, set to the standard N-H bond length of the CHARMM force field.

The derivatives for the distance (D) are given by

$$\frac{\partial D}{\partial q_k} = \begin{cases} \dfrac{q^{j}_{CO} - q^{i}_{N1}}{D} & \text{for} \quad q = x, y, z \quad \text{and} \quad k = CO^{j} \\ -\dfrac{q^{j}_{CO} - q^{i}_{N1}}{D} & \text{for} \quad q = x, y, z \quad \text{and} \quad k = N1^{i} \end{cases} \qquad (5)$$

The derivatives for the angle are

$$\frac{\partial \cos\theta}{\partial q^{i}_{CA1}} = - \frac{F_A\left((q^{i}_{h} - q^{j}_{CO}) + (q^{i}_{h} - q^{i}_{N1}) \right)}{\sqrt{\sum_{q = x, y, z} (q^{i}_{h} - q^{j}_{CO})^2}\, d_{N1h}} +$$

$$\frac{F_A (q^{i}_{h} - q^{j}_{CO}) \sum_{q=x,y,z} (q^{i}_{h} - q^{j}_{CO})(q^{i}_{h} - q^{i}_{N1})}{\left(\sqrt{\sum_{q = x, y, z} (q^{i}_{h} - q^{j}_{CO})^2} \right)^3 d_{N1h}} \quad \text{for } q = x, y, z \qquad (6)$$

$$\frac{\partial \cos\theta}{\partial q_{CO}^{i-1}} = -\frac{F_B\left((q_h^i - q_{CO}^j) + (q_h^i - q_{N1}^j)\right)}{\sqrt{\sum_{q=x,y,z}(q_h^i - q_{CO}^j)^2}\, d_{N1h}} +$$

$$\frac{F_B(q_h^i - q_{CO}^j)\sum_{q=x,y,z}(q_h^i - q_{CO}^j)(q_h^i - q_{N1}^i)}{\left(\sqrt{\sum_{q=x,y,z}(q_h^i - q_{CO}^j)^2}\right)^3 d_{N1h}} \quad \text{for} \quad q = x, y, z \tag{7}$$

$$\frac{\partial \cos\theta}{\partial q_{N1}^i} = \frac{(1 - F_A - F_B)(q_h^i - q_{N1}^i) - (F_A + F_B)(q_h^i - q_{CO}^j)}{\sqrt{\sum_{q=x,y,z}(q_h^i - q_{CO}^j)^2}\, d_{N1h}} +$$

$$\frac{(1 - F_A - F_B)(q_h^i - q_{CO}^j)\sum_{q=x,y,z}(q_h^i - q_{CO}^j)(q_h^i - q_{N1}^i)}{\left(\sqrt{\sum_{q=x,y,z}(q_h^i - q_{CO}^j)^2}\right)^3 d_{N1h}} \tag{8}$$

$$\text{for} \quad q = x, y, z$$

$$\frac{\partial \cos\theta}{\partial q_{CO}^j} = \frac{q_h^i - q_{N1}^i}{\sqrt{\sum_{q=x,y,z}(q_h^i - q_{CO}^j)^2}\, d_{N1h}}$$

$$- \frac{(q_h^i - q_{CO}^j)\sum_{q=x,y,z}(q_h^i - q_{CO}^j)(q_h^i - q_{N1}^i)}{\left(\sqrt{\sum_{q=x,y,z}(q_h^i - q_{CO}^j)^2}\right)^3 d_{N1h}} \quad \text{for } q = x, y, z \tag{9}$$

PRIMO Distance-dependent Spline Interpolated Potentials Fit into CHARMM explicit Dipeptide Simulations

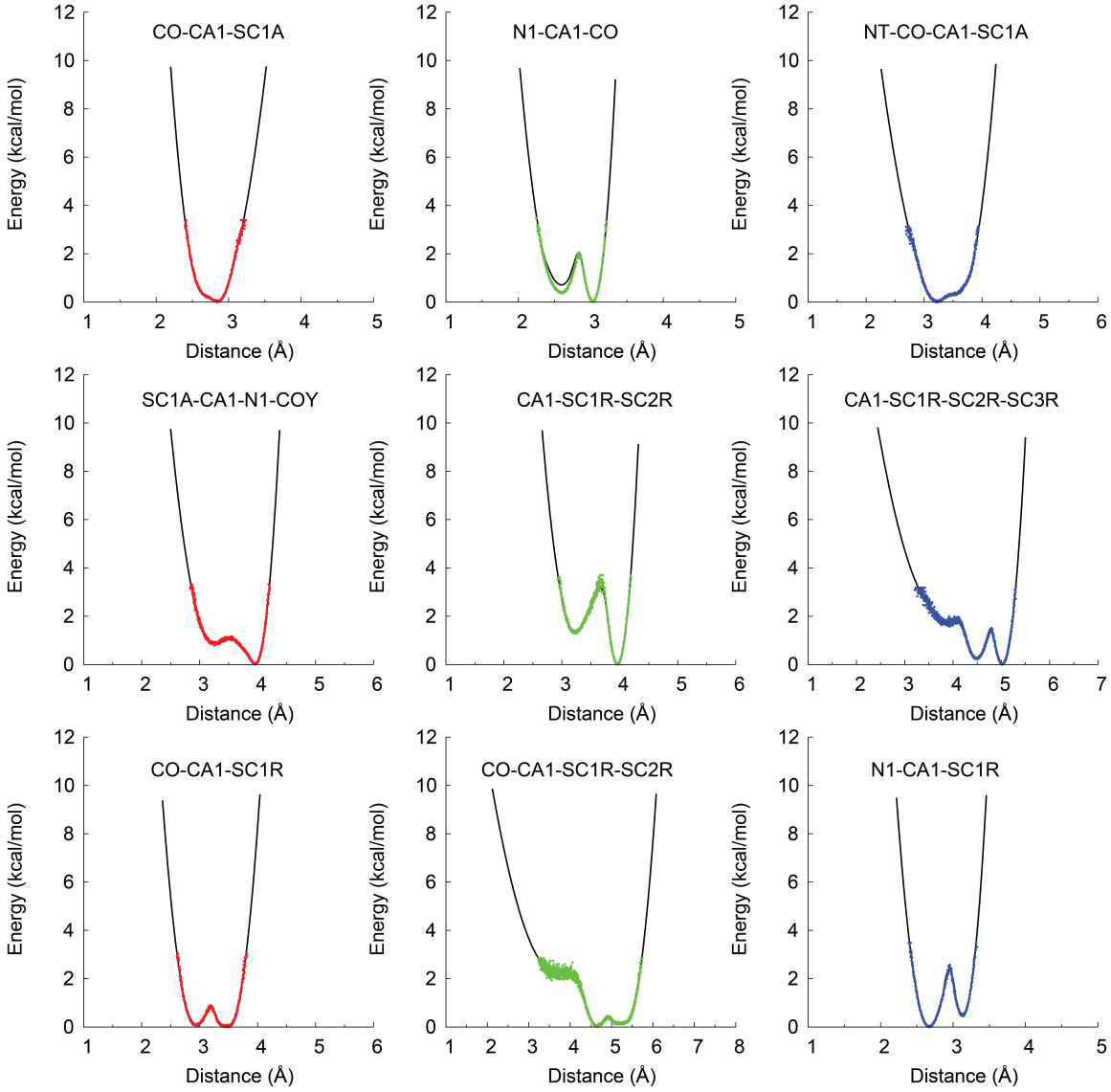

Figure S4: See page S32.

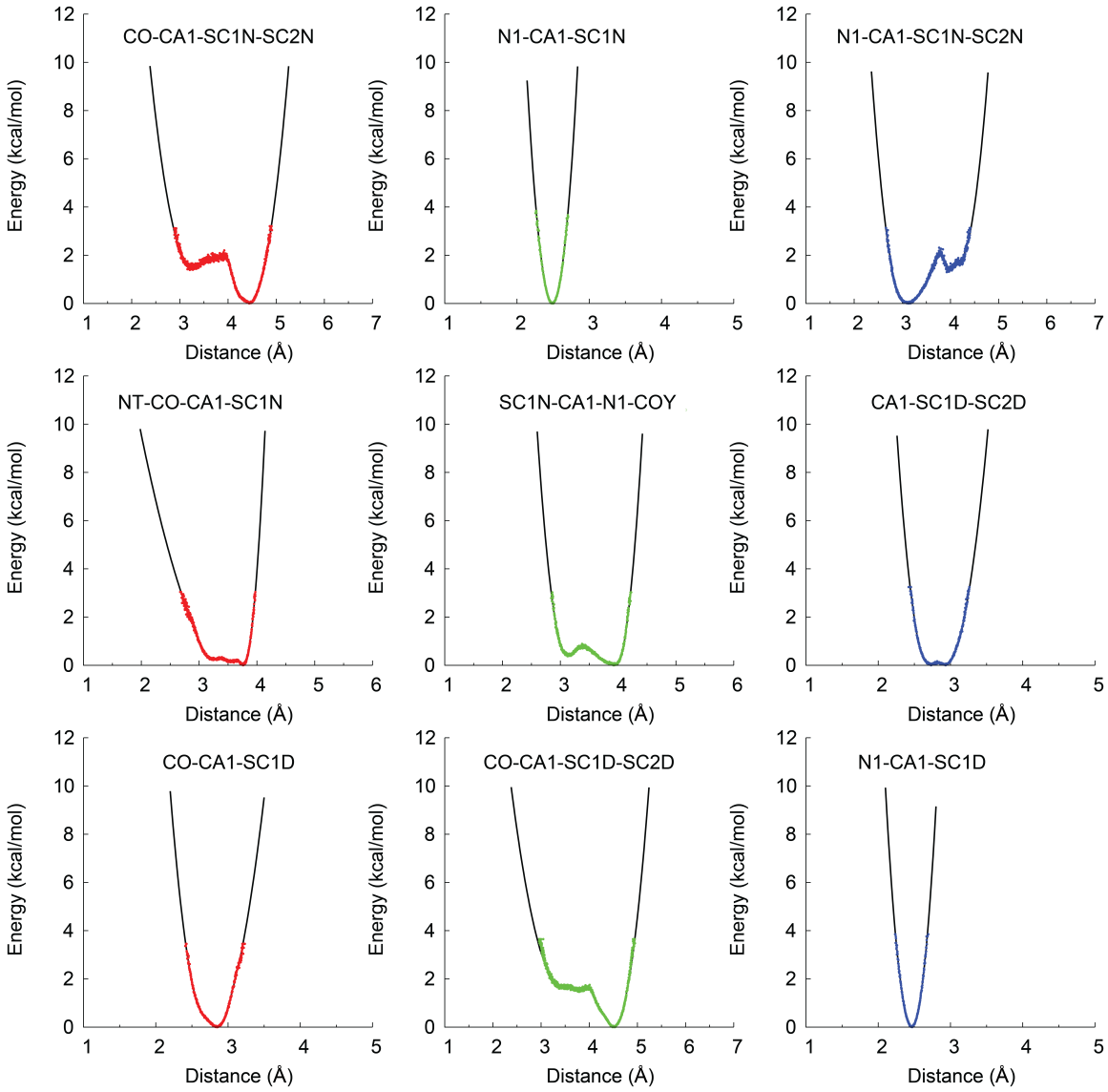

Figure S4: See page S32.

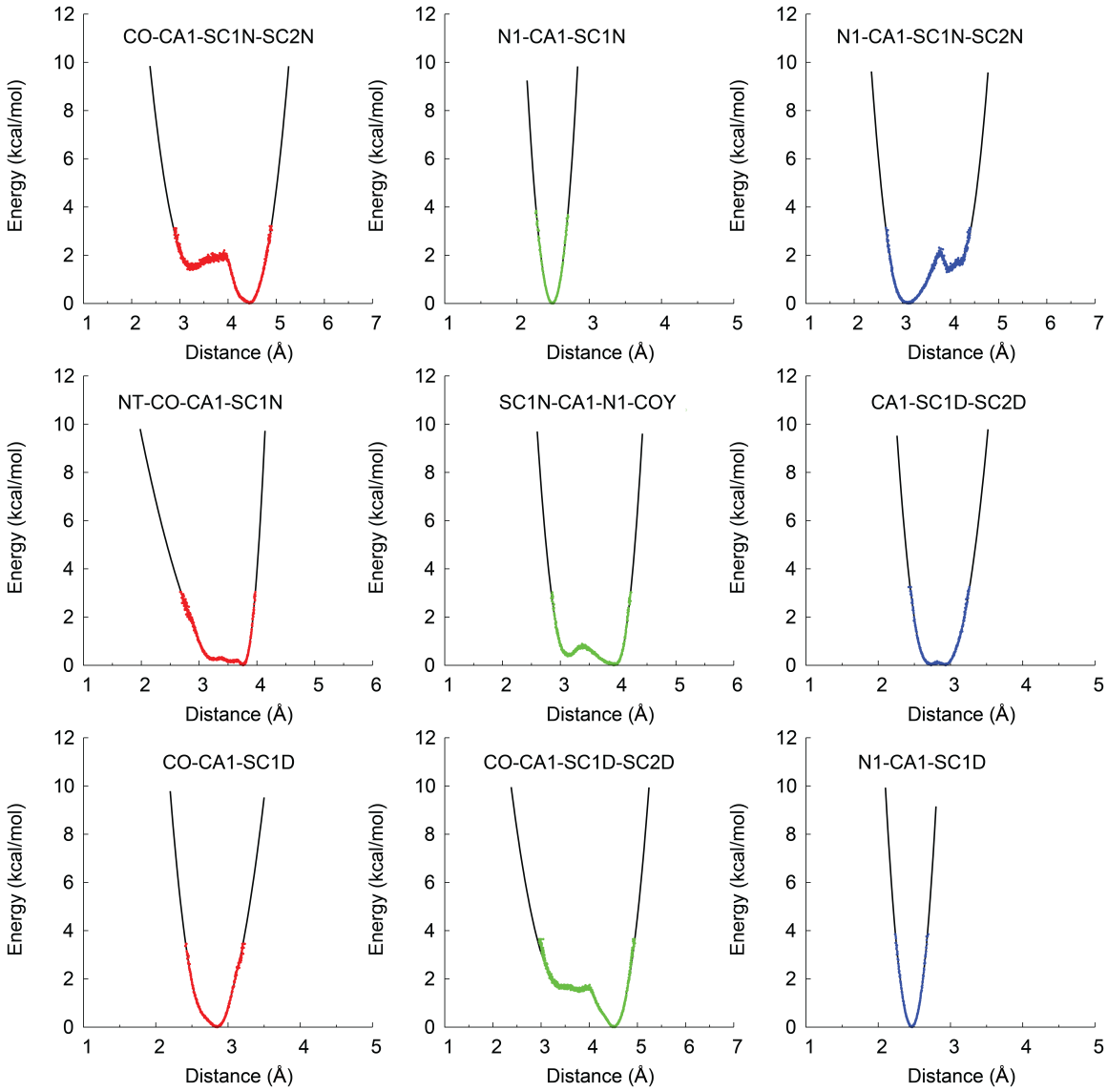

Figure S4: See page S32.

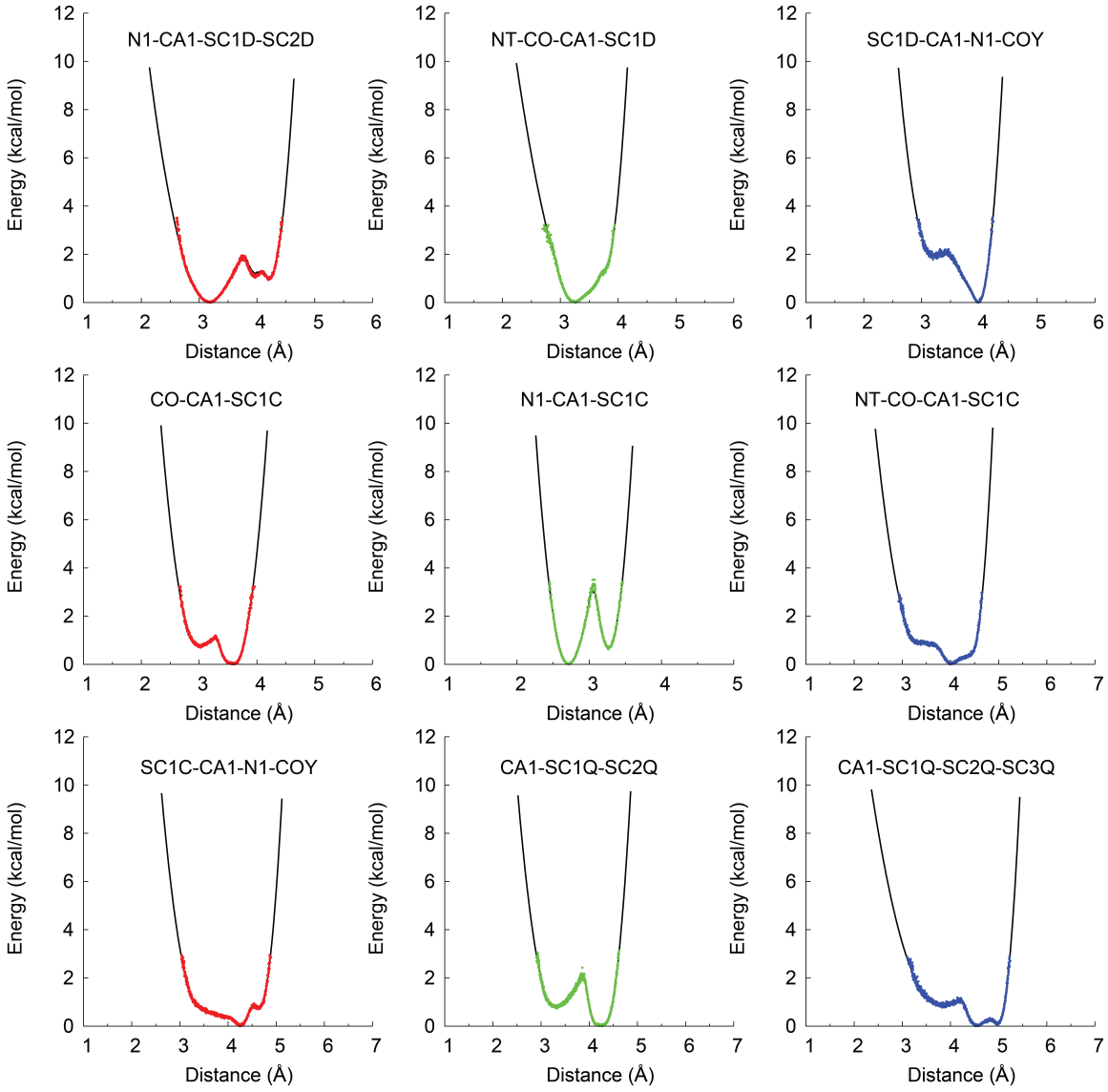
N1-CA1-SC1D-SC2D
NT-CO-CA1-SC1D
SC1D-CA1-N1-COY
CO-CA1-SC1C
N1-CA1-SC1C
NT-CO-CA1-SC1C
SC1C-CA1-N1-COY
CA1-SC1Q-SC2Q
CA1-SC1Q-SC2Q-SC3Q
Energy (kcal/mol)
Distance (Å)

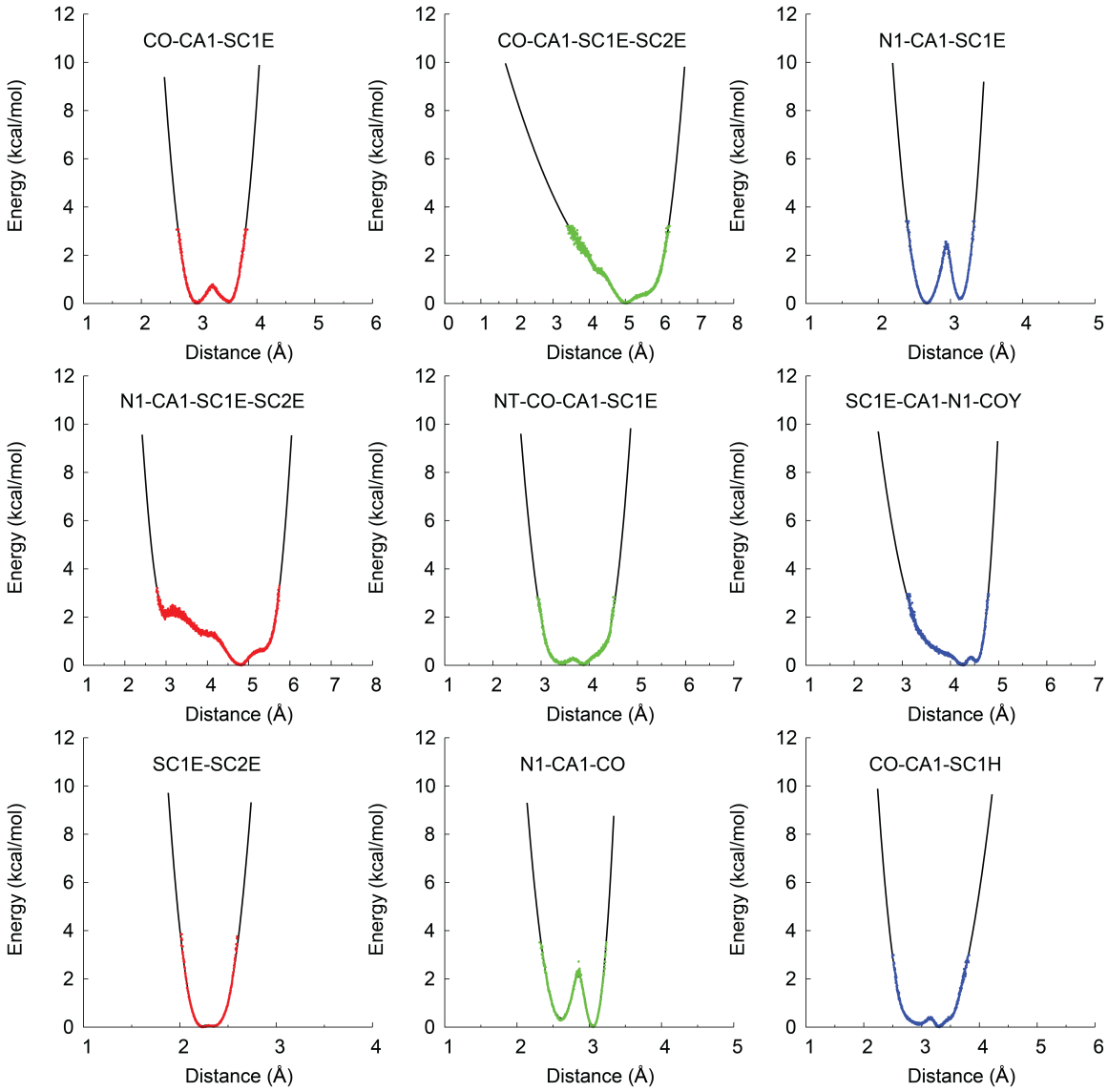

Figure S4: See page S32.

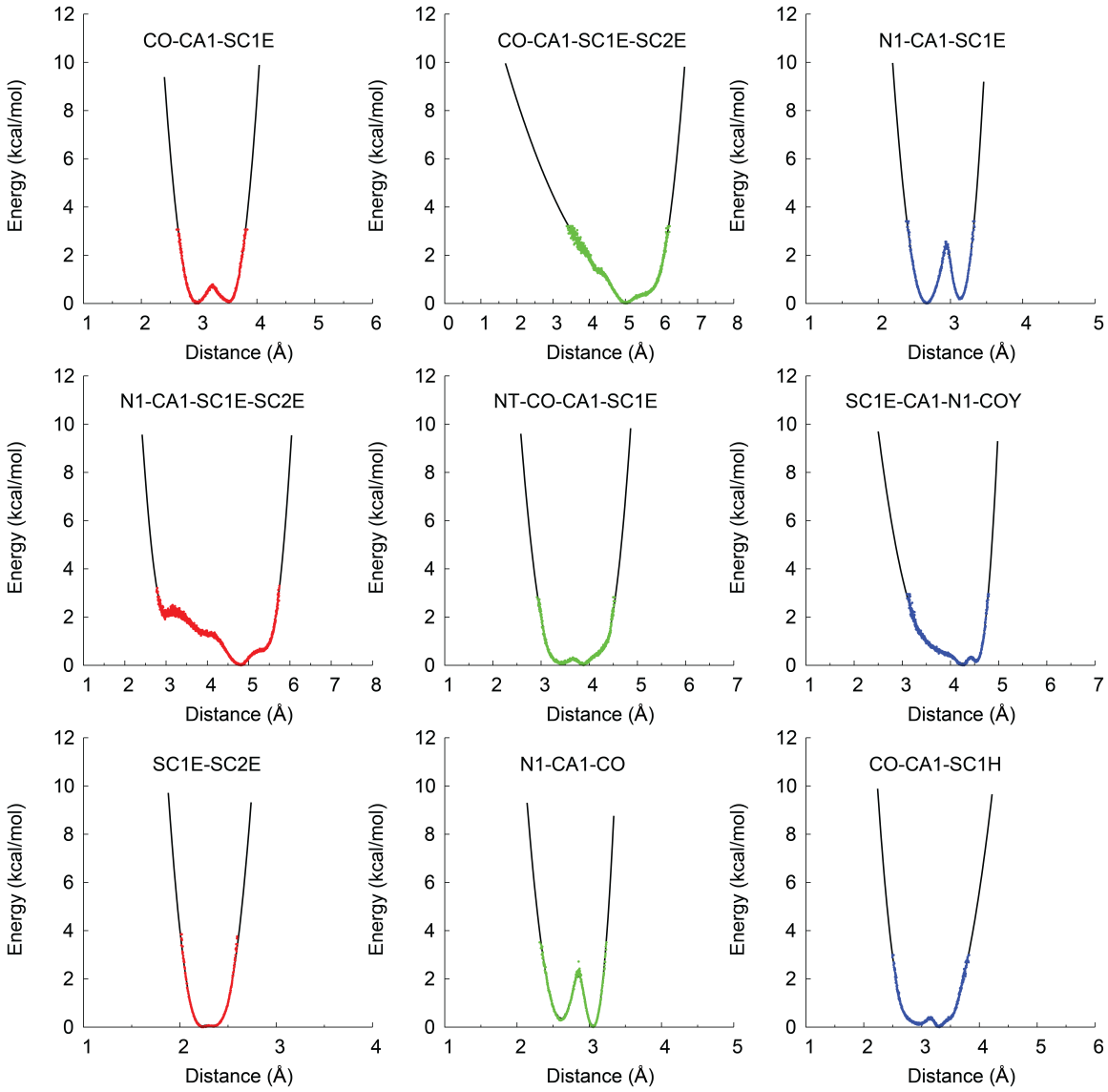

Figure S4: See page S32.

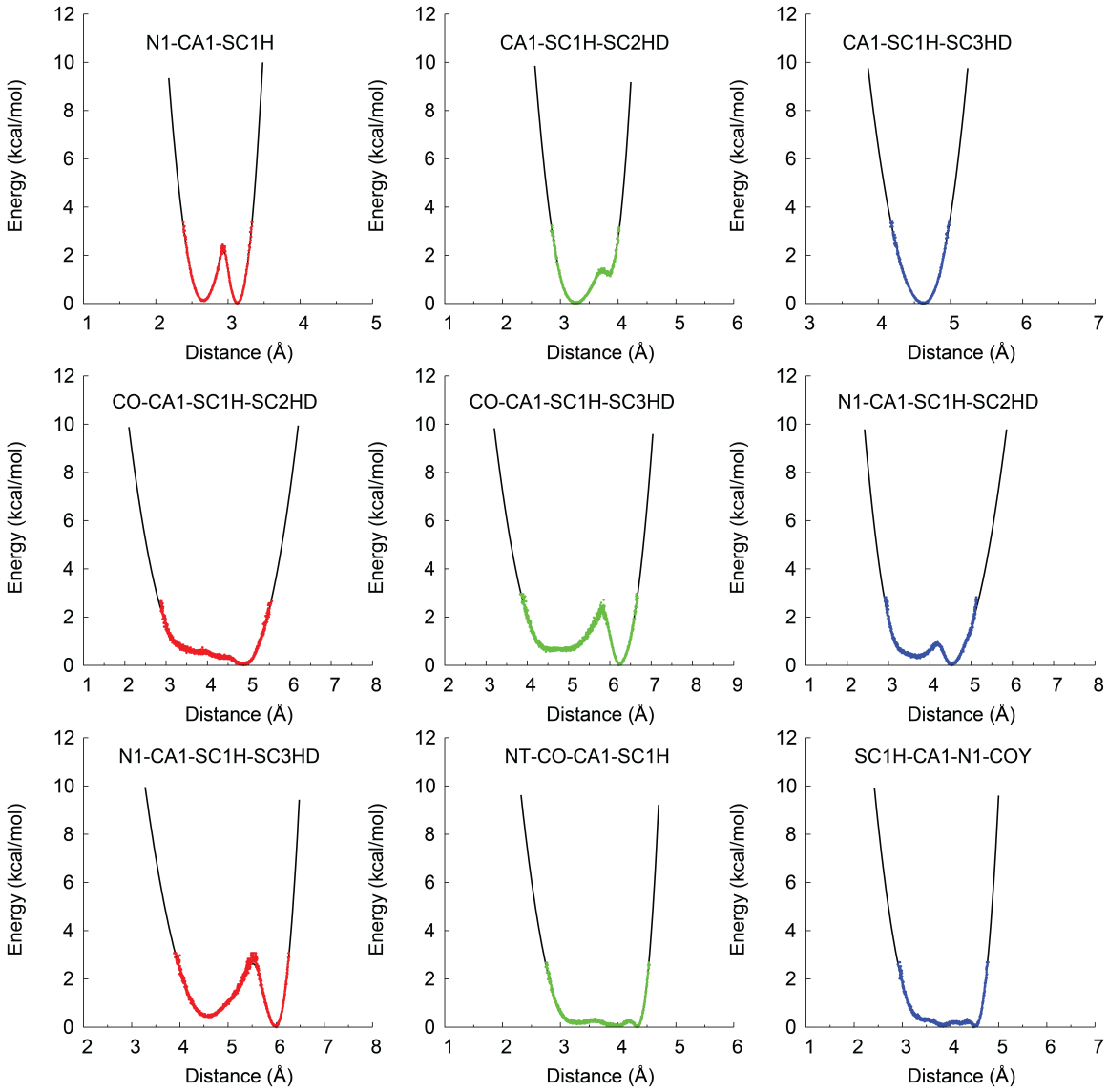

Figure S4: See page S32.

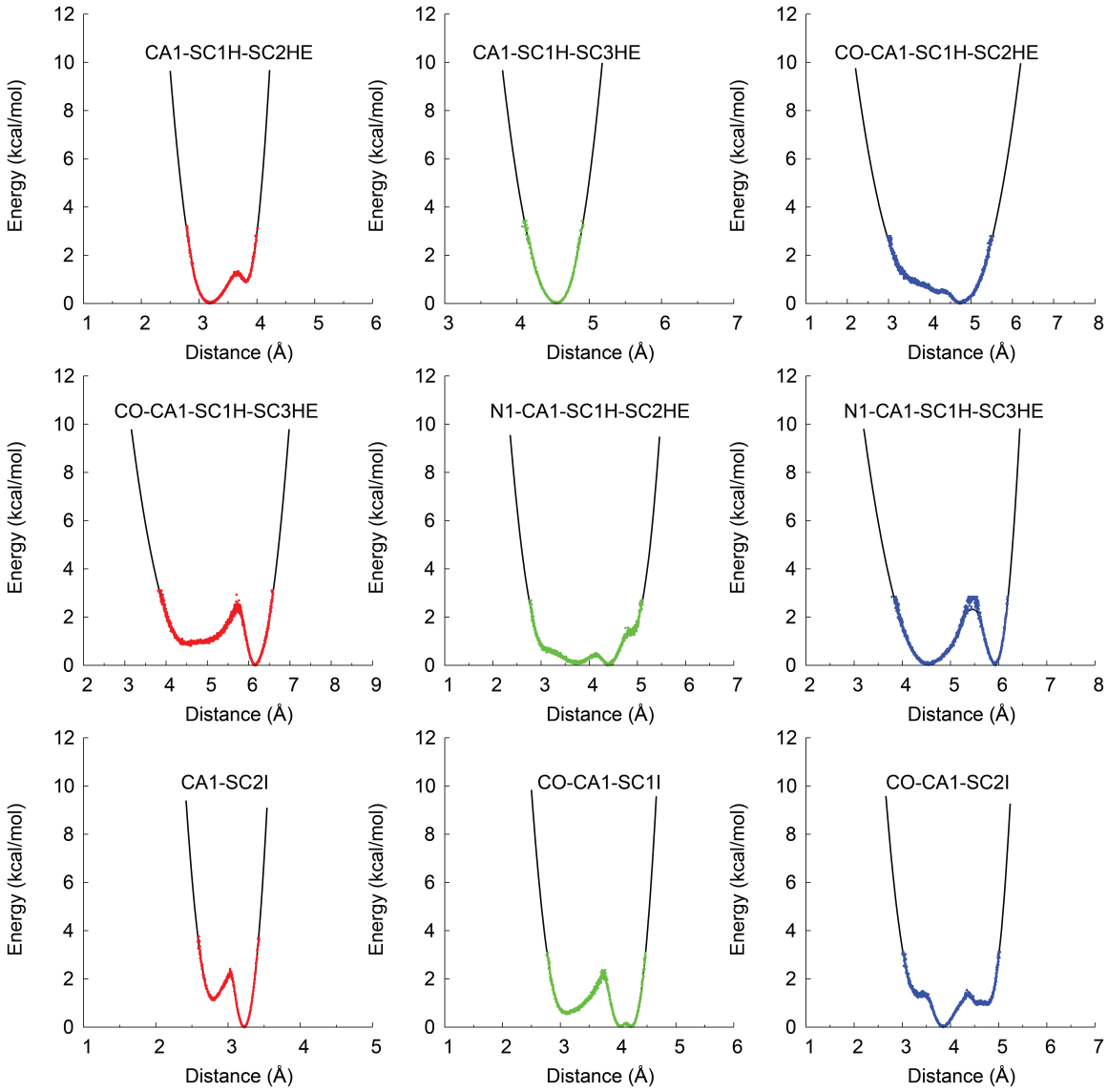

Figure S4: See page S32.

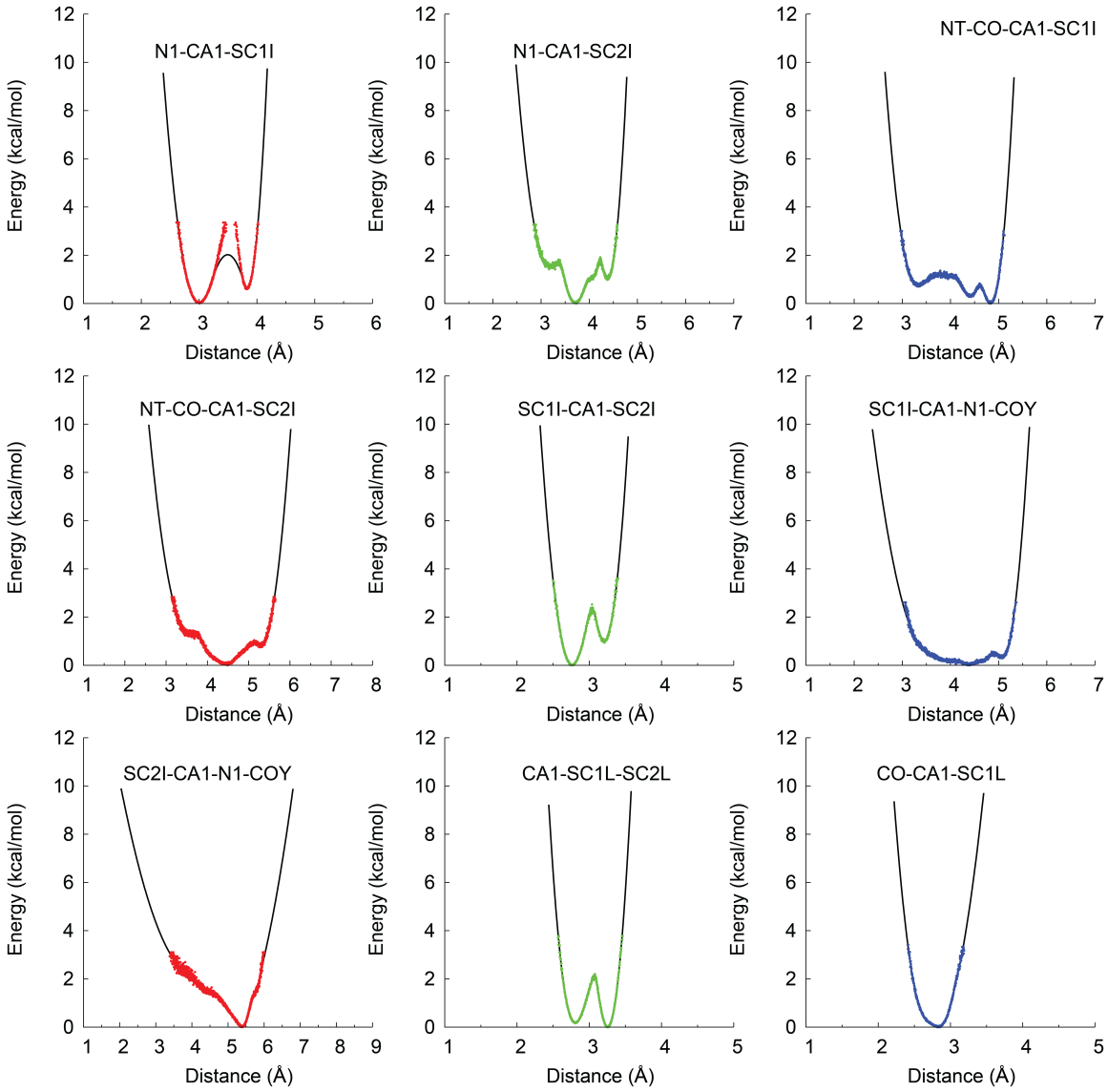

Figure S4: See page S32.

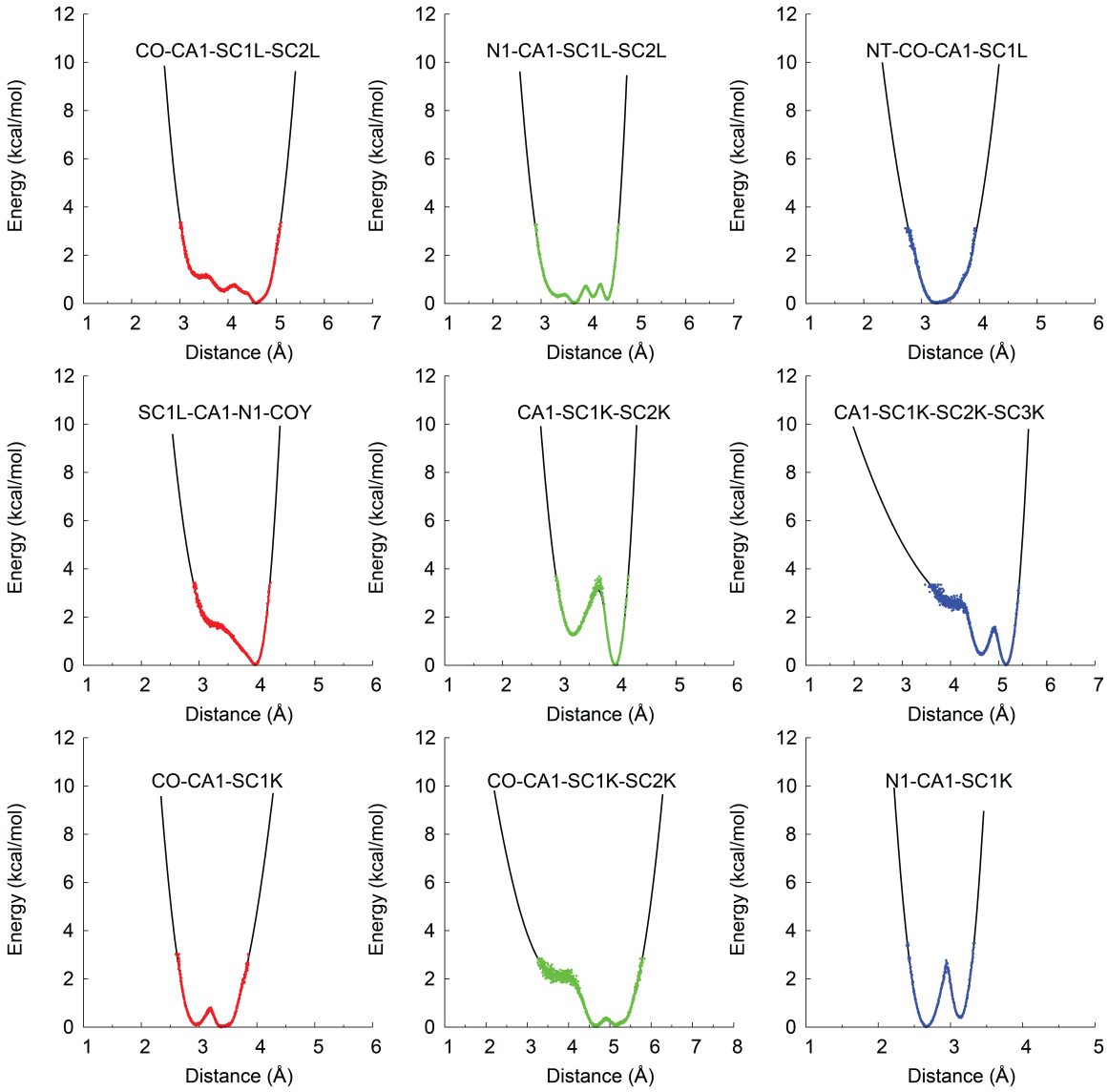

Figure S4: See page S32.

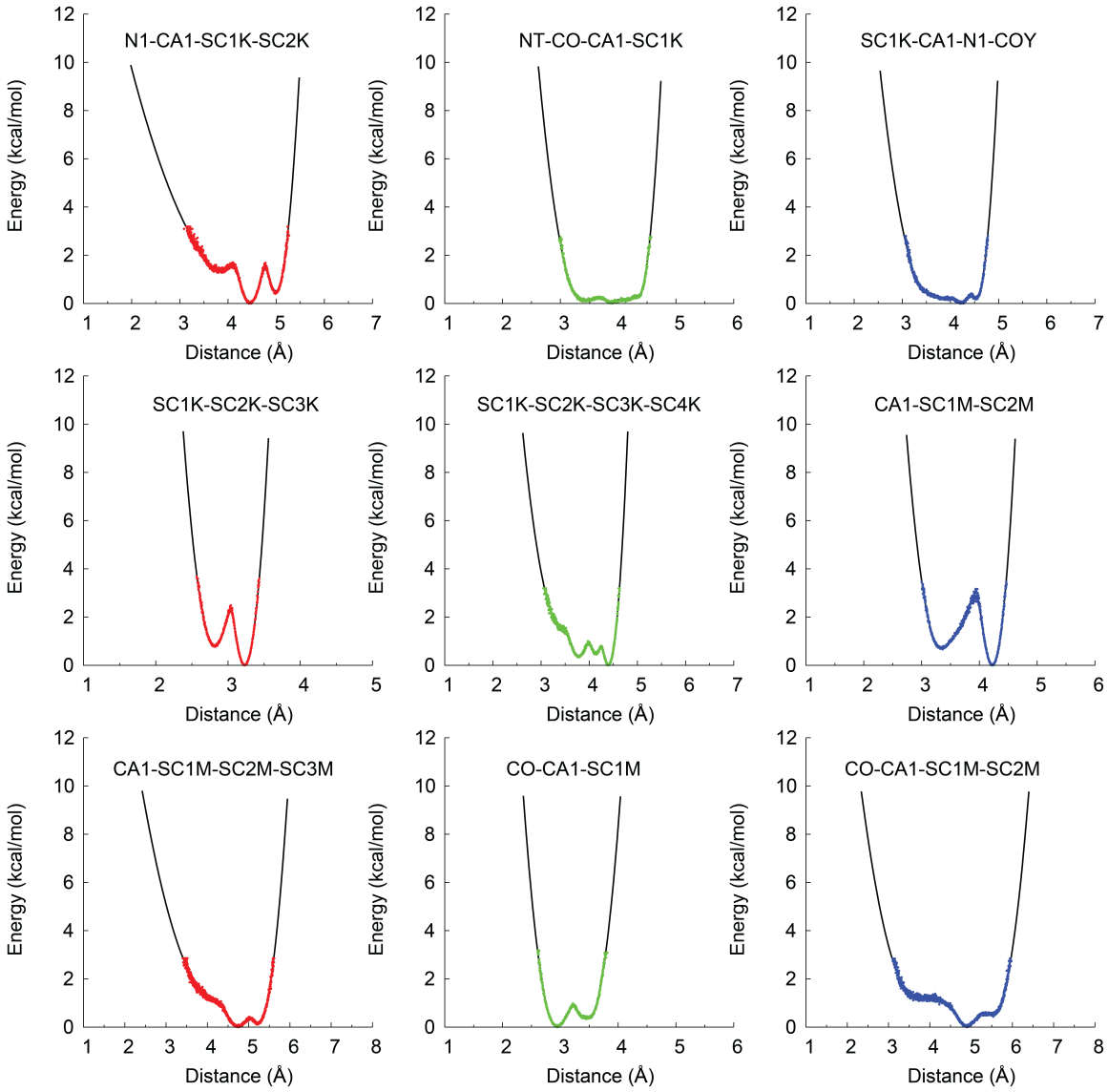

Figure S4: See page S32.

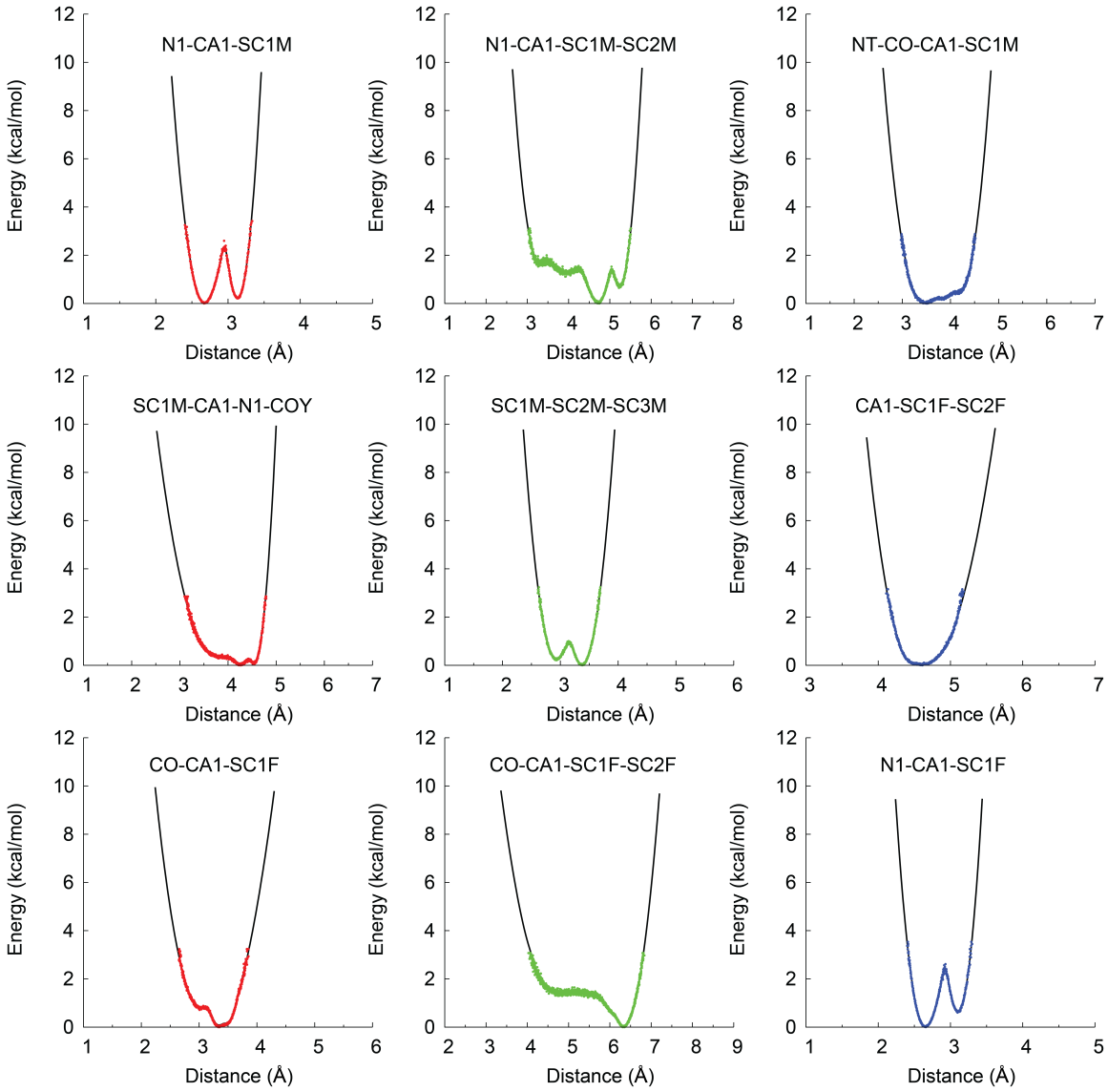

Figure S4: See page S32.

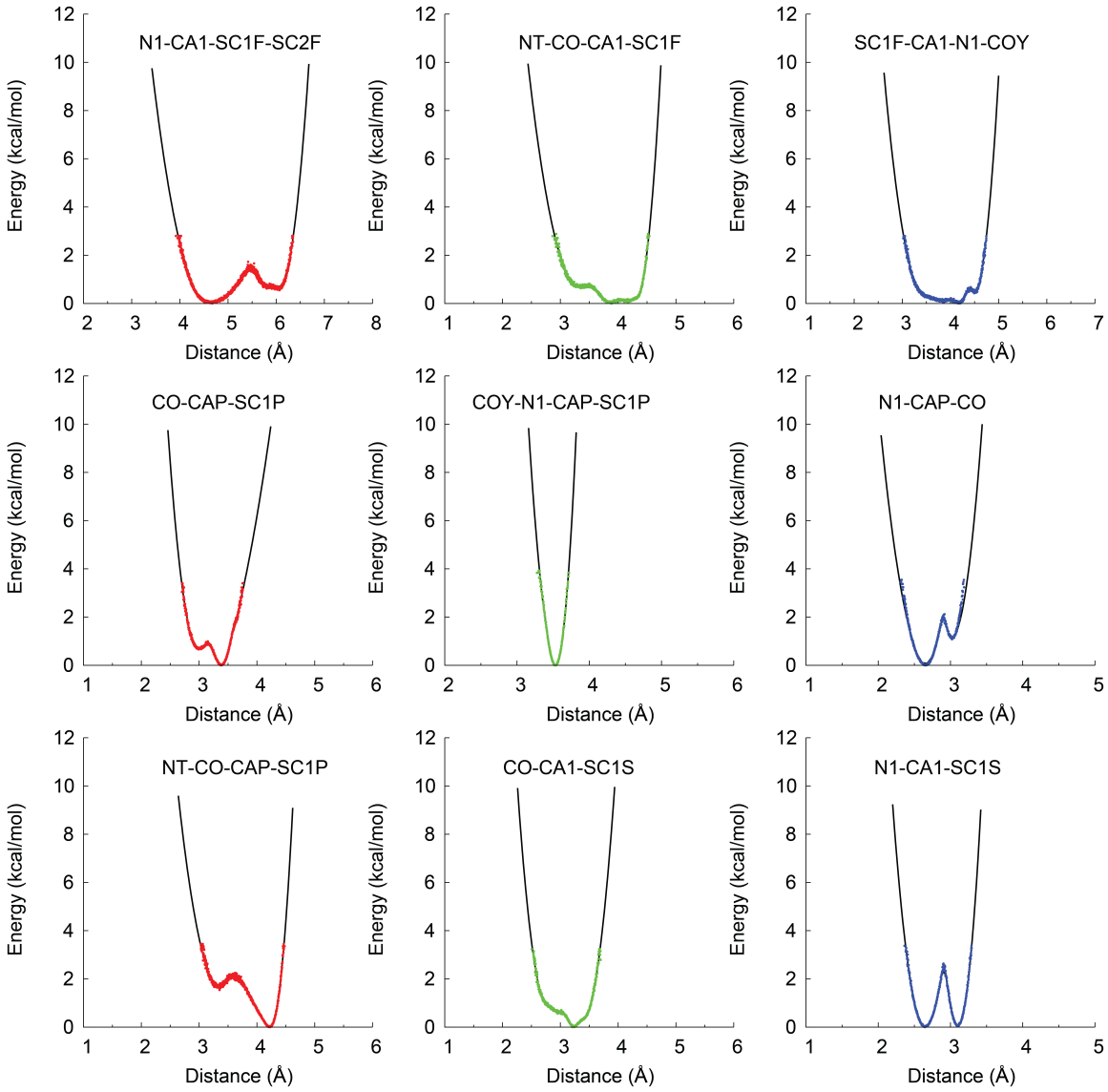

Figure S4: See page S32.

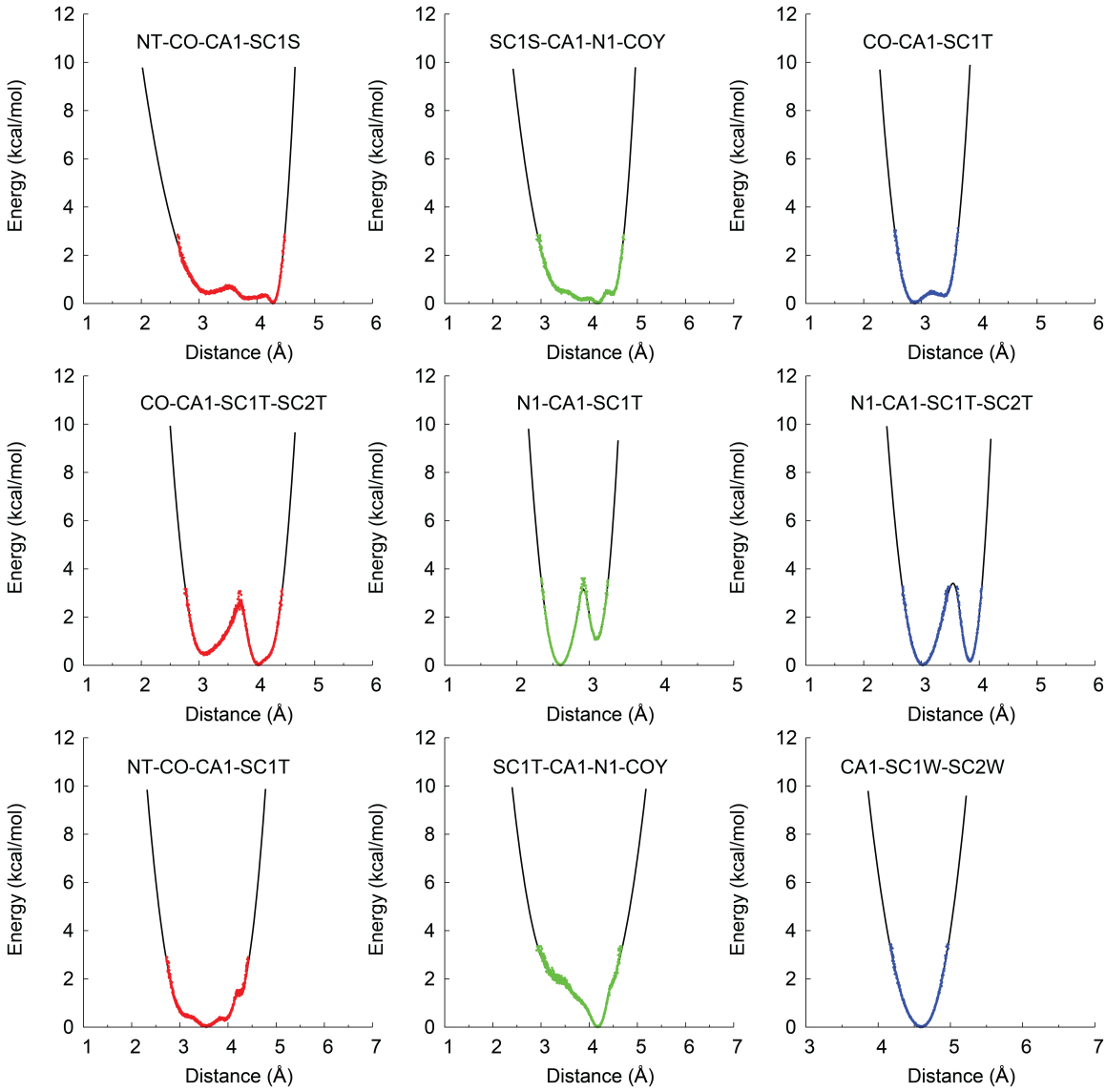

Figure S4: See page S32.

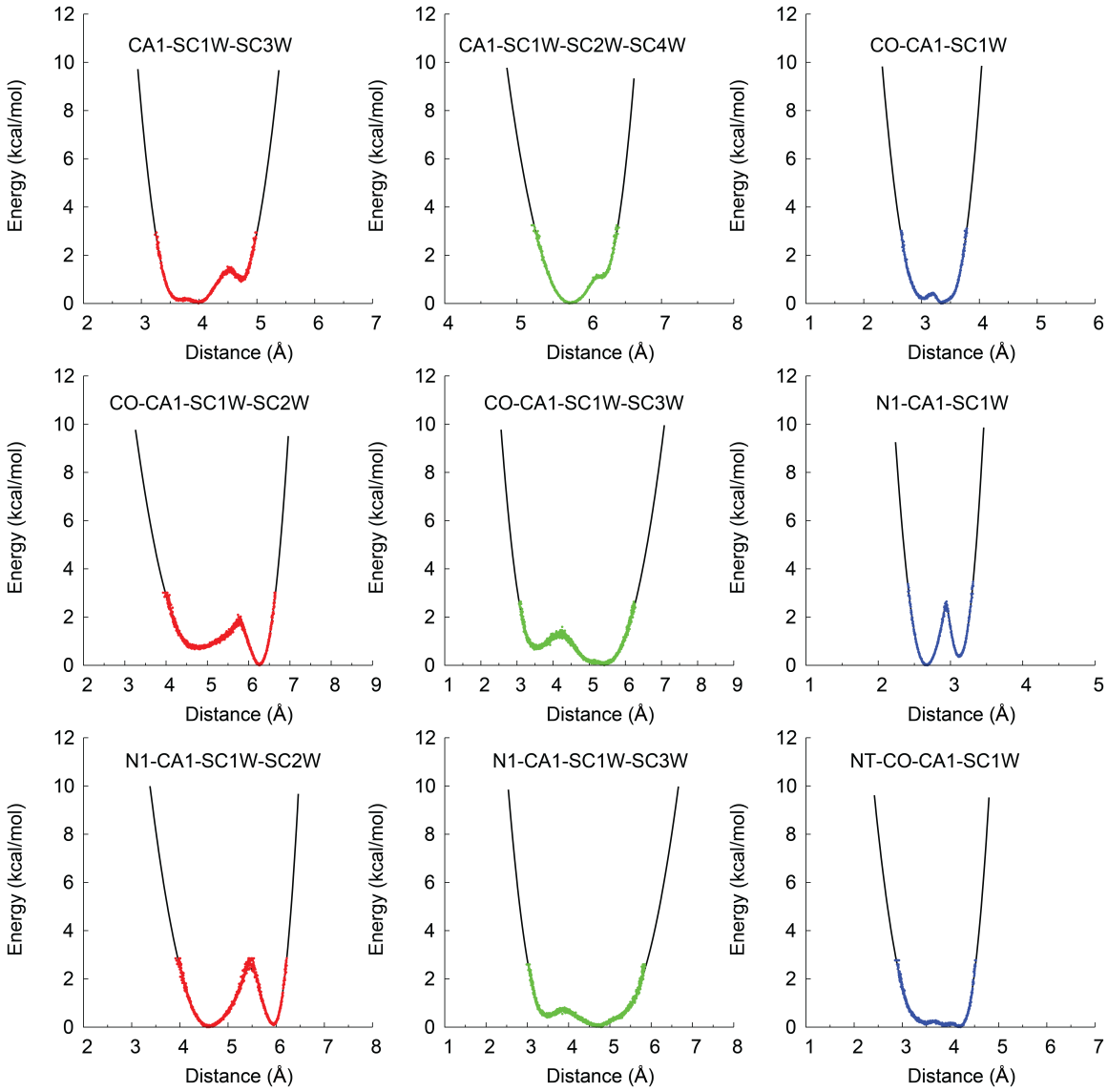

Figure S4: See page S32.

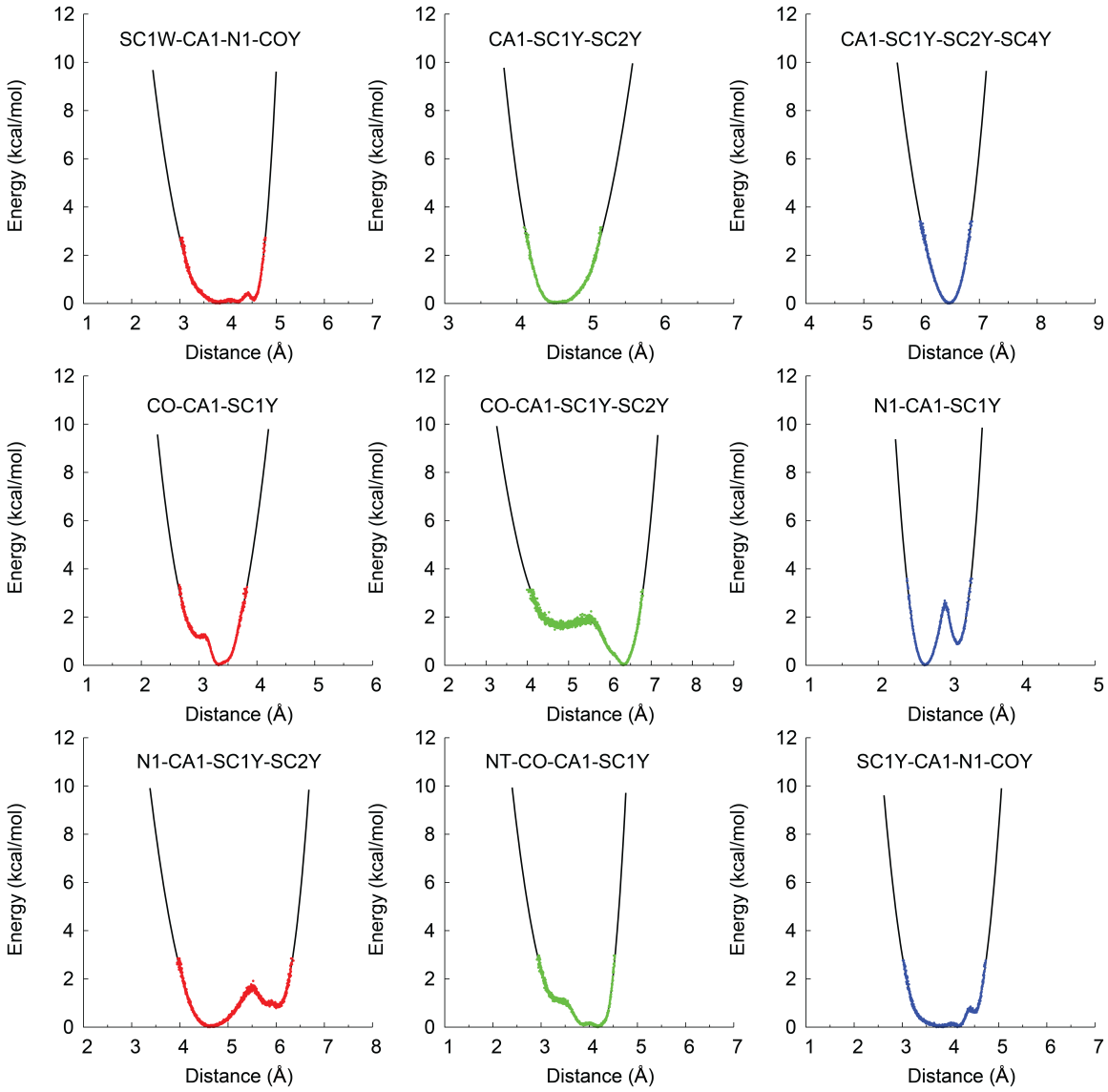

Figure S4: See page S32.

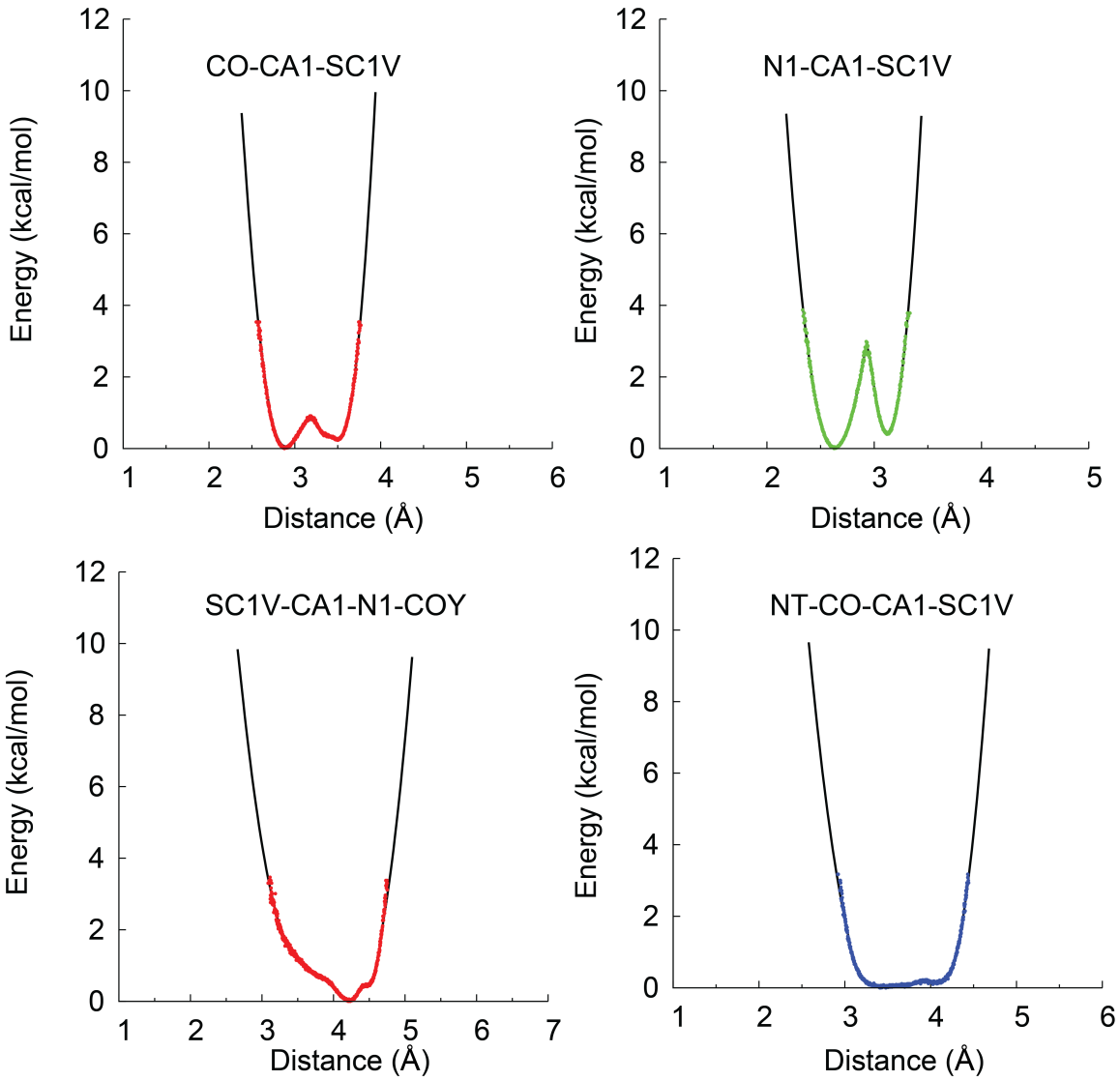

Figure S4: PRIMO distance spline potentials for bond, angle, and torsion terms for all naturally occuring amino acids. The spline (black) is fitted into the sampling (red) from CHARMM dipeptide simulations.

Comparison of Sampling of Internal Degrees of Freedom in AXA and CHARMM Explicit Dipeptide Simulations

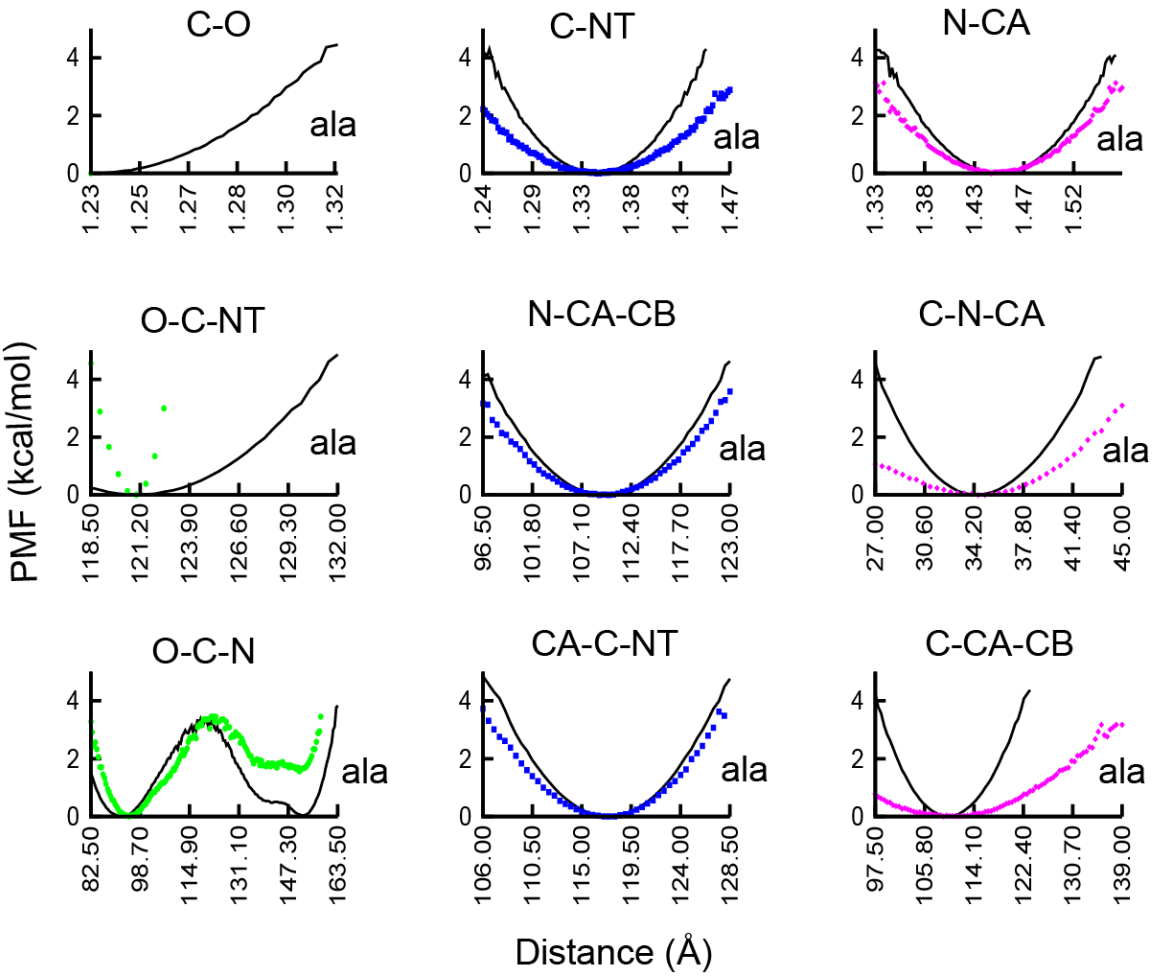

Figure S5: See page S75.

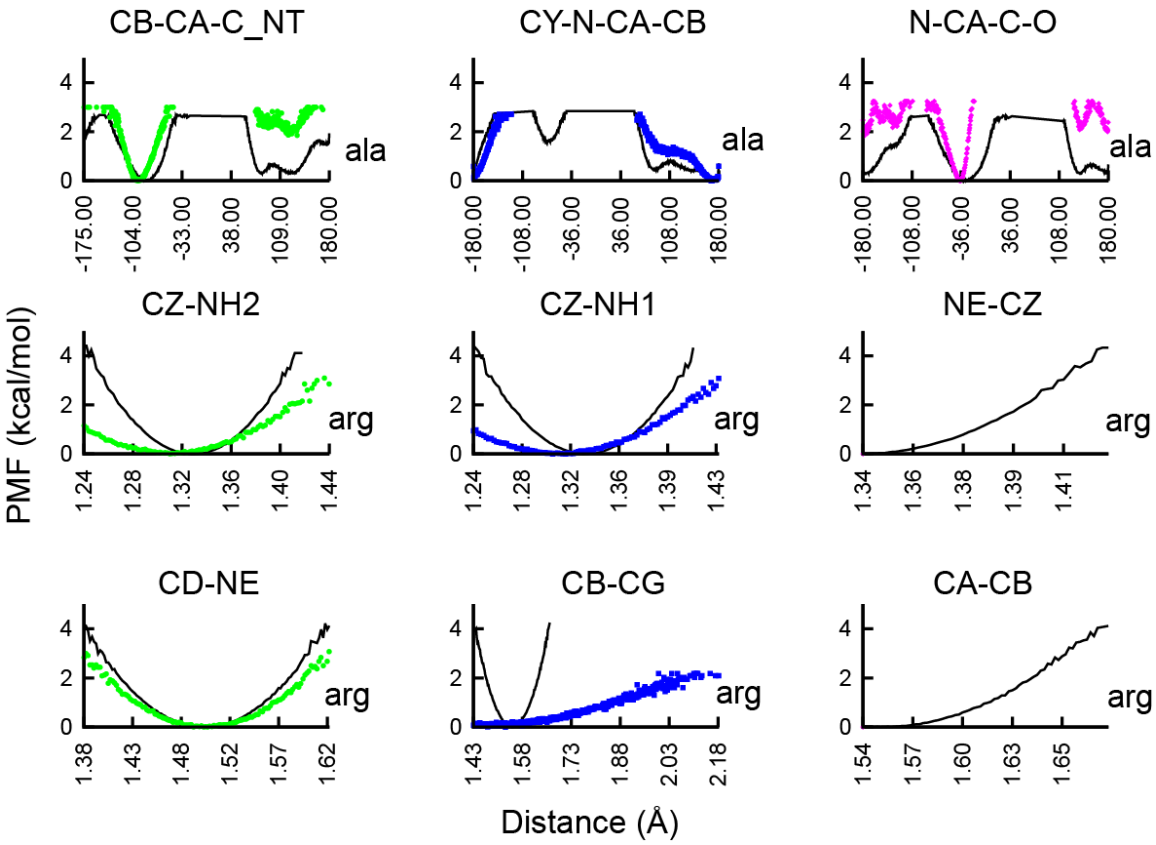

Figure S5: See page S75.

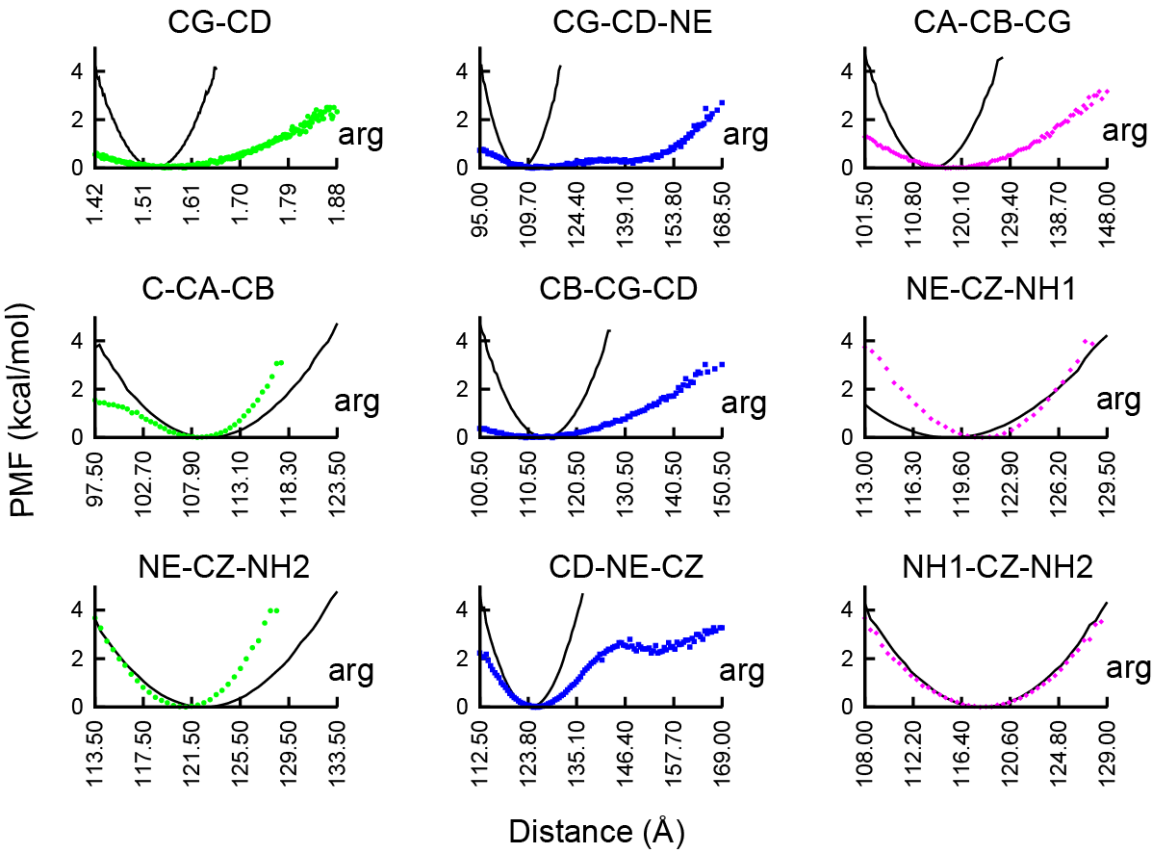

Figure S5: See page S75.

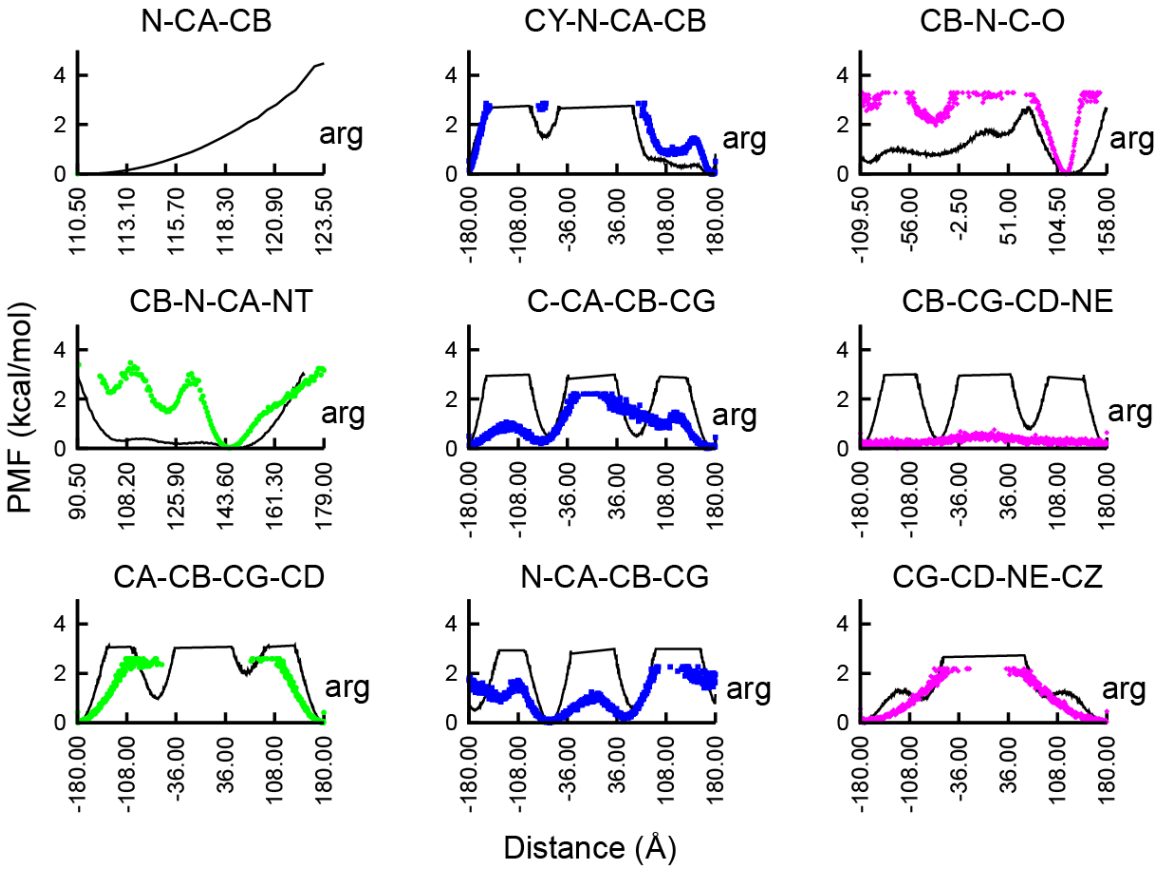

Figure S5: See page S75.

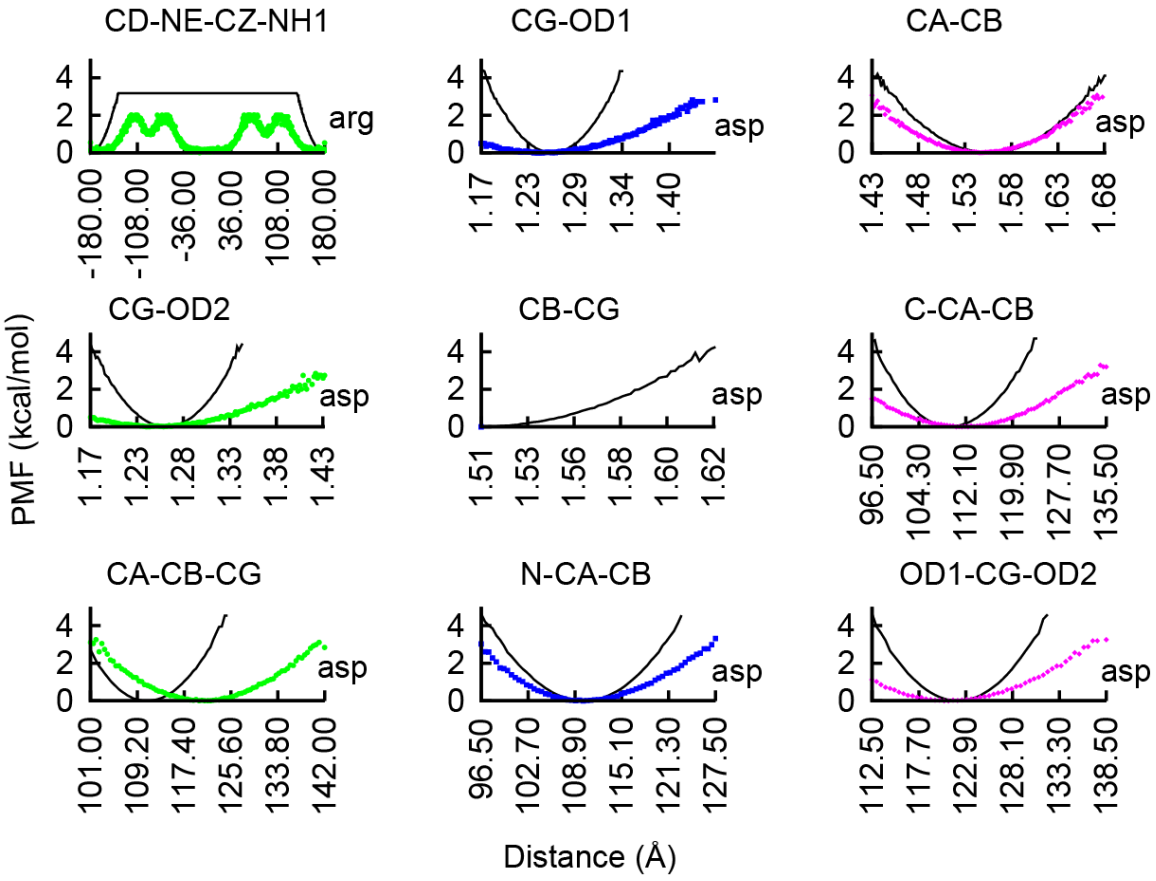

Figure S5: See page S75.

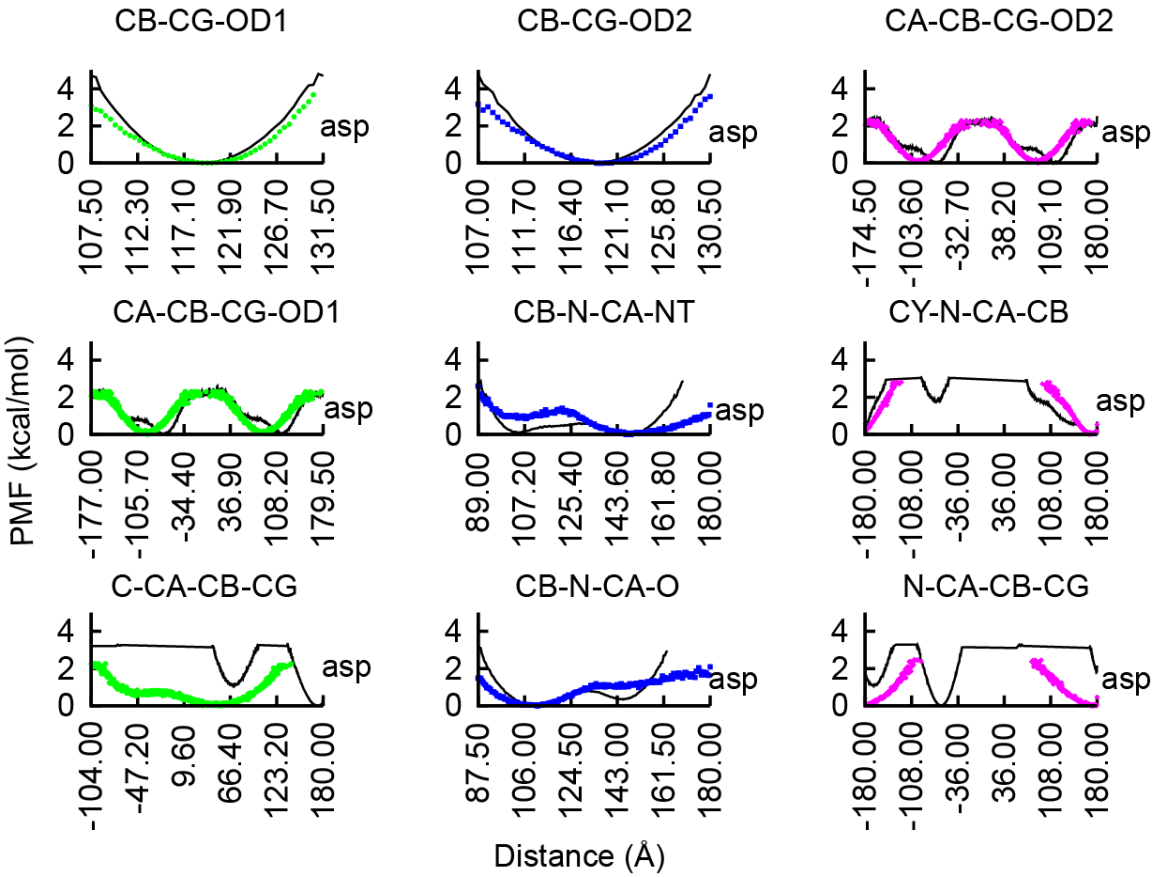

Figure S5: See page S75.

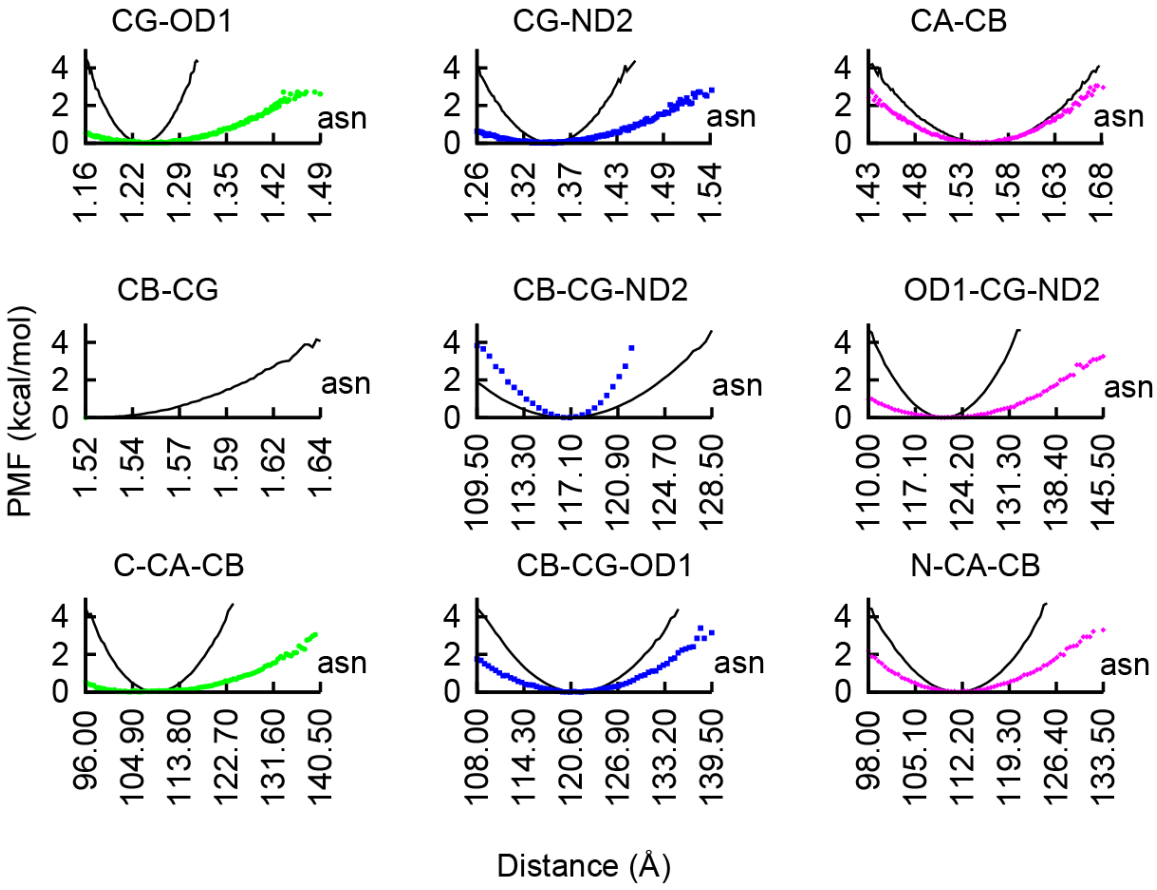

Figure S5: See page S75.

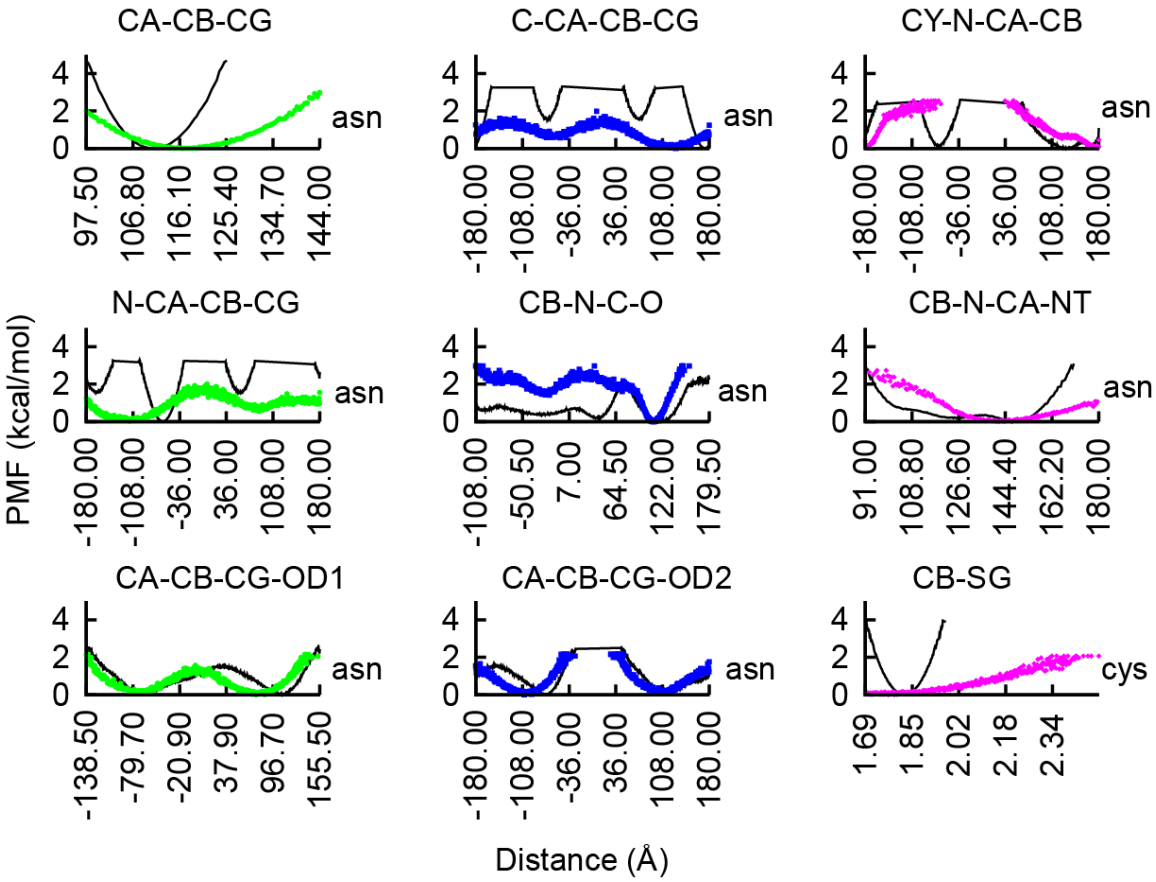

Figure S5: See page S75.

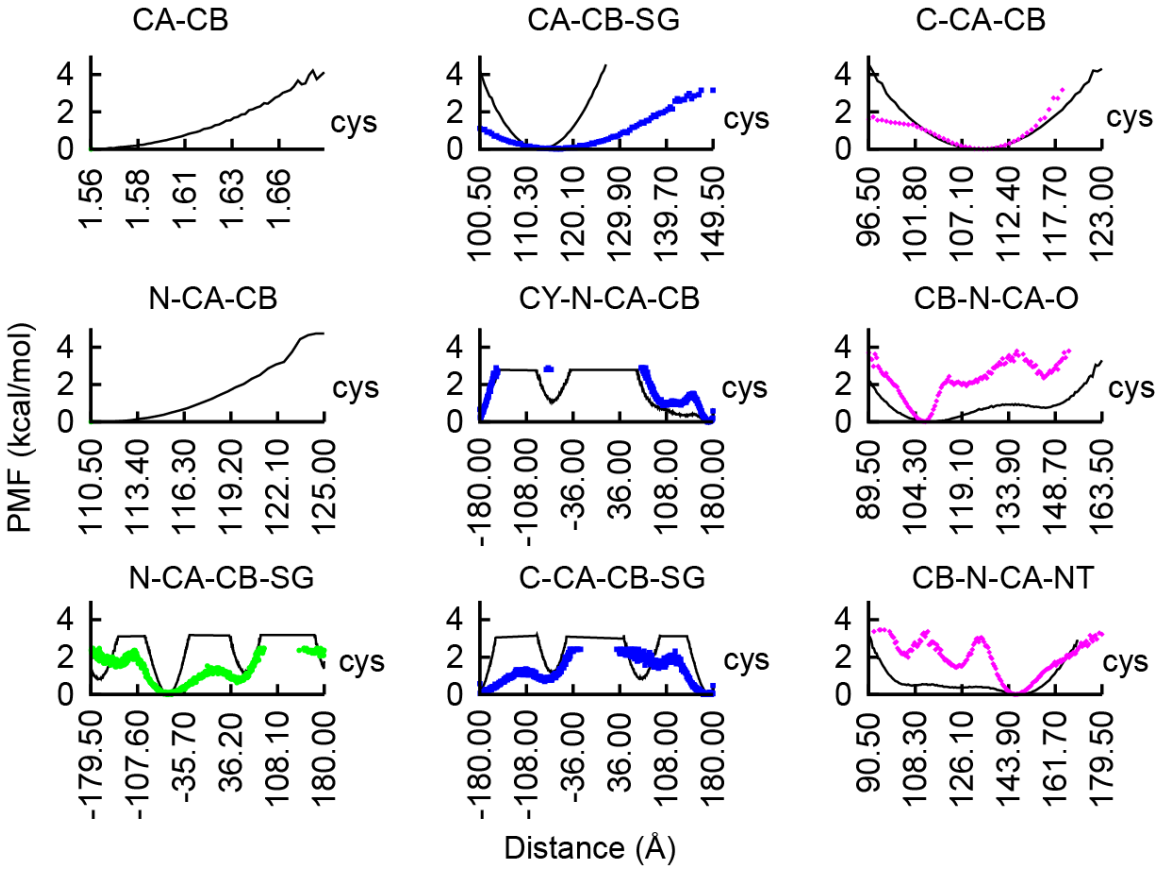

Figure S5: See page S75.

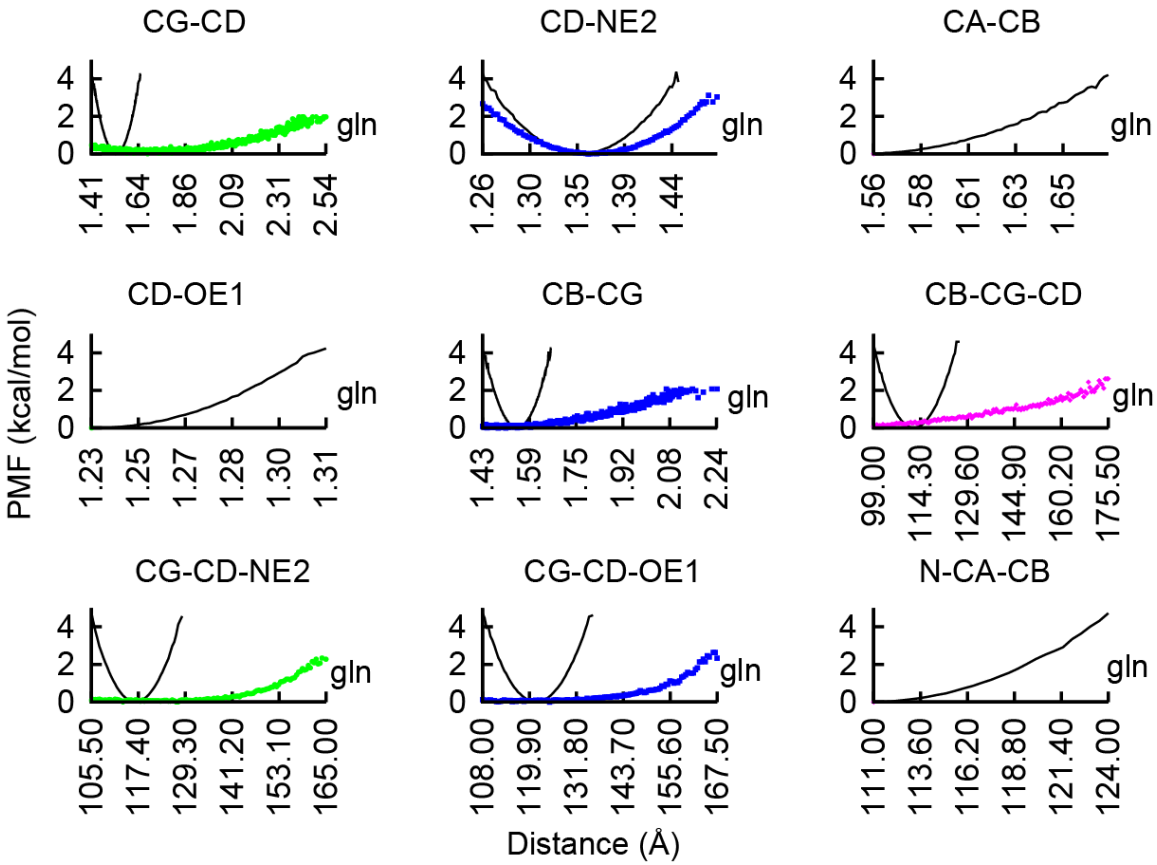

Figure S5: See page S75.

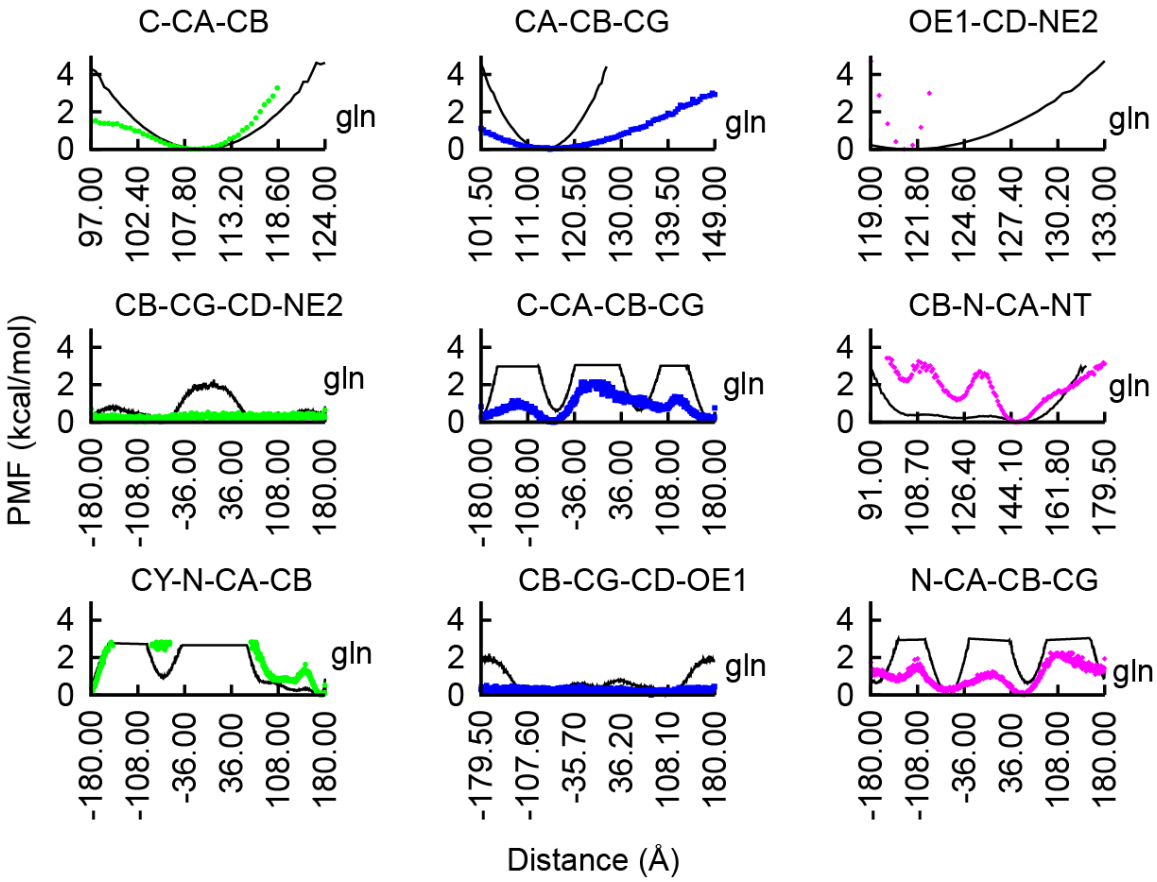

Figure S5: See page S75.

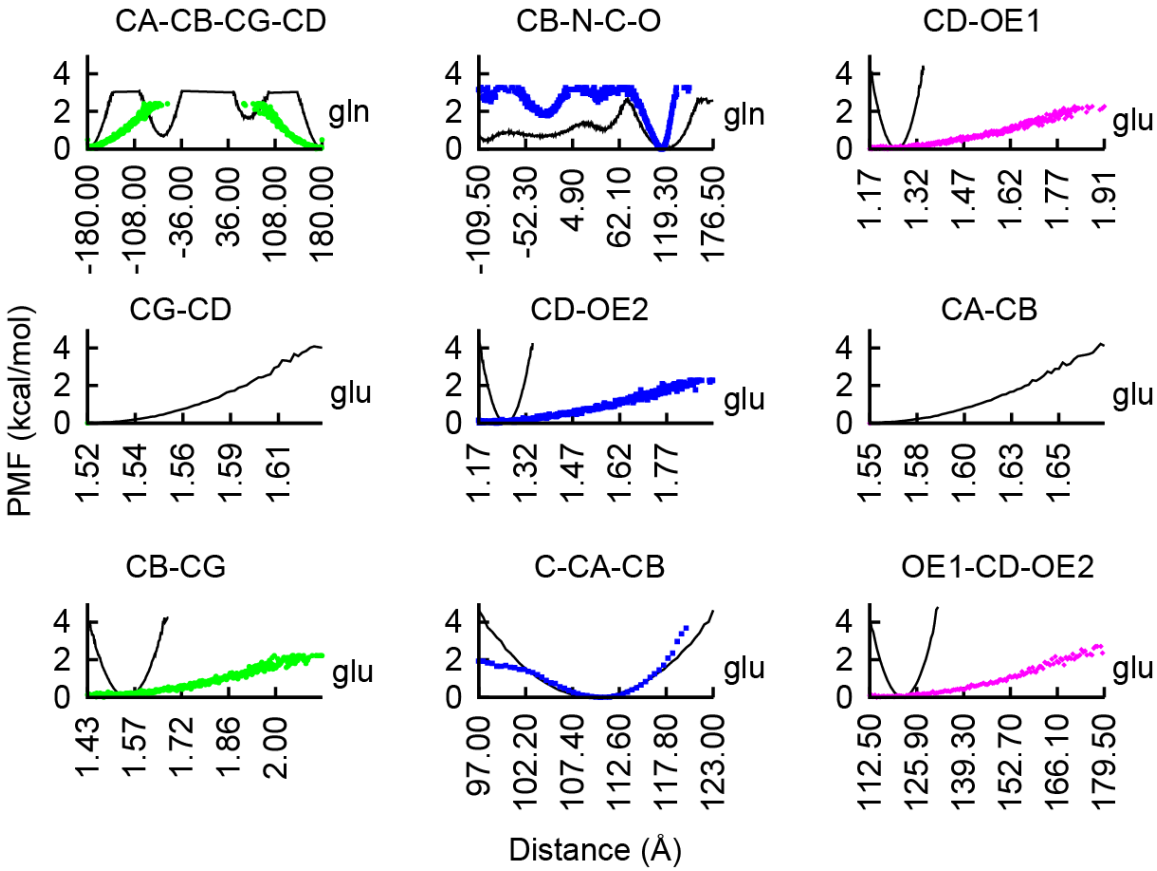

Figure S5: See page S75.

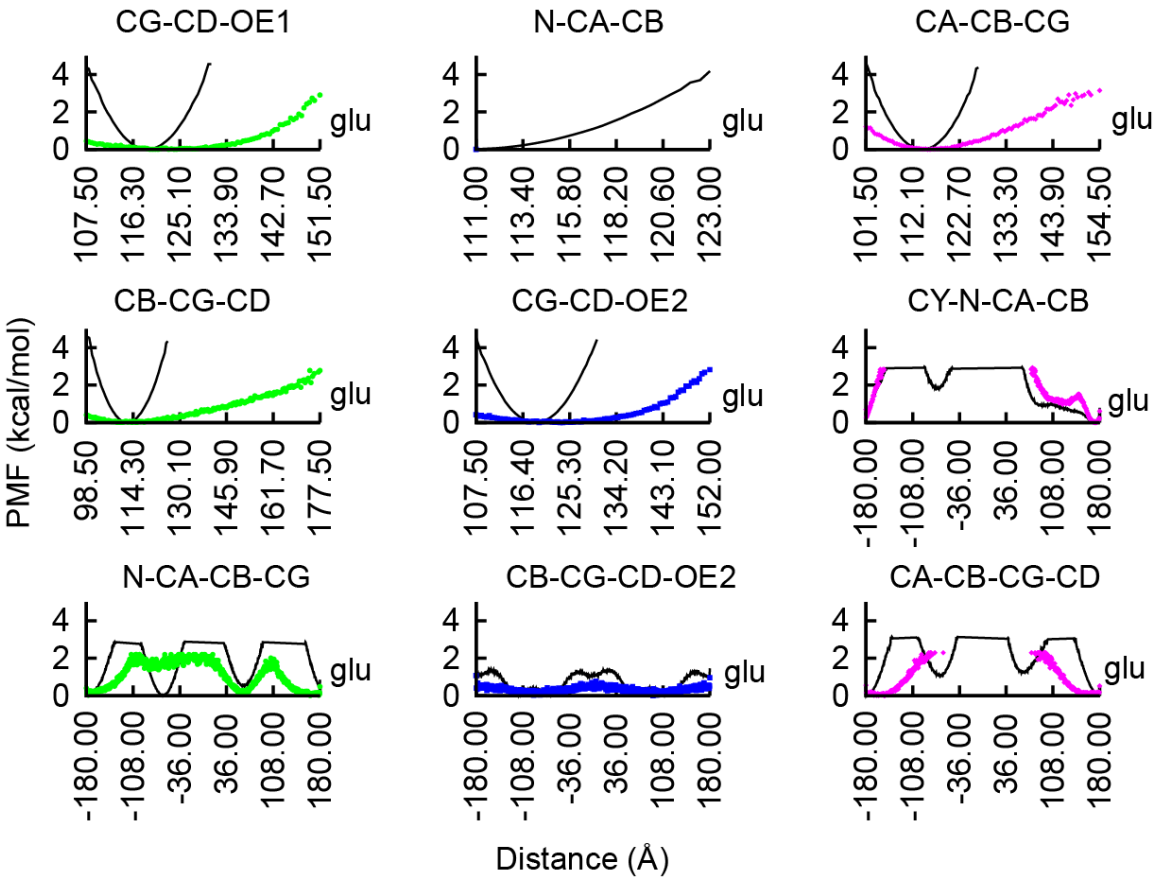

Figure S5: See page S75.

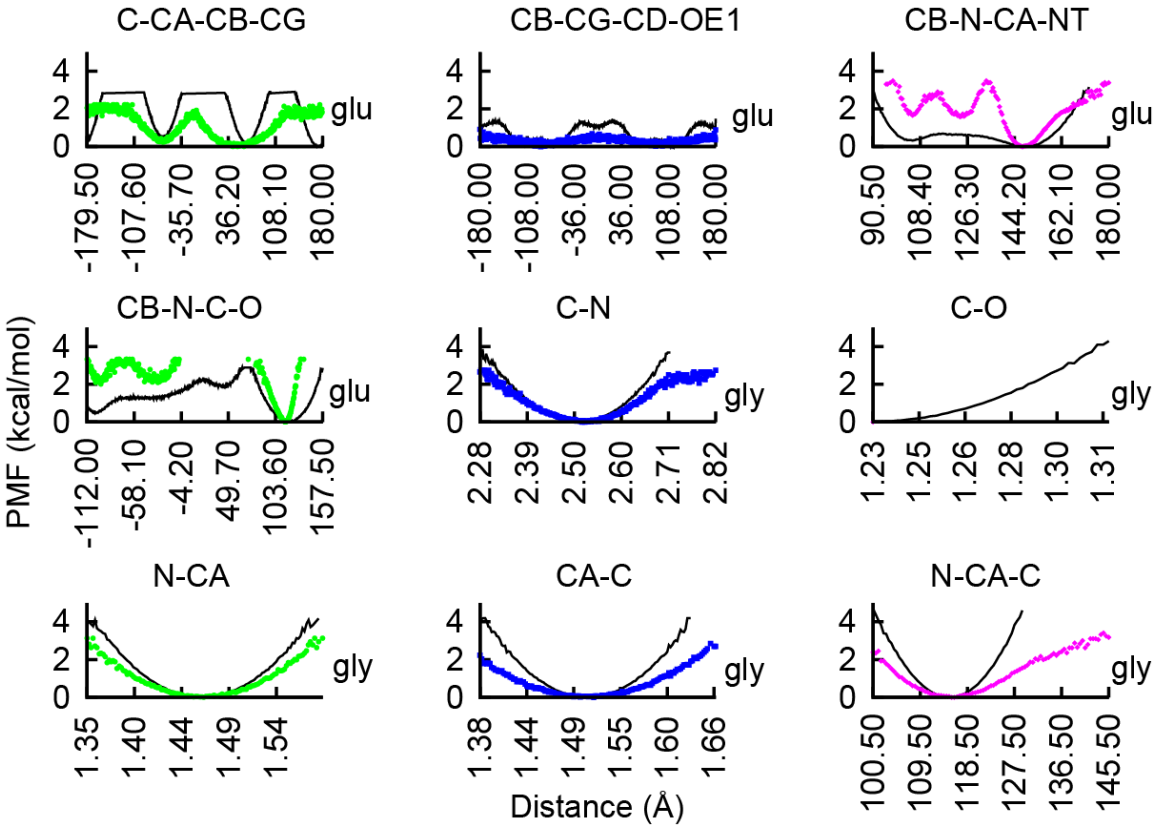

Figure S5: See page S75.

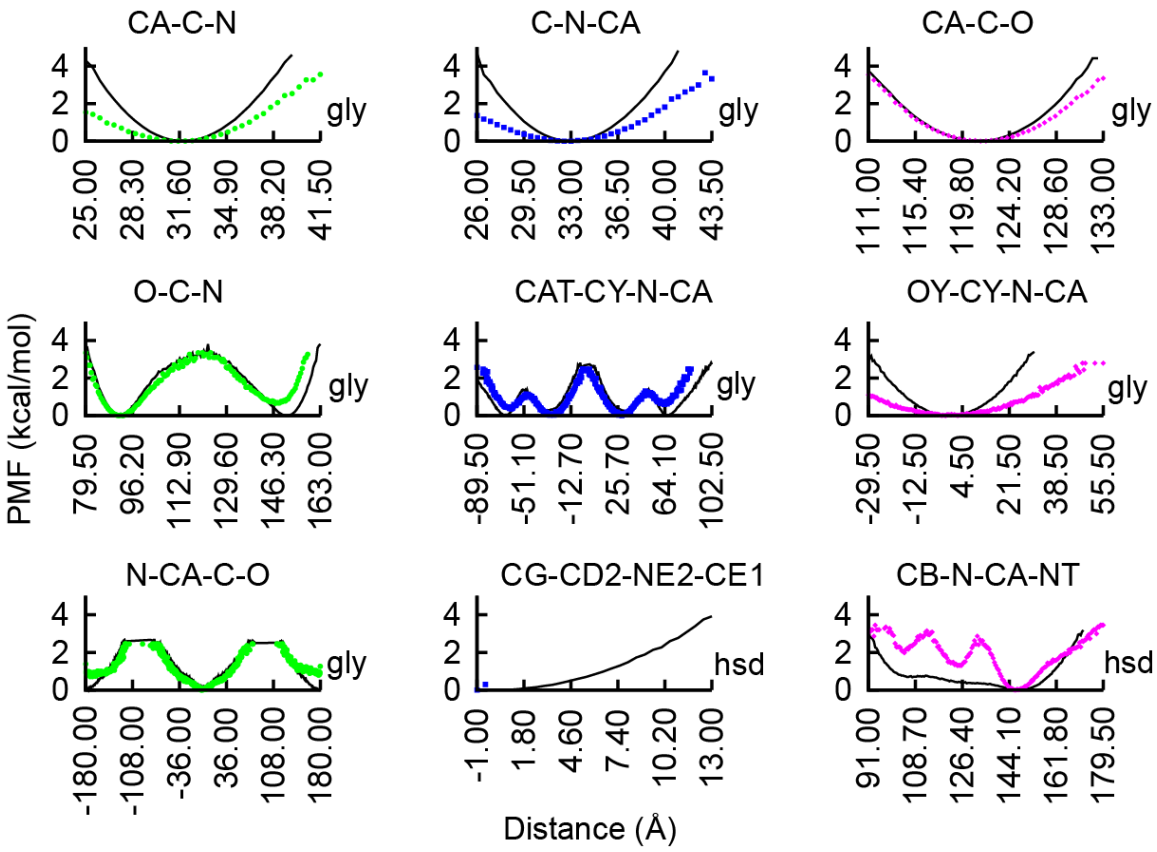

Figure S5: See page S75.

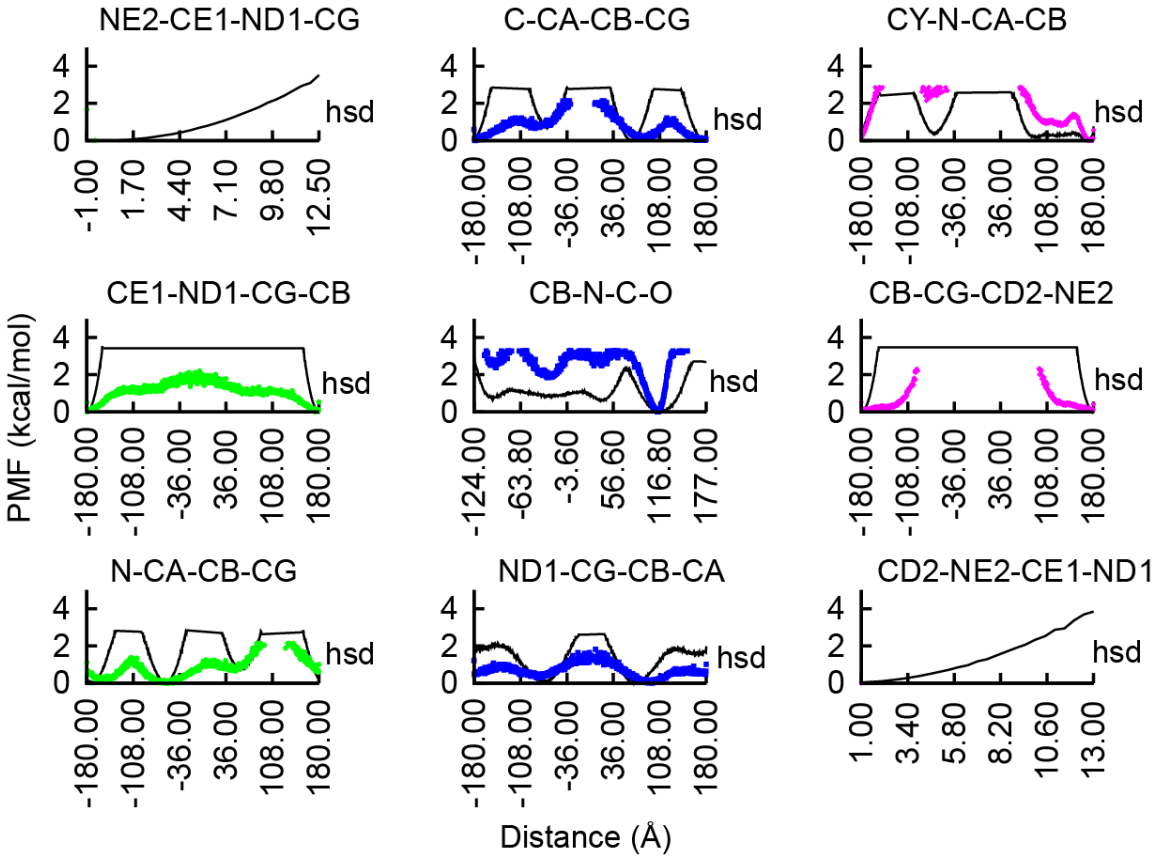

Figure S5: See page S75.

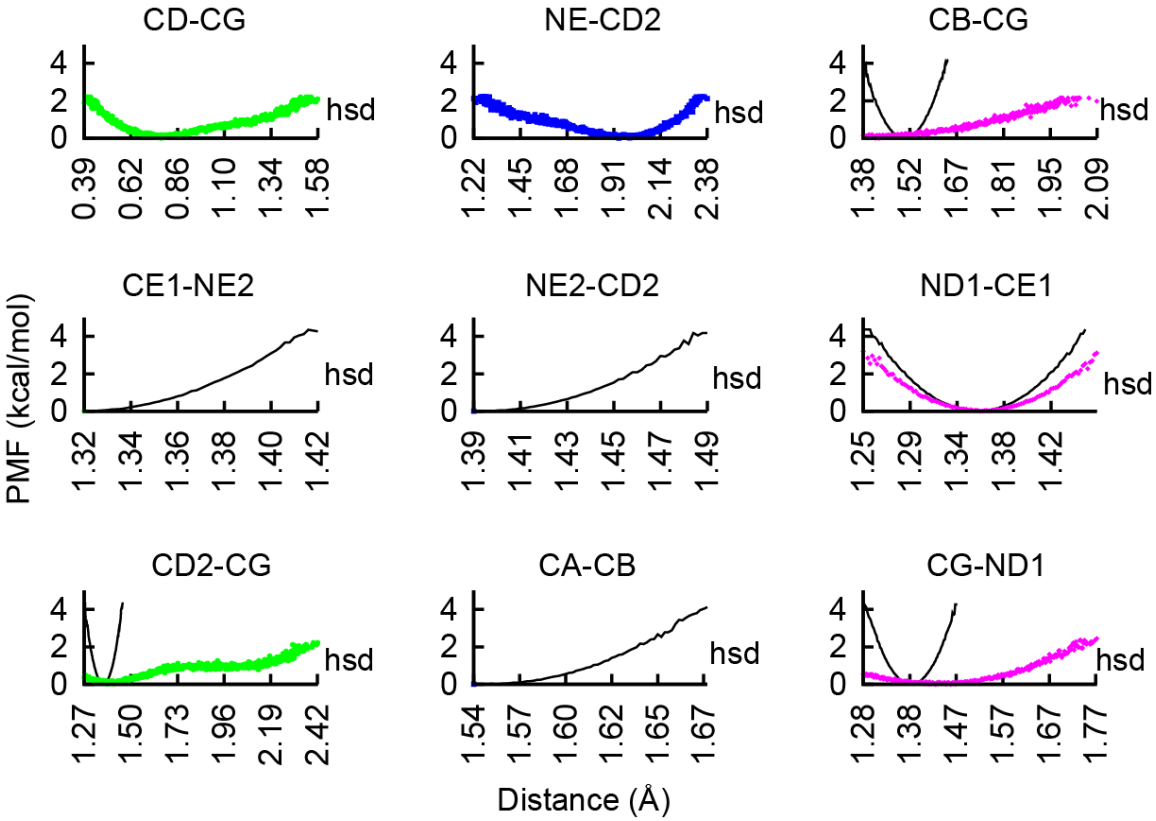

Figure S5: See page S75.

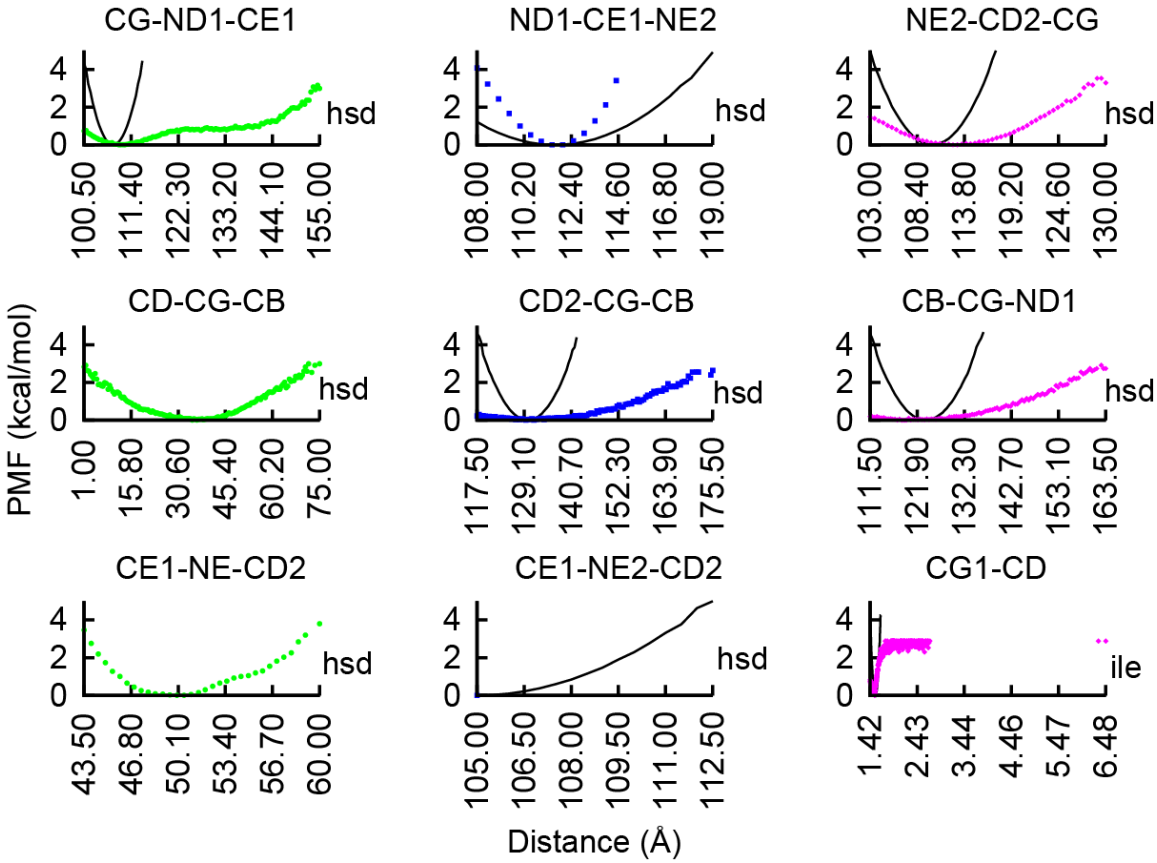

Figure S5: See page S75.

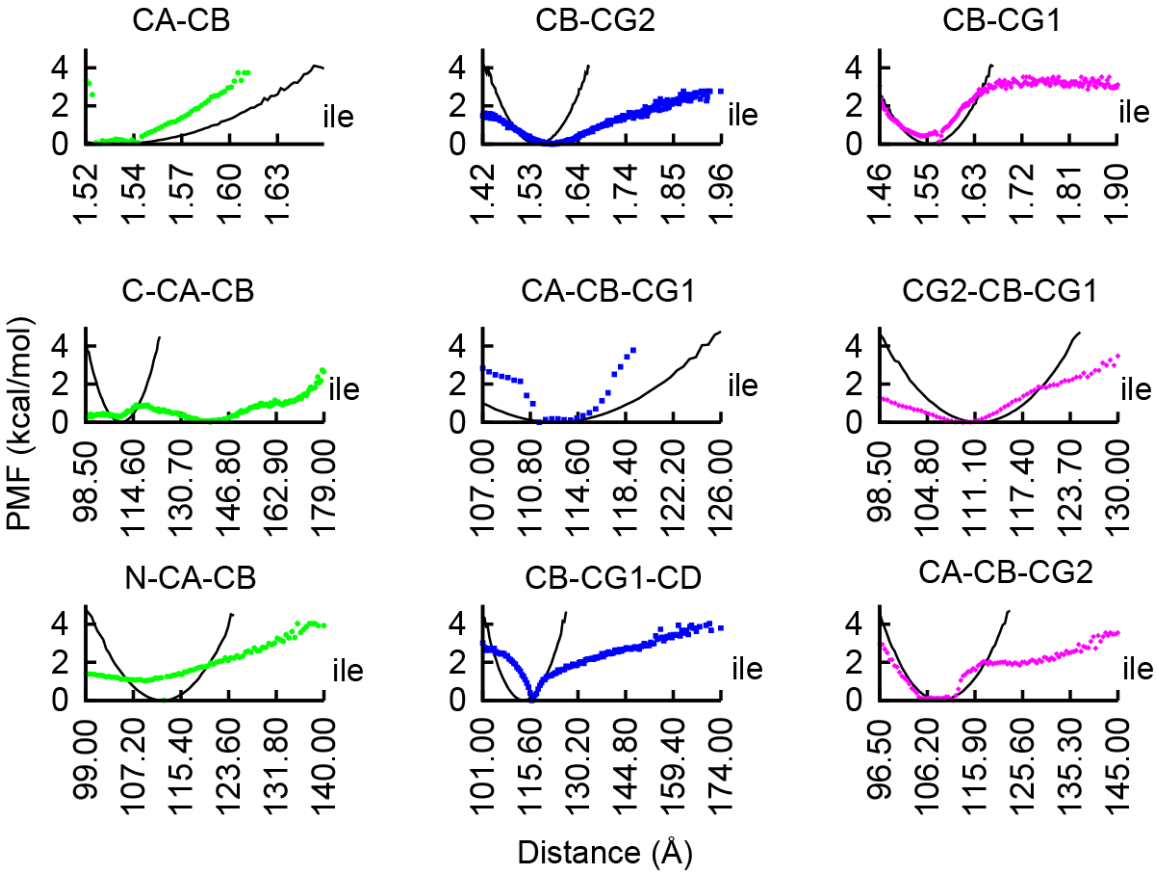

Figure S5: See page S75.

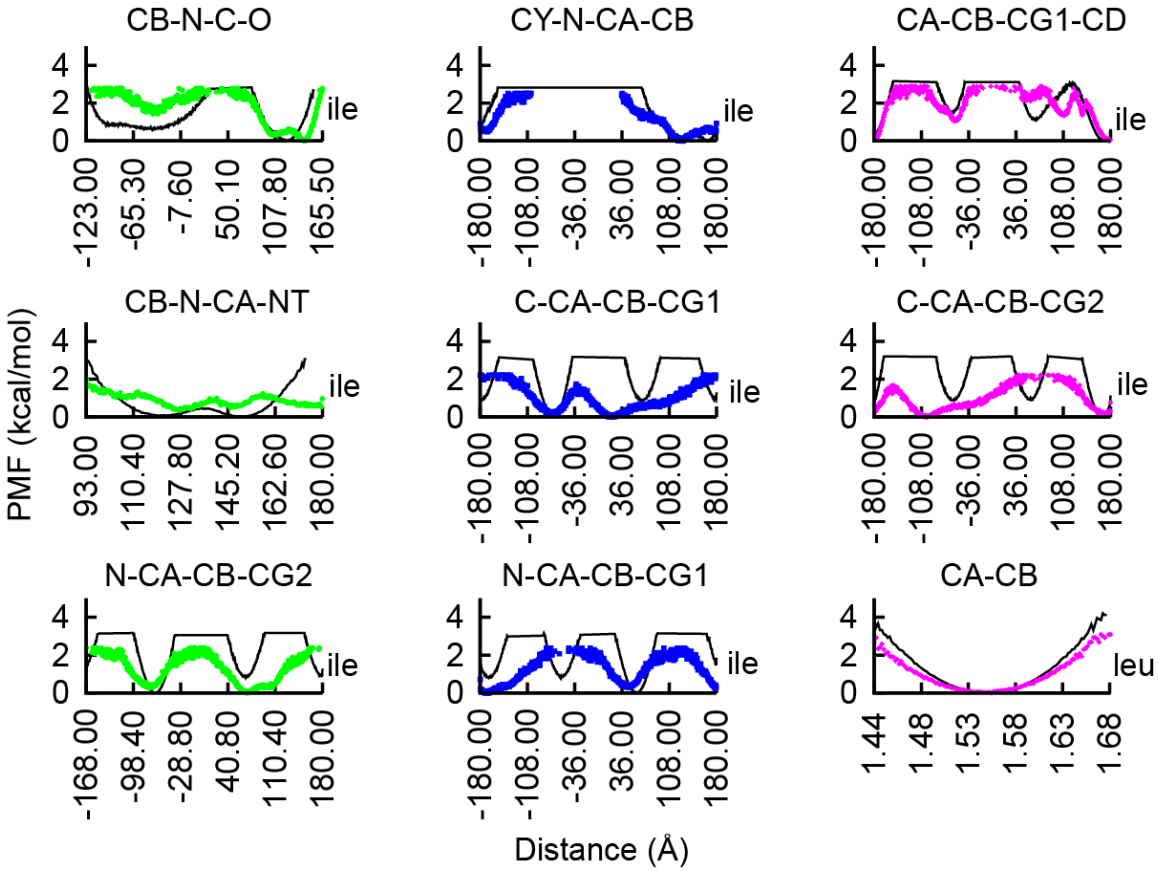

Figure S5: See page S75.

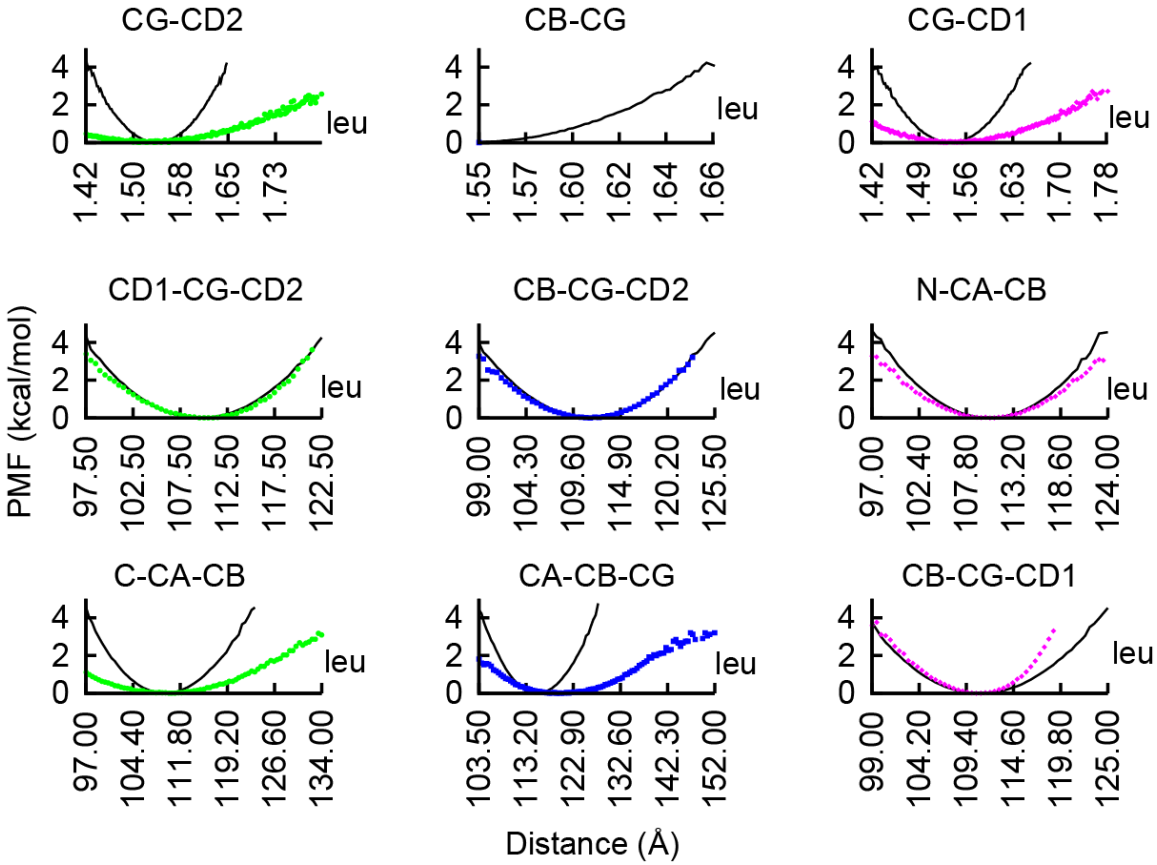

Figure S6: See page S75.

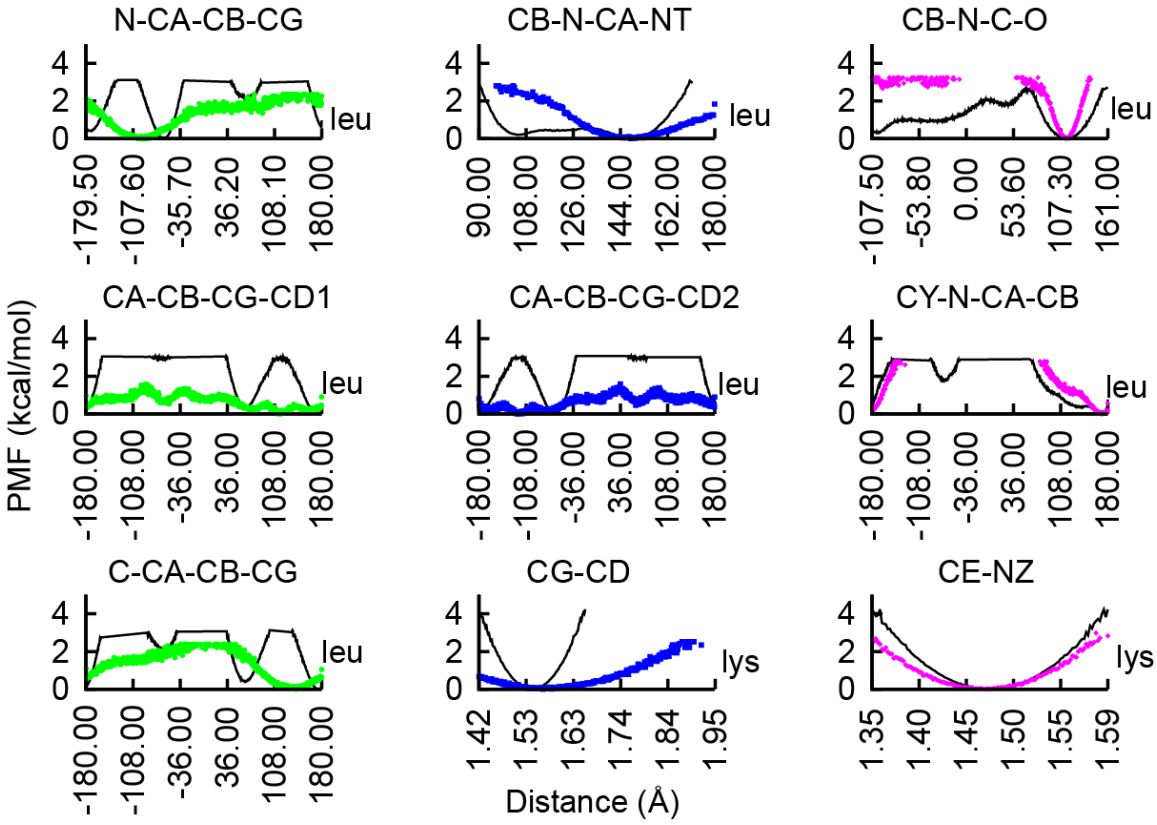

Figure S5: See page S75.

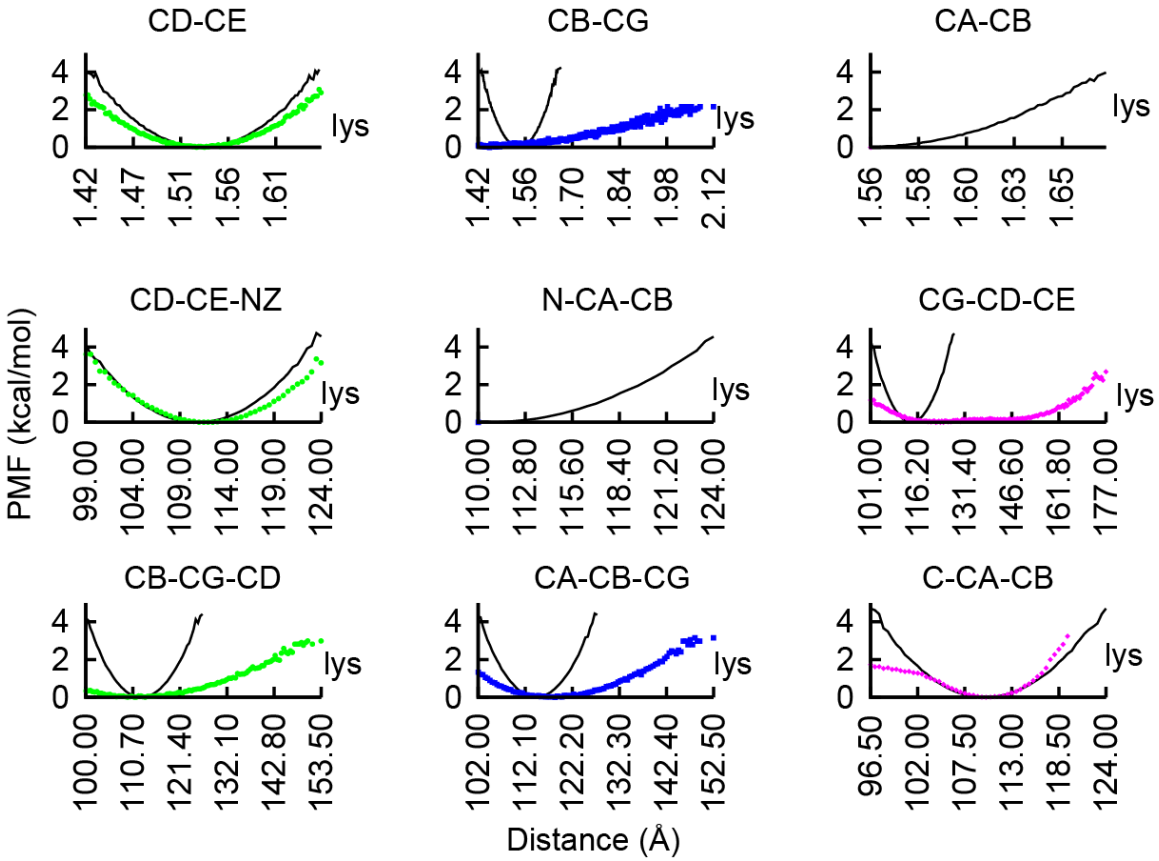

Figure S5: See page S75.

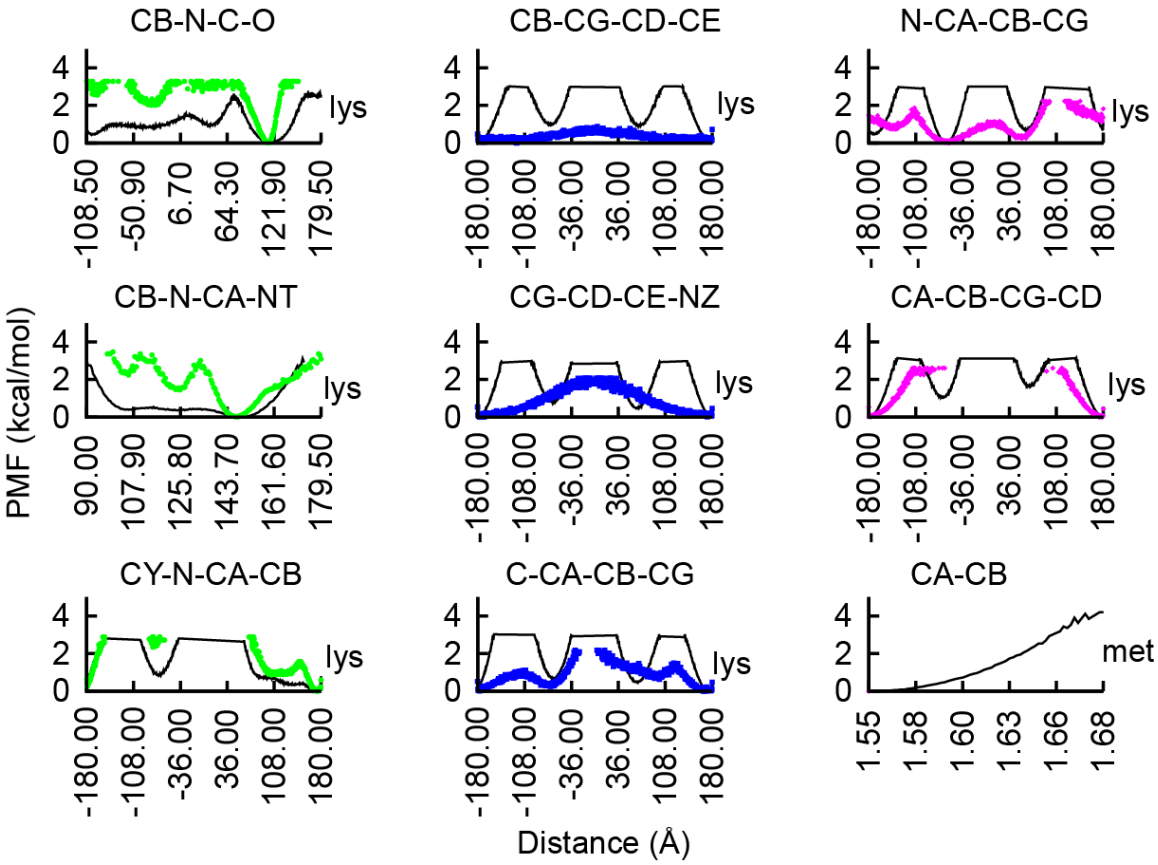

Figure S5: See page S75.

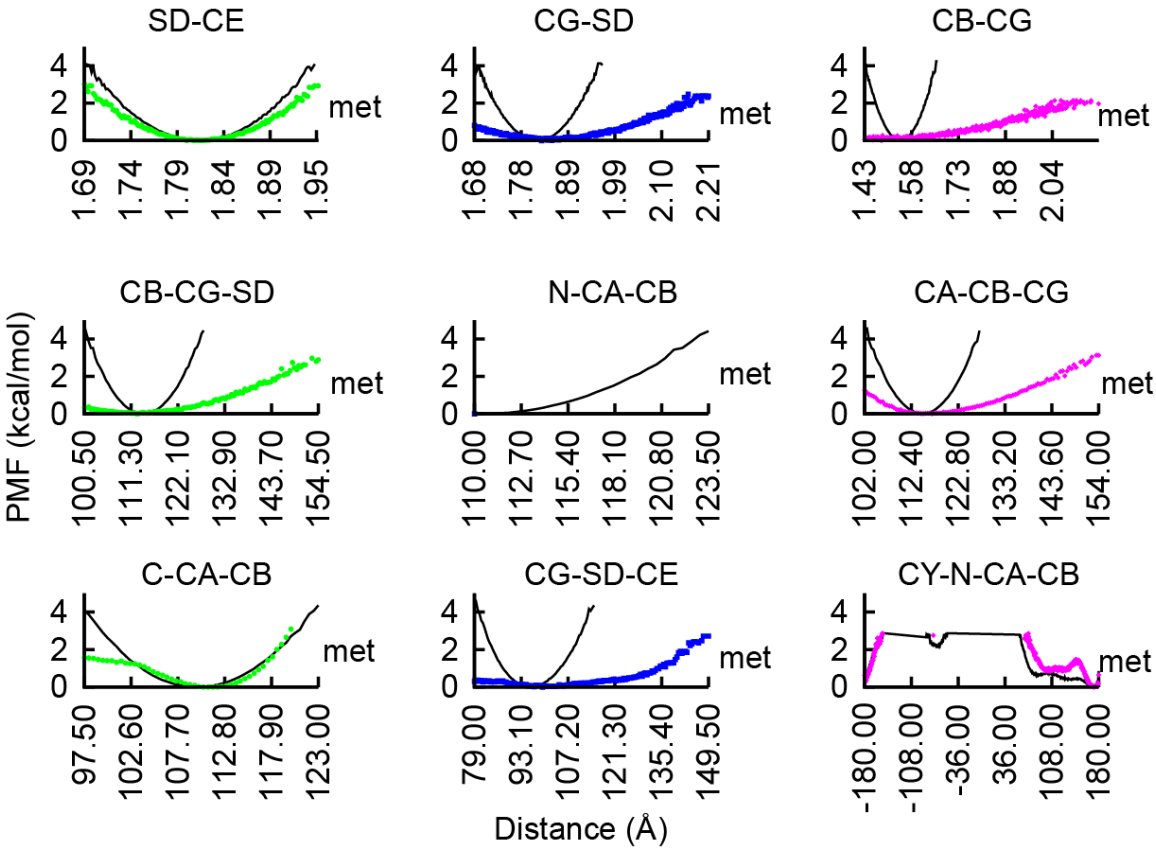

Figure S5: See page S75.

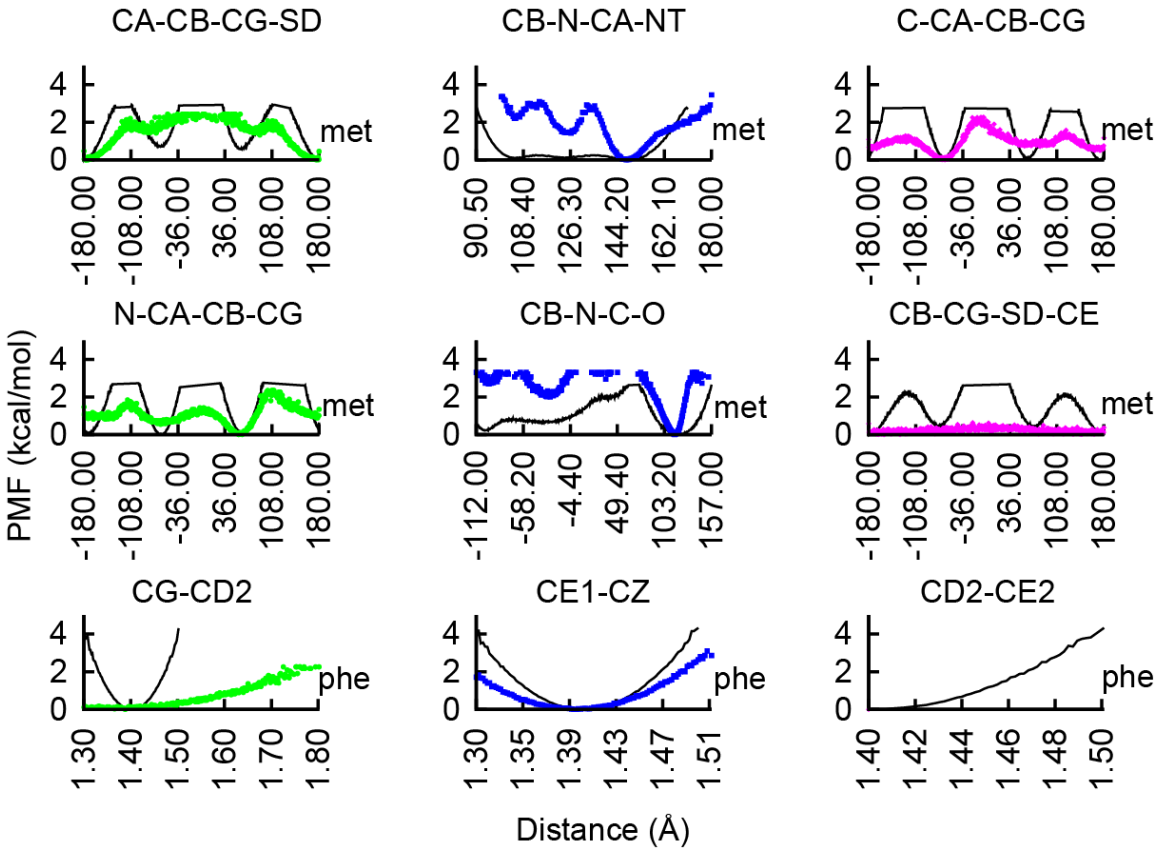

Figure S5: See page S75.

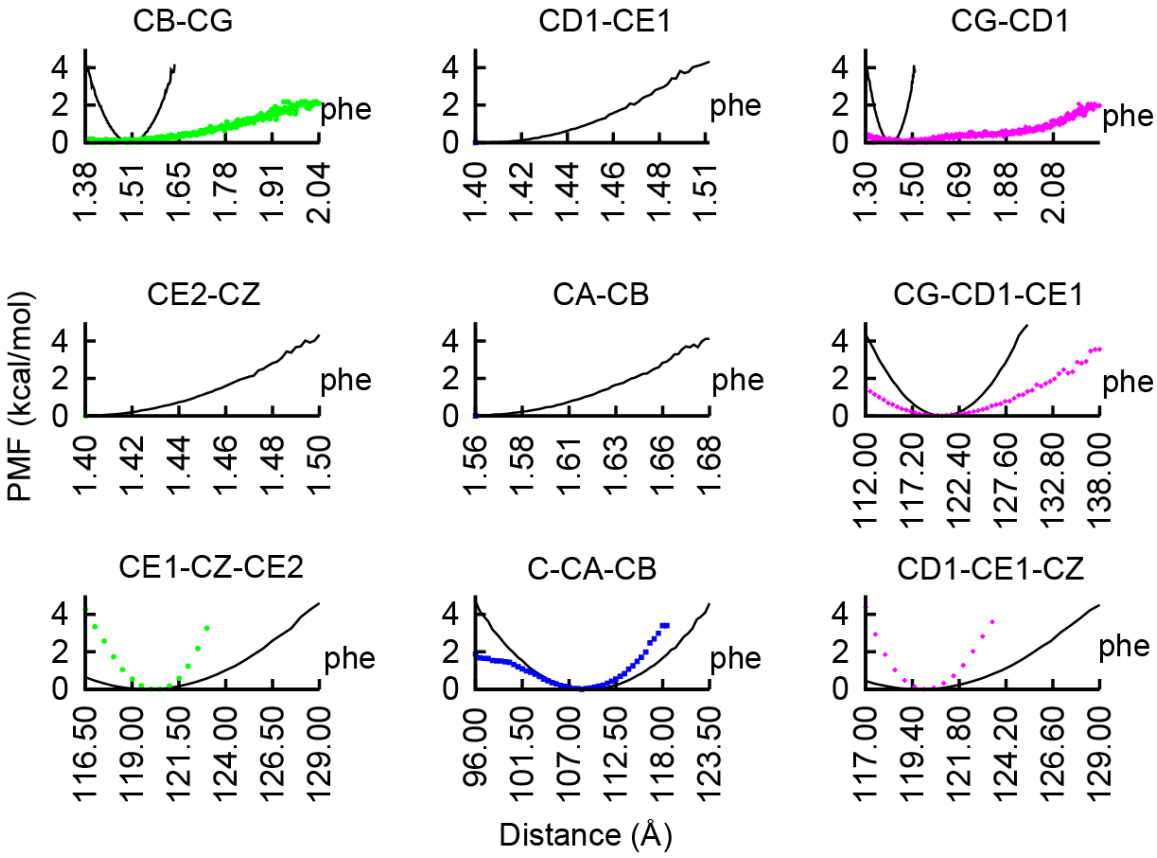

Figure S5: See page S75.

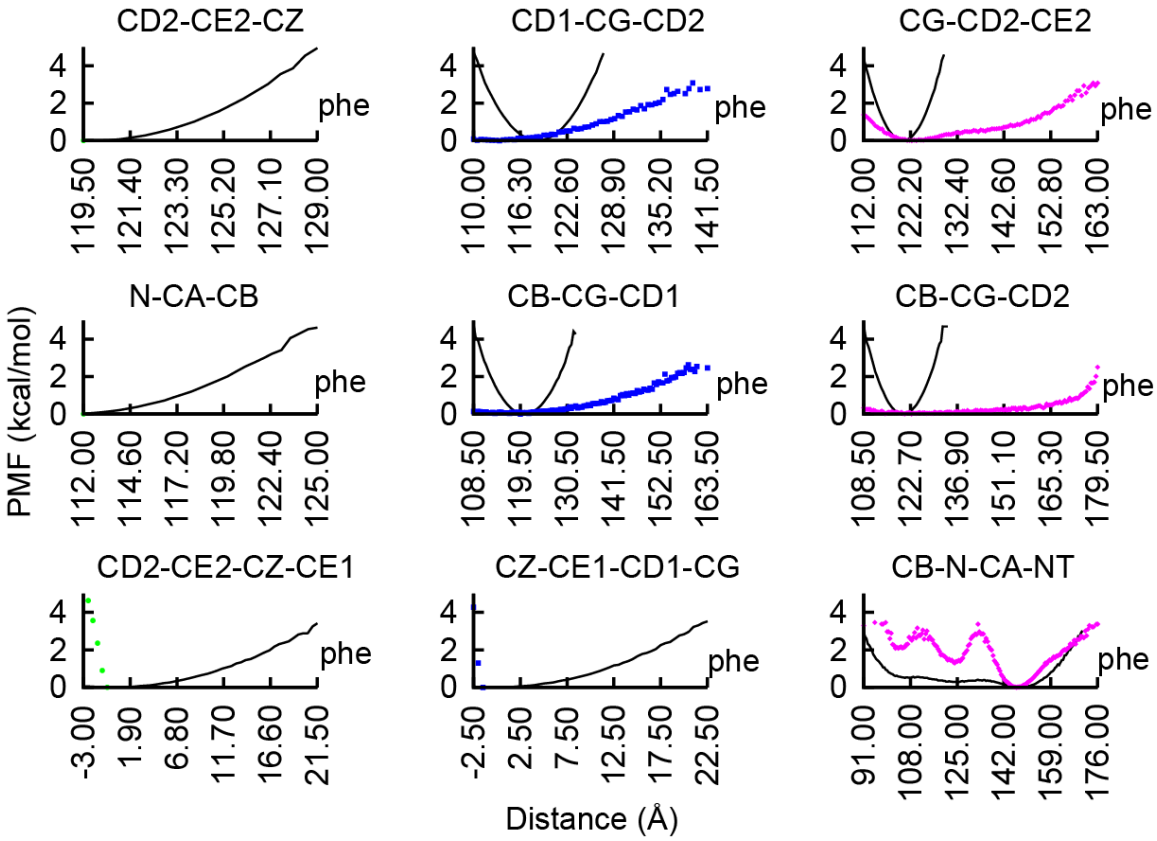

Figure S5: See page S75.

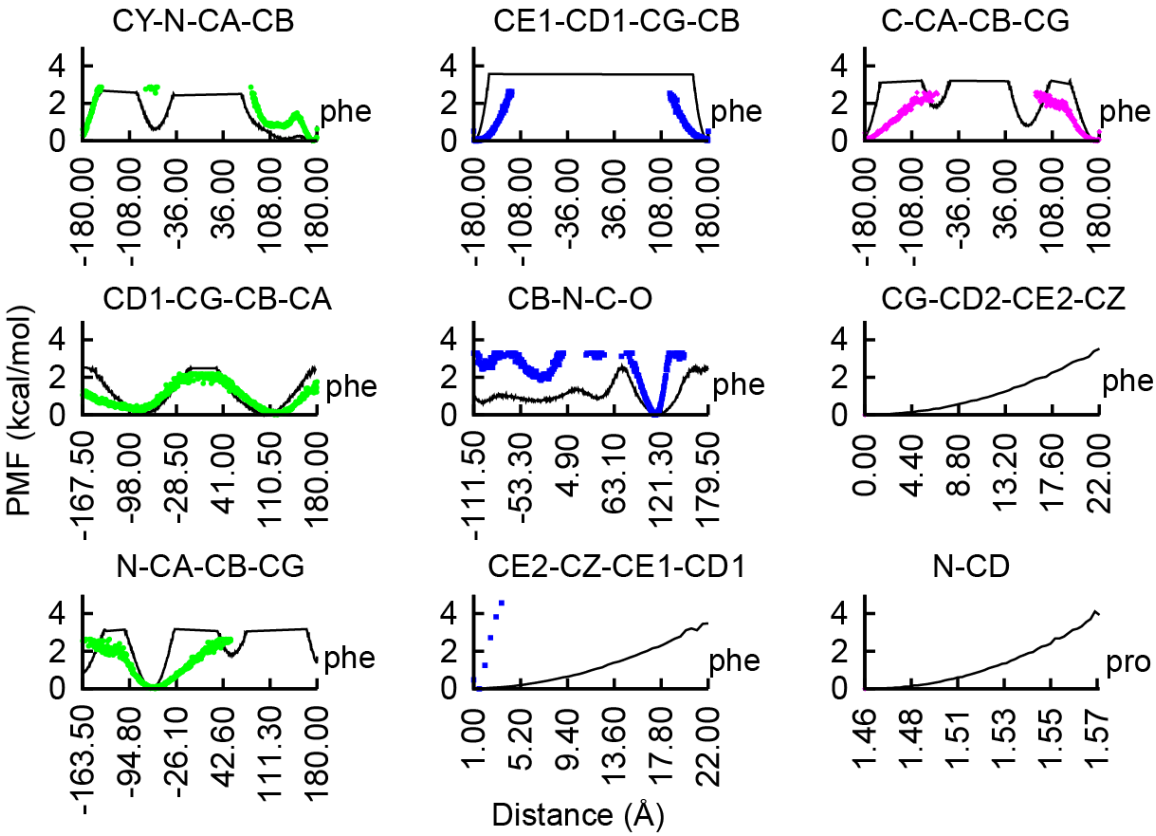

Figure S5: See page S75.

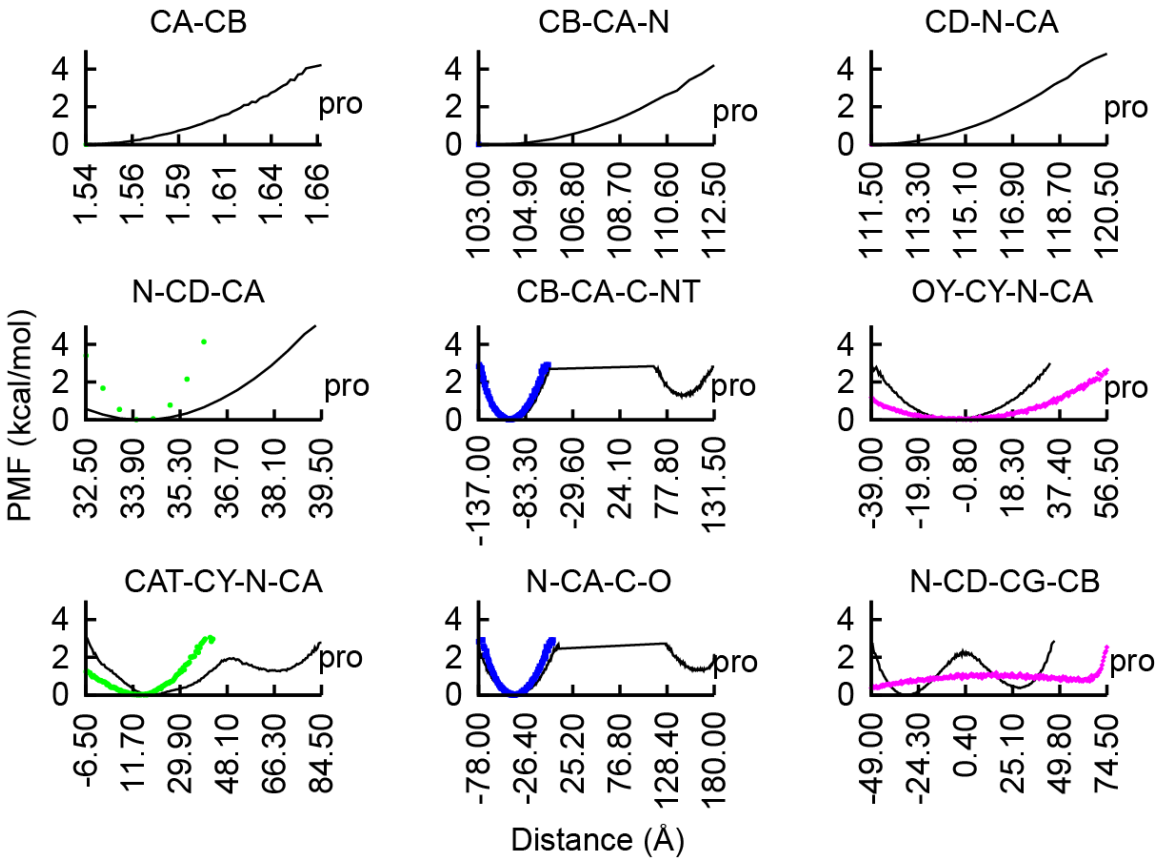

Figure S5: See page S75.

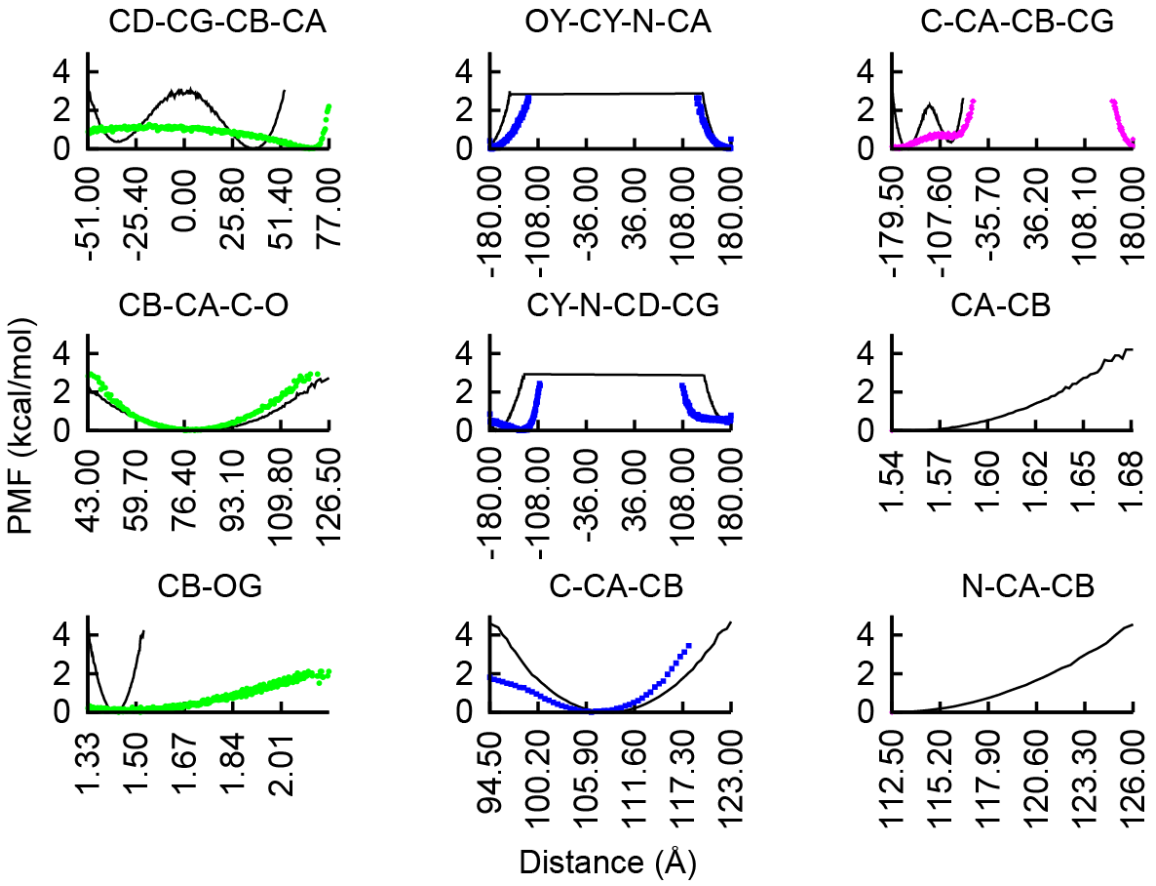

Figure S5: See page S75.

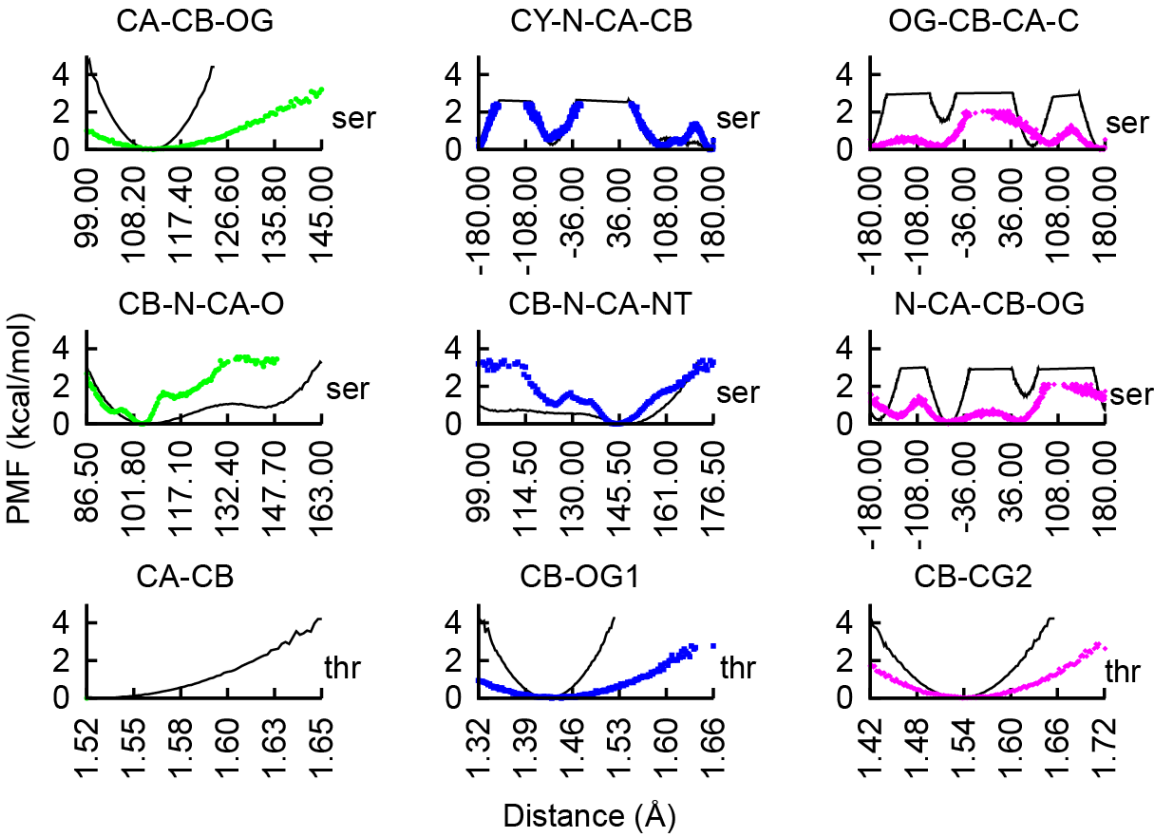

Figure S5: See page S75.

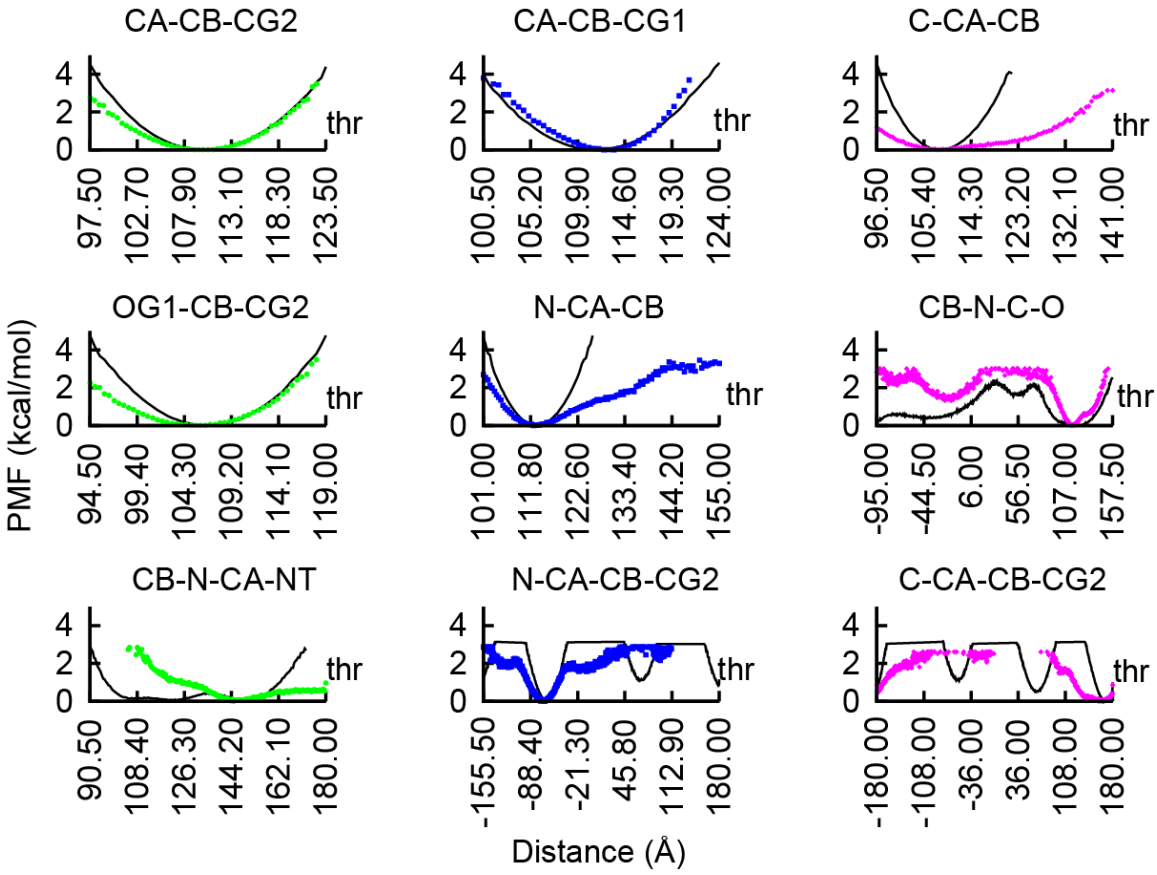

Figure S5: See page S75.

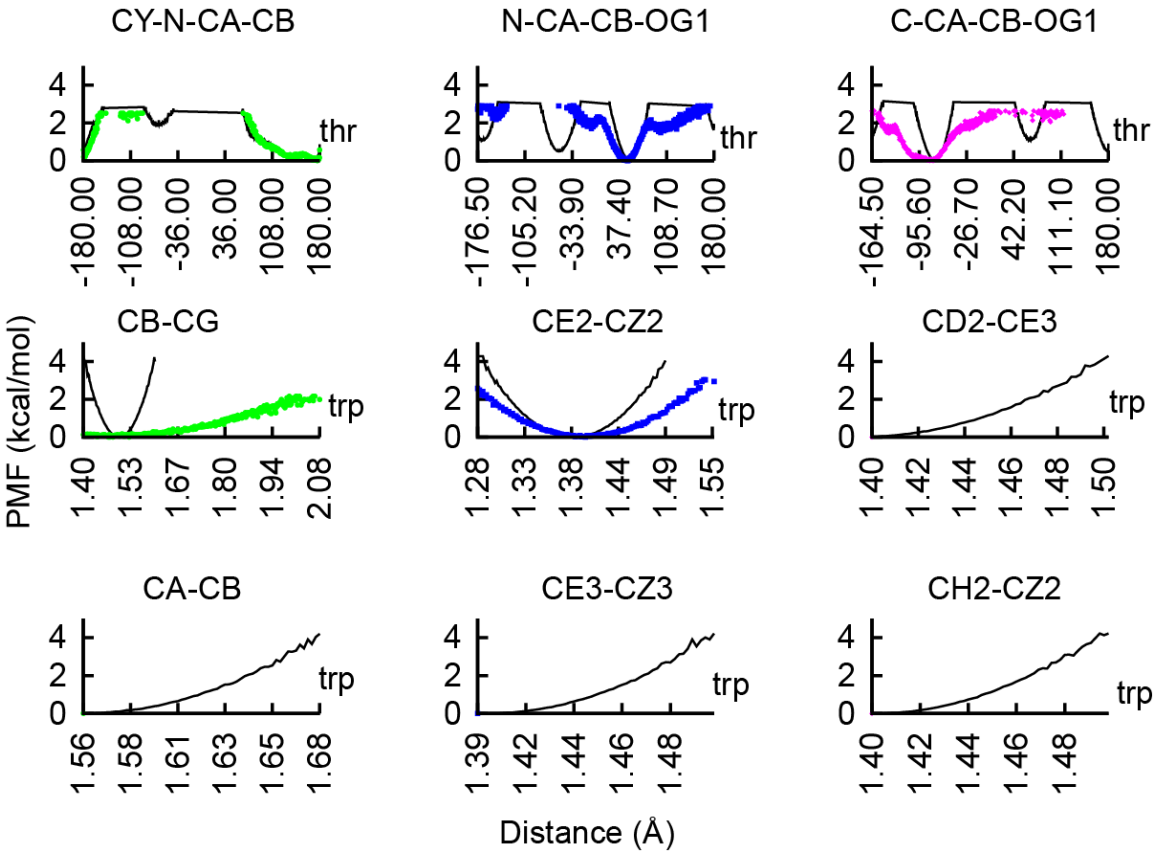

Figure S5: See page S75.

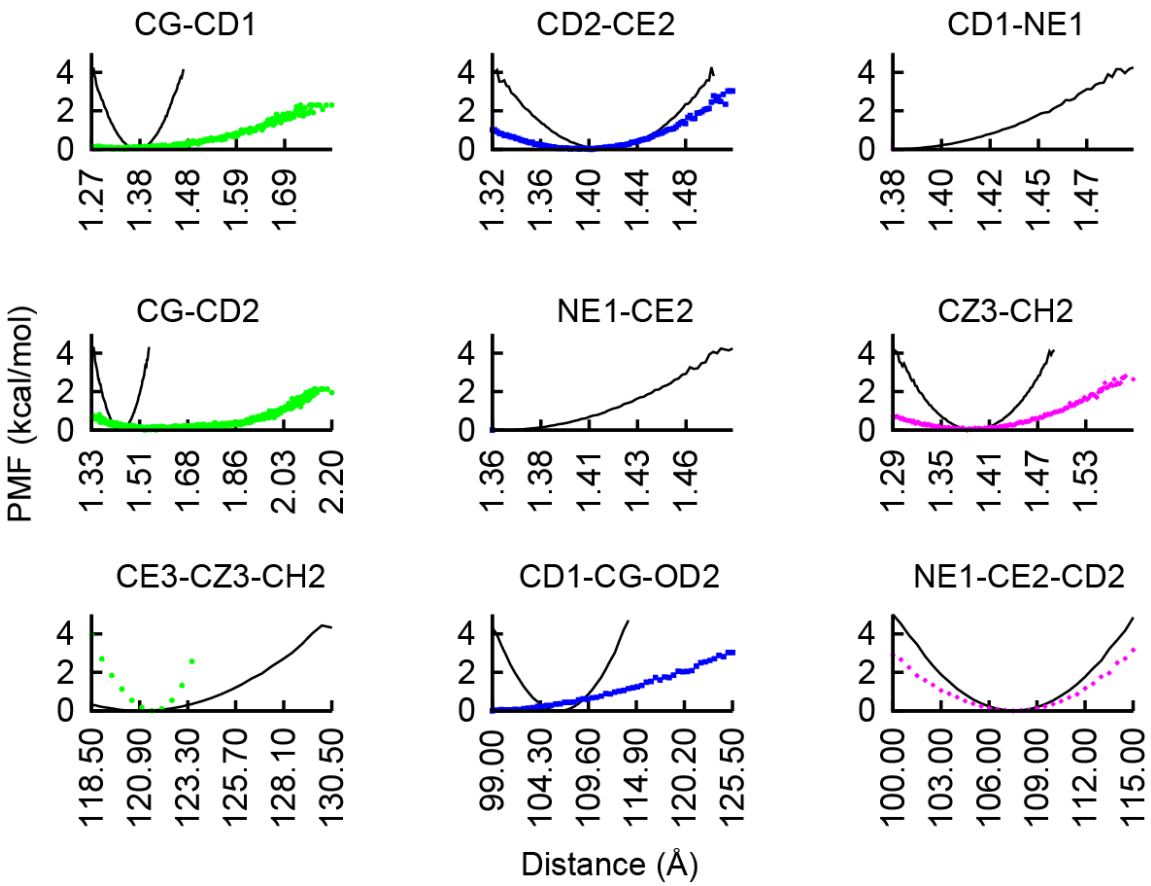

Figure S5: See page S75.

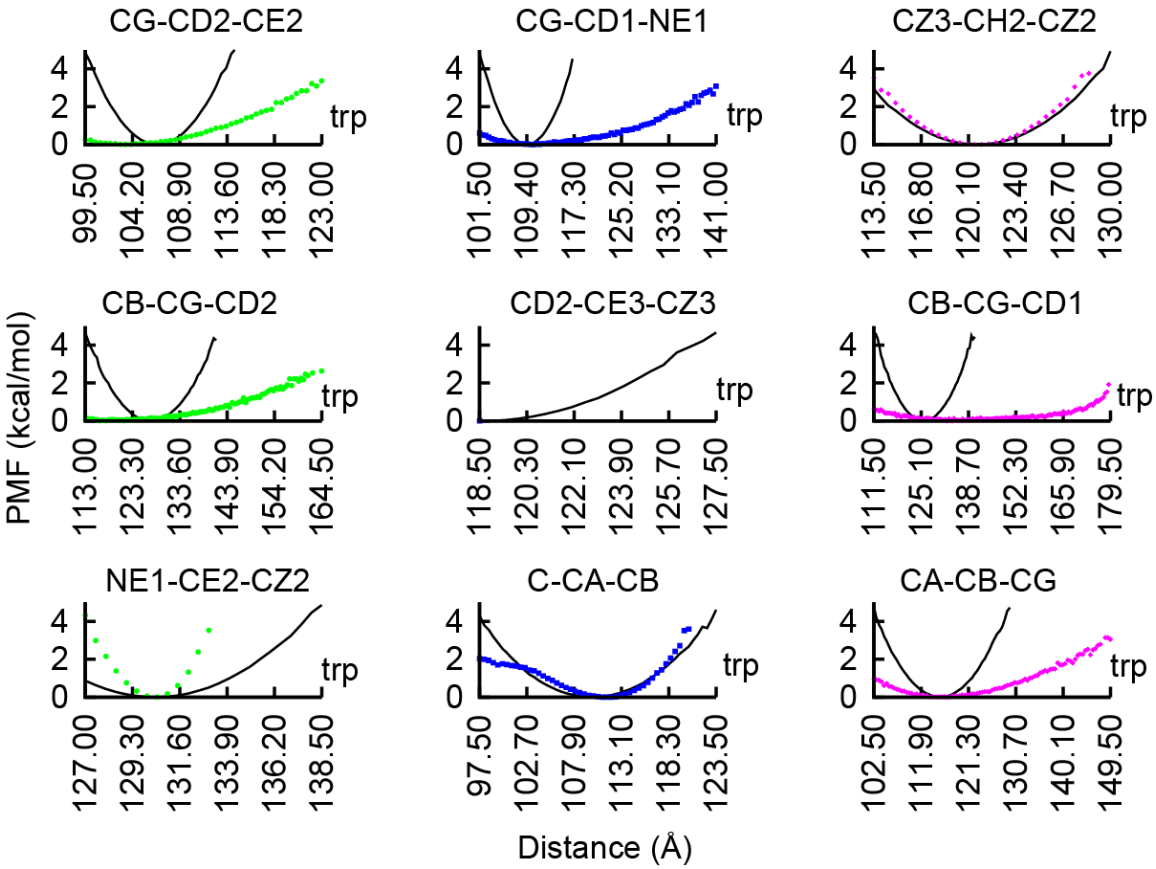

Figure S5: See page S75.

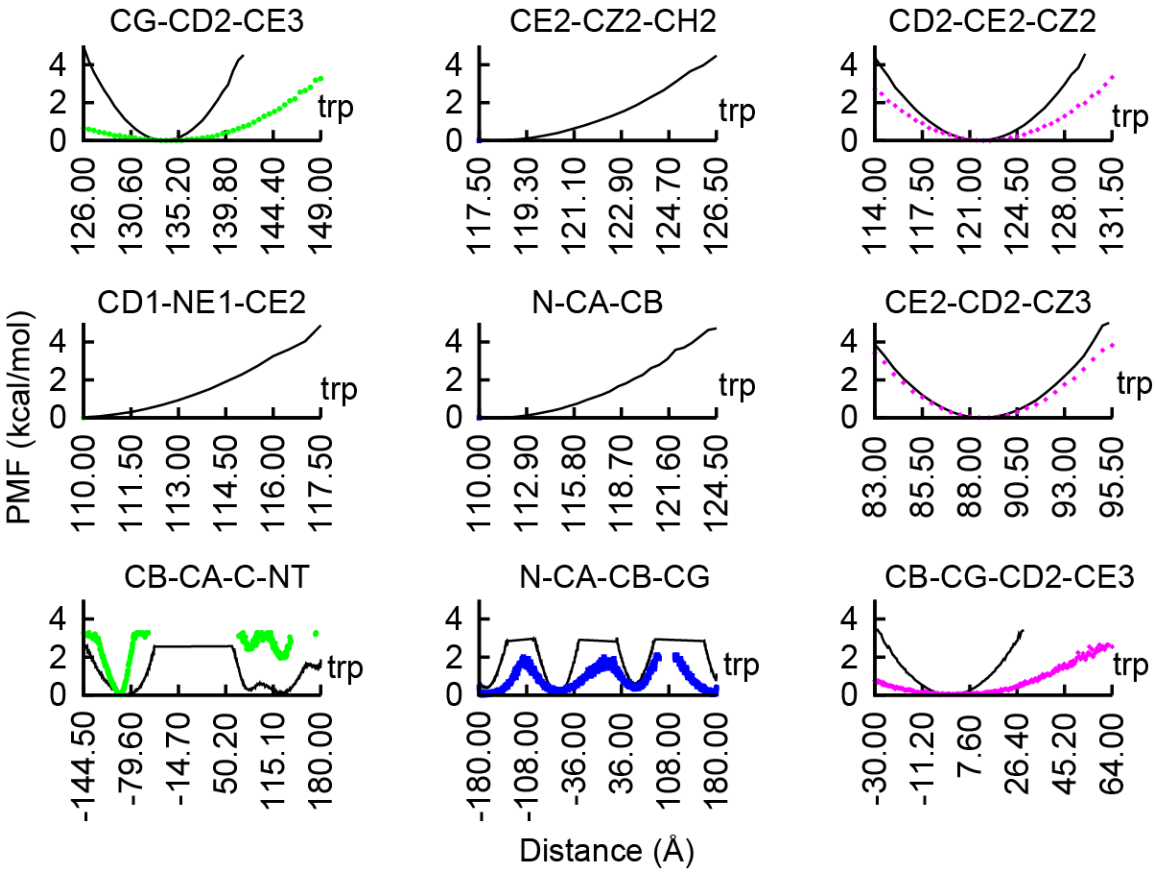

Figure S5: See page S75.

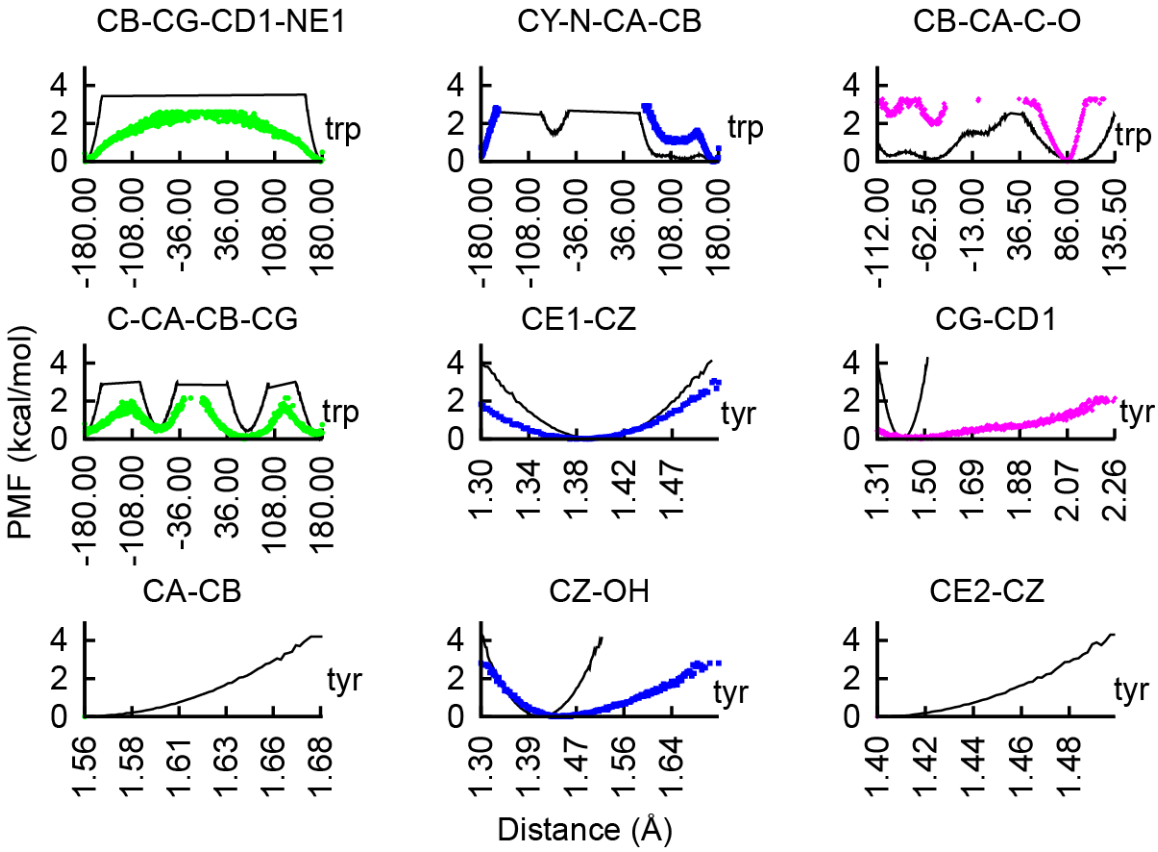

Figure S5: See page S75.

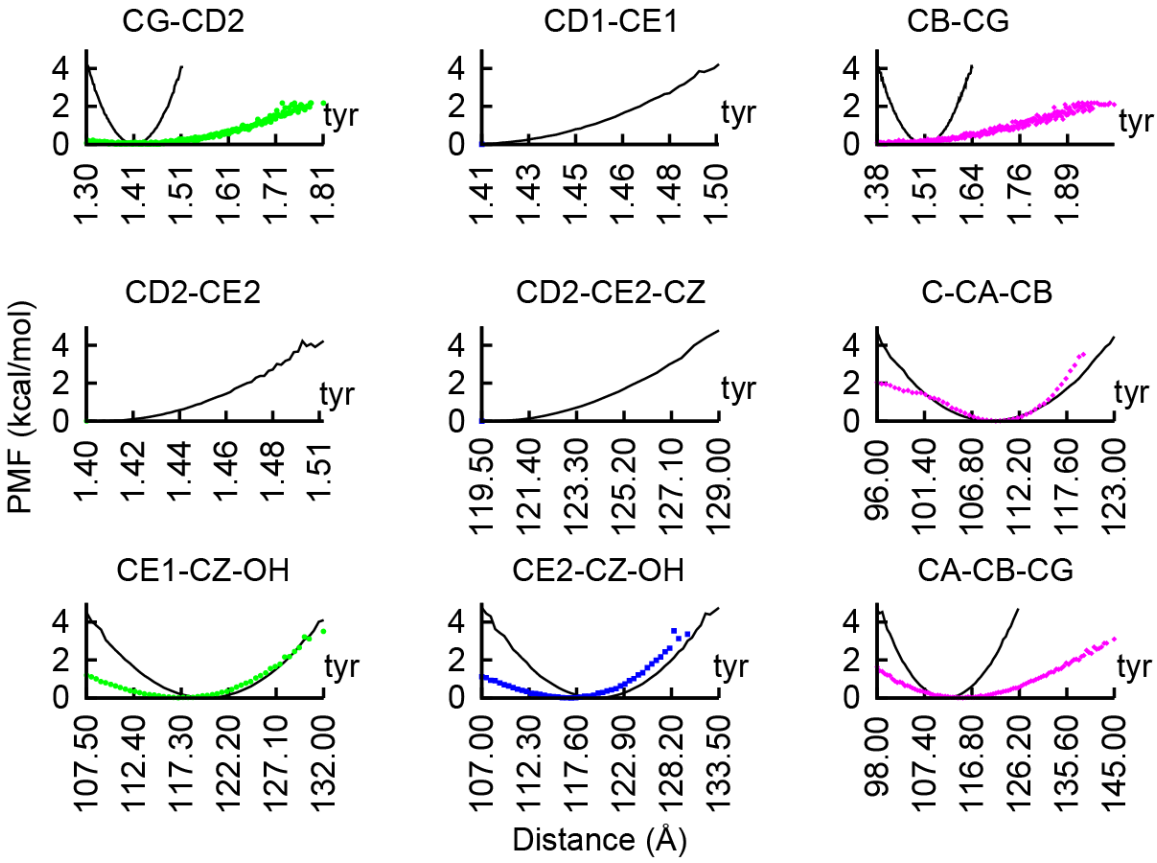

Figure S5: See page S75.

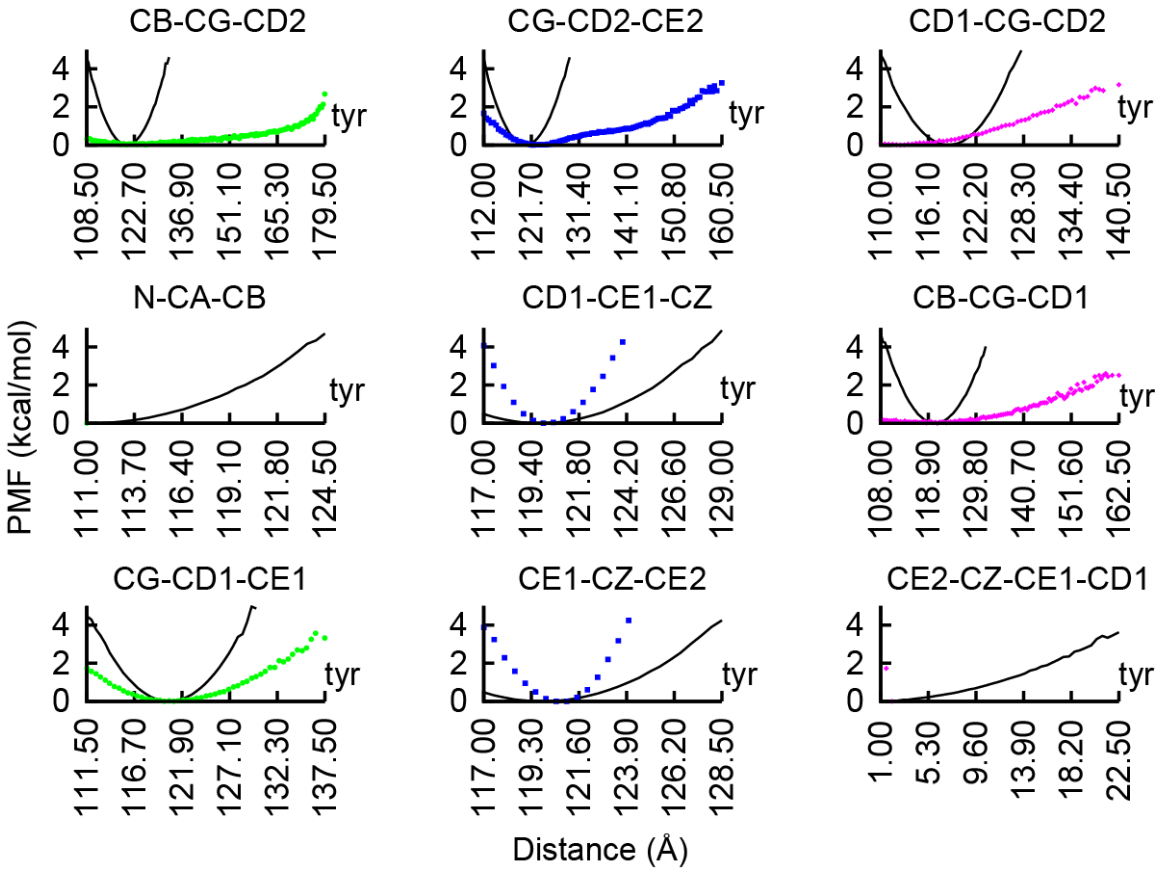

Figure S5: See page S75.

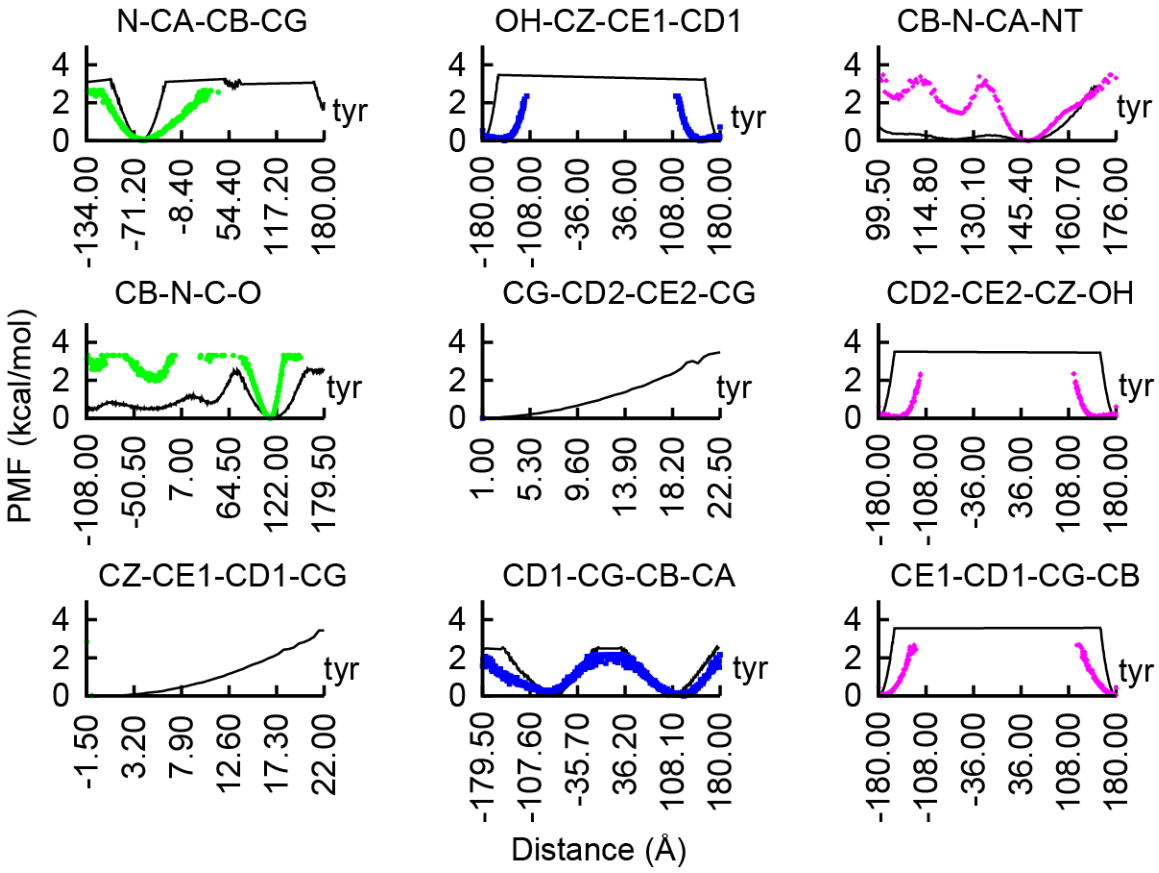

Figure S5: See page S75.

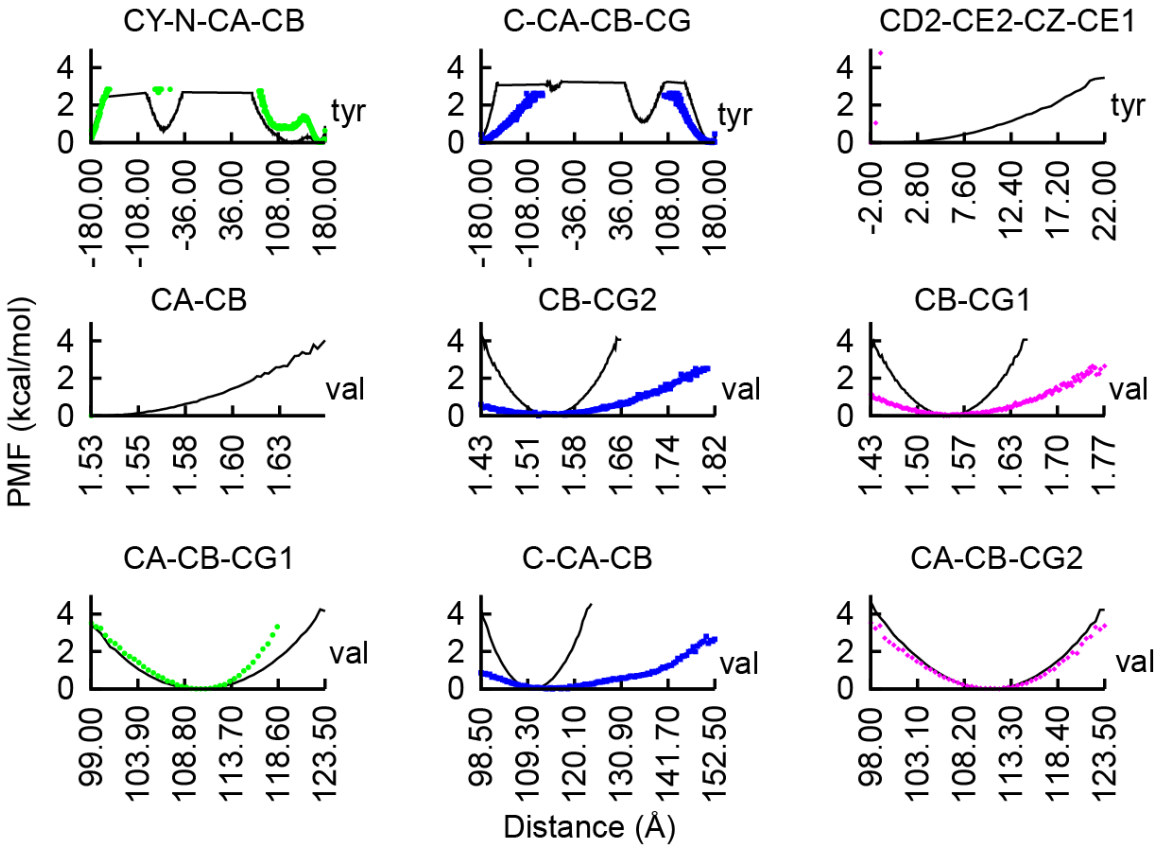

Figure S5: See page S75.

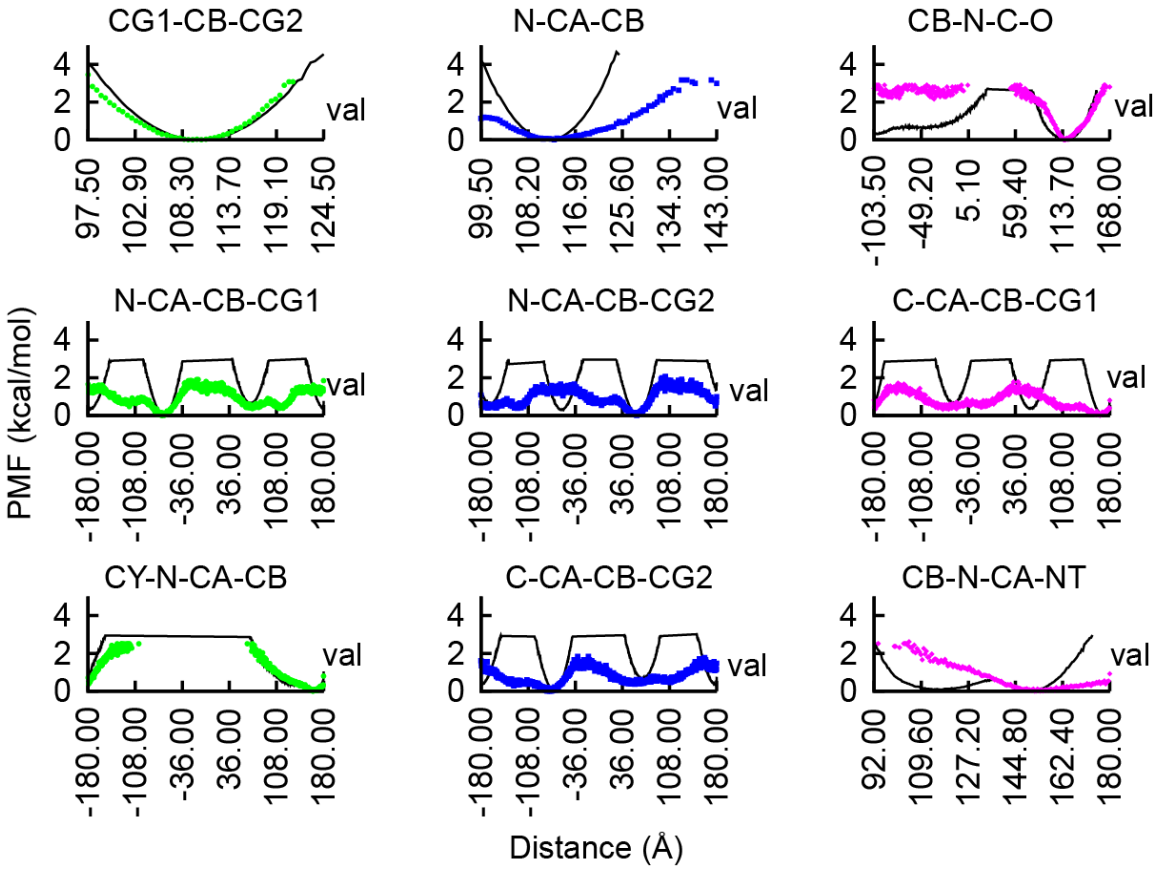

Figure S5: Comparison of distribution of internal degrees of freedom (bonds, angles, and dihedrals) from PRIMO AXA simulations (color) with the CHARMM explicit dipeptide simulations (black). Here, X can be any of 20 naturally occurring amino acids and is shown in the figure (bottom right).

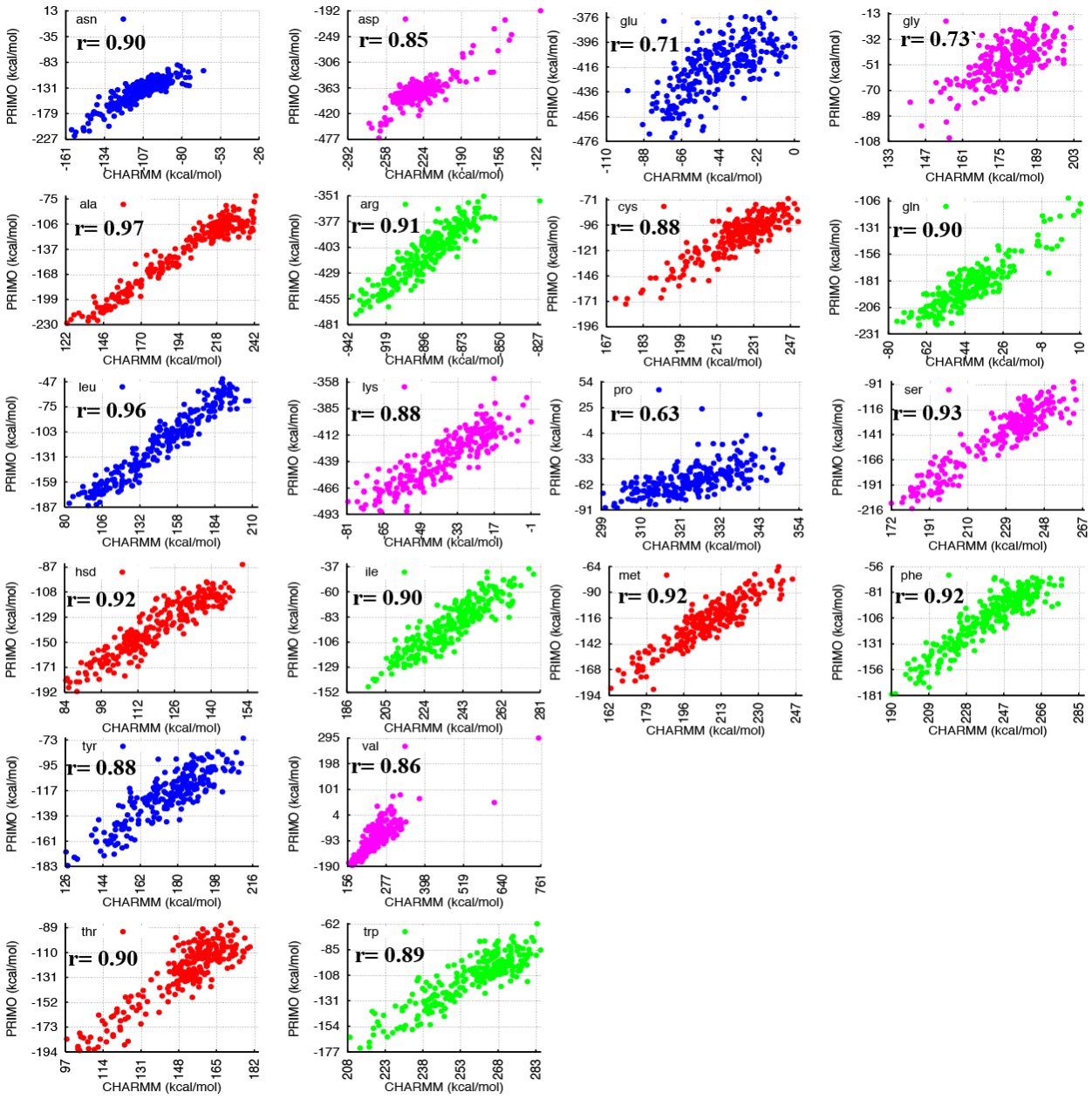

Figure S6: (color online) PRIMO versus CHARMM total energies for $(AAXAA)_4$ decoys with corresponding linear correlation coefficients r.

φ/ψ Sampling in AXA Simulations

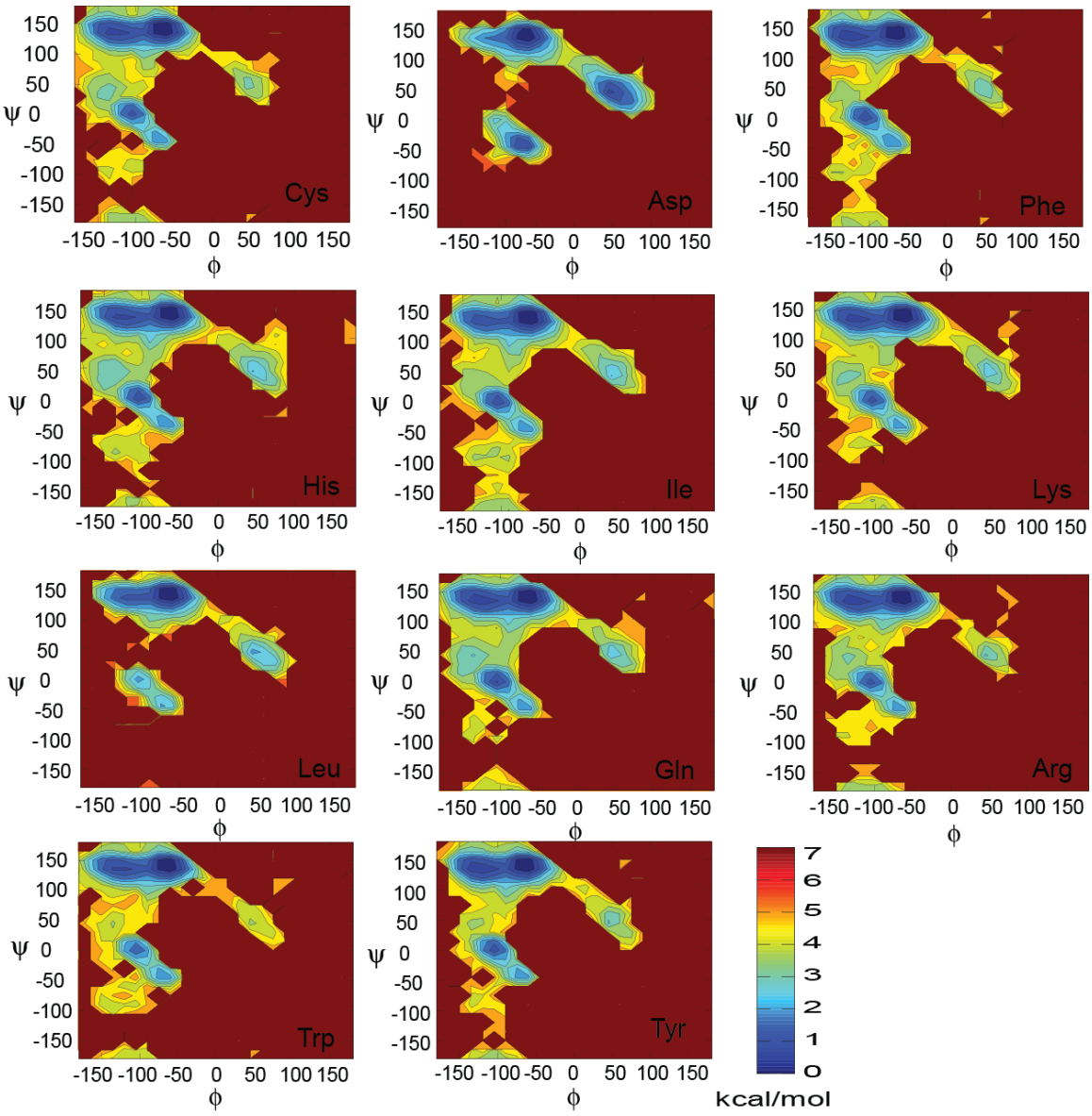

Figure S7: Potentials of mean force for the sampling of φ/ψ backbone torsion angles in selected amino acid residues from AXA simulations. A color bar indicating energy levels is provided on the right.

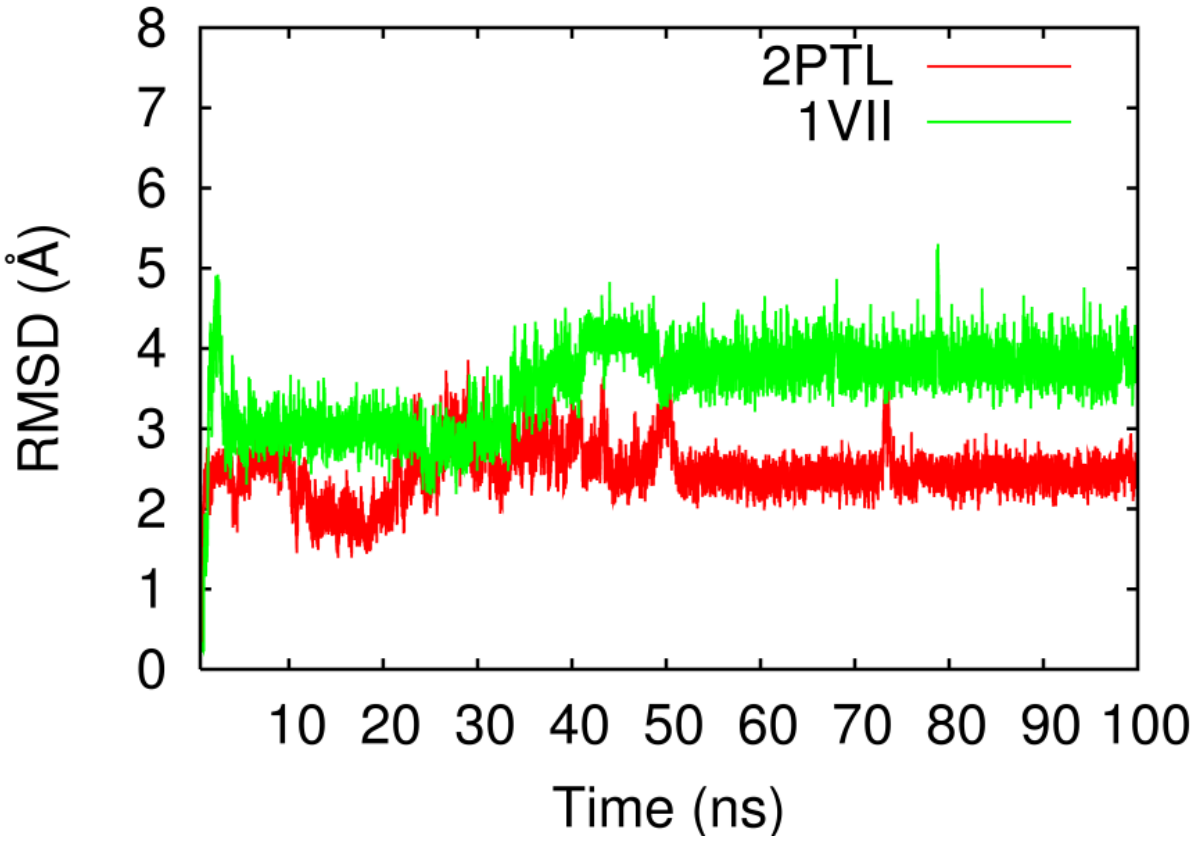

Figure S8: Time evolution of Cα RMSD for 1VII and 2PTL.

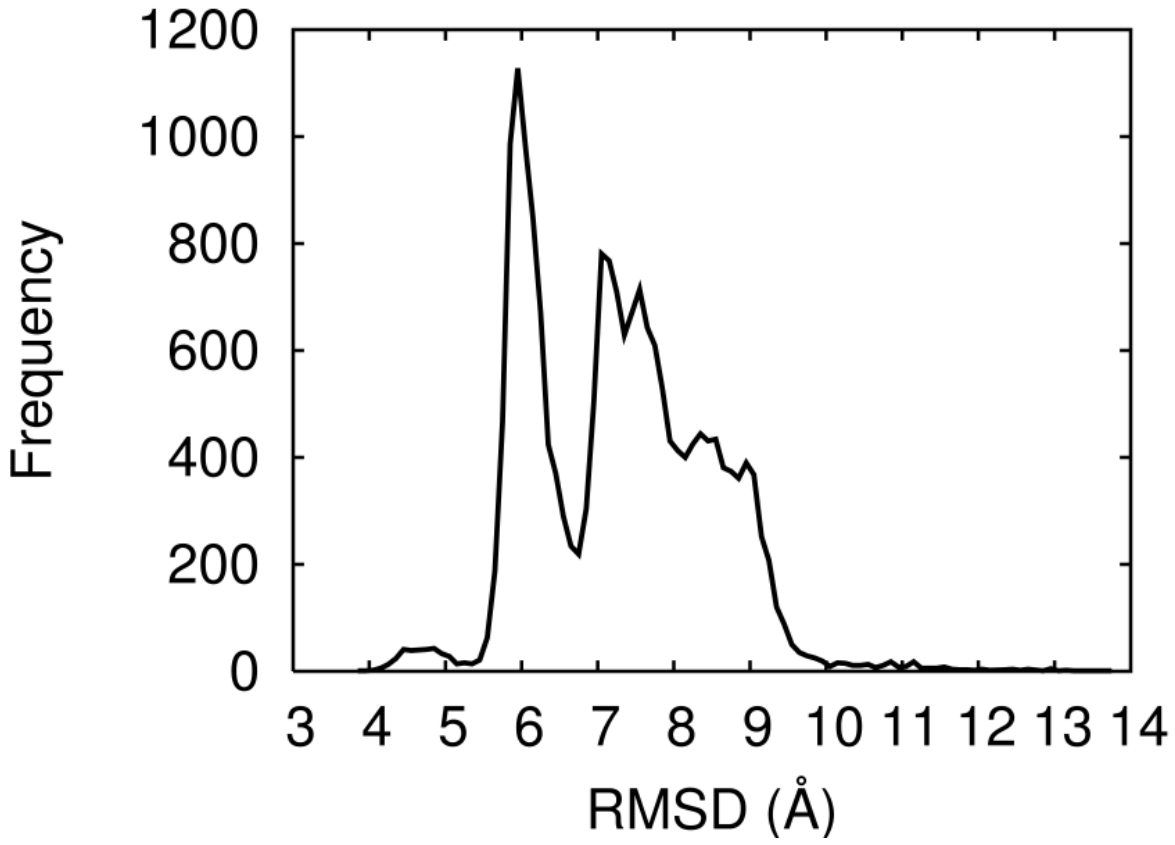

Figure S9: Distribution of backbone RMSD values for WW domain at 300 K in PRIMO REMD simulations.

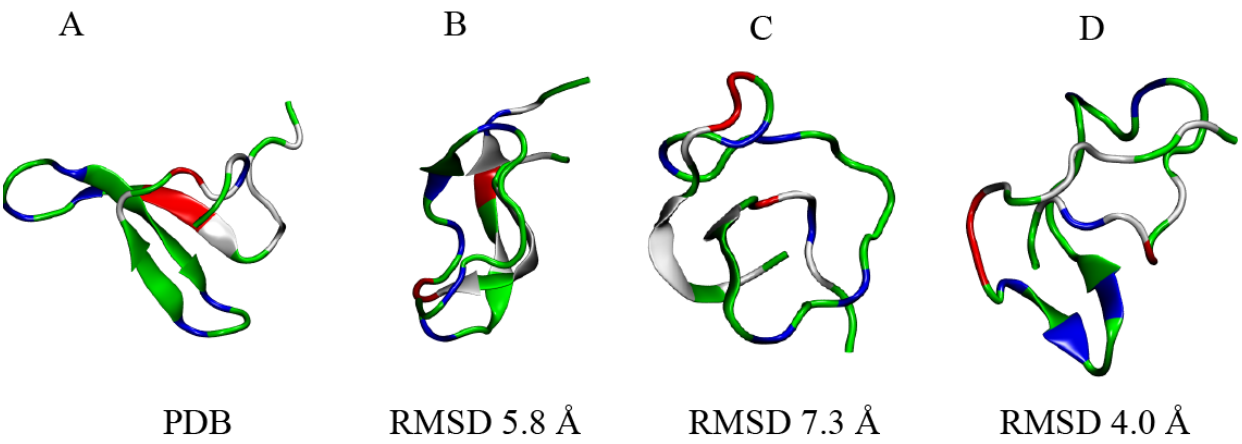

Figure S10: Representative structures from the REMD simulations of WW domain.

REFERENCES

(1) Gopal, S. M.; Mukherjee, S.; Yi Ming, C.; Feig, M. *Proteins* **2011**, *78*, 1266-1281.

(2) Cheng, Y-M.; Gopal, S. M.; Law, S.; Feig, M. *IEEE/ACM Transactions on Computational Biology and Bioinformatics* **2012**, *6*, 476-486.